Chapter 1

1. Introduction

1.1 Background

The detection of weak signal pulses in noise has been a problem for radars ever since they were invented. Curiously enough, early radars used the most intelligent system to determine the presence of weak signals: the human operator staring at an oscilloscope display. But operator performance is variable and uncertain especially as the operator tires of staring at the screen. The operator was quickly replaced by automatic target detection systems that use a threshold to detect pulses that exceed the noise floor by a preset amount. If a noise spike crosses the threshold a false target is detected, so in most radar systems the threshold must be set 14 to 16 dB above the mean noise floor for a single pulse to reduce the false alarm rate to an acceptable level. Integration of multiple target echoes allows the threshold to be lowered to 5 or 6 dB above the noise floor.

A radar must detect a target and also measure the range to the target by finding the time that it takes the transmitted pulses to travel to the target and back to the radar. Accurate measurement of the time interval is particularly important in tracking radars that provide information to weapons systems. Threshold detection is used to record the time stamp of threshold crossings. However, this measurement is strongly dependent on the noise that may either trigger a false alarm, distort the pulse shape, or even hide the expected pulse.

The idea for a new measurement technique was thus needed. Correlation detection is a way to improve the accuracy of the timing measurement that provides range information,

especially where the pulses from the radar receiver are weak and distorted. A correlation detector multiplies the transmitted pulse and received pulse shapes with all possible time delays, and then looks for the maximum output. The maximum occurs where there is a best match between the pulse shapes. This process has been widely used in geodetic Very Long Baseline Interferometry (VLBI) for instance, where stable periodical and weak signals from distant radio sources (quasars) are correlated in order to accurately determine the relative positions of the radio receiver antennas attached to different Earth land masses. It is therefore possible to build correlation detectors that can find targets with pulses that are below the noise floor, thus significantly extending the range of the radar.

The difficulty with correlation detection of weak pulses, especially those below the noise floor, is that the entire range of received pulse times must be searched repeatedly to determine whether any targets are present. If the radar has a long range, and the target can move quickly, the received pulses may not remain at the same range for long enough to allow the correlator to detect the target. This suggests that a combination of a detection technique to find weak targets and a correlator to determine the target range, and velocity towards the radar, would be a better design.

1.2 Research goal

The thesis of this research is to prove that the system that processes pulses in order to extract information based on threshold crossings and averaging of the result can be improved in timing accuracy at lower SNRs. This implies the improvement of both the detection capabilities of this system and the accuracy of the time measurement process. The type of system that is targeted can be a radar, but also any kind of measurement systems that suffers from strong noise alteration. The system is assumed to collect the signals from a single receiver.

The primary goal of this paper is therefore two-fold. The first is to compare the performance of correlation timing measurements with that of a threshold detector for a

range of received pulse levels relative to noise. The accuracy with which the time delay between two received pulses can be determined will be compared for both systems assuming ideal and distorted pulse shapes.

The second goal is to implement a detection mechanism that ensures the localization of expected pulses, and rejects noise peaks. The combination of these two goals yields a general solution that is studied, implemented, and tested in an experimental comparison. The practical results will help to quantify the improvement in the timing measurement accuracy obtained using correlation instead of a threshold detector in a system which has fast moving distorted pulses.

As mentioned above, the complex case of processing pulses that are distorted will be studied. However, we will restrict the study to Gaussian pulses for the simplicity to calculate their spectrum, and also because the shape of these pulses can approximate any kind of conventional pulses like sinx/x pulses, rectangular pulses with finite bandwidth, and Bessel pulses. The distortion will be taken into account through the consideration of different amplitudes, different pulse widths, and different symmetry or asymmetry characteristics within a pair of received pulses.

The range of frequencies for the pulse will be about 300kHz, corresponding to pulse widths of about 3μs. Noise is assumed to be AWGN, that is an additive white Gaussian noise. Noise bandwidths equal to that given by a matched filter and higher will be studied in order to consider cases where filtering is not – or cannot be – perfect.

1.3 Document overview

This Chapter is a brief introduction to the motivations for the use of accurate detection systems in the case of radar technology, as well as any other method requiring precise time measurements of pulse occurrence.

Chapter 2 presents an overview of the use of correlation in telecommunication systems such as GPS, radar, and CDMA systems, but also in the more general problem of signal Time Delay Of Arrival (TDOA). The fundamental properties of correlation are reviewed in order to understand the wide use of this technique.

Chapter 3 presents the mathematical formulation of the theoretical accuracy of threshold timing measurements. This study is a required first step for an analytical comparison between both correlation and threshold measurements.

Chapter 4 is focused on the derivation of the theoretical accuracy of threshold measurements adapted to correlation. The obtained formula is then tested using simulations in order to corroborate the analytical results.

Chapter 5 is dedicated to the comparison between threshold and correlation timing measurements. The comparison will be based on the mathematical models obtained previously, as well as computer-based simulations for distorted pulses that theoretical developments can’t model.

Chapter 6 describes a combination of detection methods in order to prevent the failure of the timing measurement process due to the presence of high noise levels. The improvements due to the methods M-out-of-N detection and integration, are presented from a practical and mathematical point of view. An experimental comparison between theoretical and practical results is established.

Chapter 7 constitutes a summary of all the developments presented in this paper adapted to the case of a practical system requiring timing measurement improvement. It gathers all the methods: detection, integration, and correlation or threshold in order to design a complete solution for this specific problem. The solution is then implemented and tested with real samples of signals. The results of this simulation are analyzed and compared to the original specification in order to evaluate the validity of the design. A comparison

between threshold and correlation timing measurements is also discussed for the specific case of this problem.

Chapter 8 presents the research conclusion and recommendation for further research.

Appendix A presents the code developed in MATLAB for the practical experiment of Chapter 7.

Chapter 2

2. Background and literature review

The simplest method to measure the time delay between two pulses is the use of a threshold that localize the edge of each received pulse, or both edges in order to identify the center of each peak. This principle is illustrated in Figure 2.1.

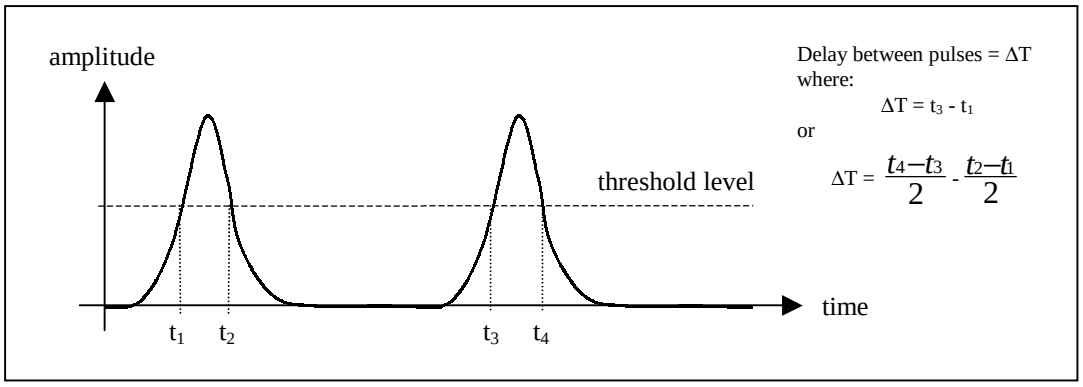

Figure 2-1Time delay measurement with a threshold

Yet, a threshold measurement performed on a Gaussian pulse with a SNR of 6dB can yield ambiguous results due to false alarms or missed detection, as illustrated in Figure 2.2. On the same figure, a signal received with a SNR of 16dB is represented in order to give an idea of the noise distortion as the SNR is increased.

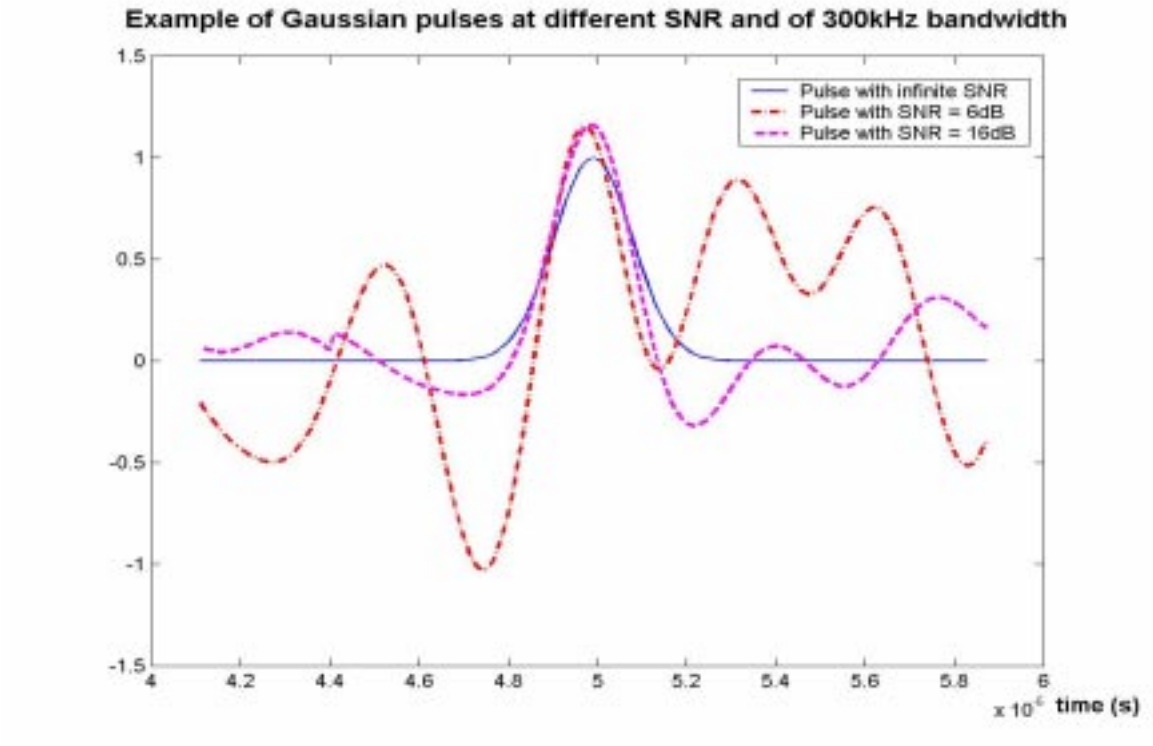

Figure 2-2 Gaussian pulses at different SNRs

Correlation is a time measurement tool that has already been used. One application is the time difference of arrival (TDOA) of signals at two or more spatially separated receivers. Yet, the main work performed in this domain does not imply a detection process since the configuration of the sensors and the properties of the propagation medium directly yield an estimation of the TDOA. Correlation used for TDOA employs random-like signals, and the geometry of the problem implies the use of two detectors. This is different from our problem, yet the issues raised for the TDOA of wideband signals convey an understanding of the motivation for the use of correlation.

Two areas therefore need to be reviewed and analyzed. One concerns detection theory, which is the capability of selecting a desired signal, while the second is related to time measurement tools in order to perform accurate measurements on this signal.

This chapter starts by reviewing the mathematical correlation method. It highlights the main properties that make correlation an interesting tool in time delay measurement.

Section 2.1 is devoted to the important concept of matched filter theory. This part follows the presentation of correlation since it is both a property of this process, and a requirement when looking for signal to noise ratio optimization.
Matched filter theory actually brings out the connection with detection developments. Section 2.2 reviews detection theory, yet this part avoids being too broad in order to rapidly focus on the methods of interest.
Finally, Section 2.3 surveys the statistical approaches used in the TDOA problem. It starts by a quick review of estimation theory applied to the case of a signal embedded in white noise. This section is needed to rapidly understand the main issues of the TDOA problem, and is focused on the literature that is applicable to our study.

2.1 Presentation of the Correlation tool

2.1.1 A Mathematical Approach

The mathematical form of the correlation is the following. Let us consider two functions f and g that depend on a parameter t. If c is the correlation of the two signals, then:

$$c(t) = \int_{-\infty}^{+\infty} f(u).\overline{g(u-t)}dt = f(u) * \overline{g(-u)} \qquad (2.1)$$

where $*$ is the convolution operator, and $\overline{g(t)}$ denotes the complex conjugate of function g.

As seen with this expression, the correlation of two signals supposes that the integral converges. Yet, as mentioned in [Nah69], correlation is linked to the concept of signal spectral density. Thus, the integral converges if the signals are of finite energy, which is always practically the case.

In many cases as in digital signal processing, the signals are discrete functions of time. If $f_n=f(n.\Delta t)$ and $g_n=g(n.\Delta t)$ are considered as two signals where Δt is the quantization time, then the definition of correlation becomes:

$$c_m = \sum_{n=-\infty}^{+\infty} f_n . \overline{g_{n-m}} \tag{2.2}$$

Correlation is a well-known way of finding the time difference between two signals. This directly results from its definition. The correlation of two functions f and g at time τ: $\varphi_{fg}(\tau)$ is equal to the area of the product of f at time t and g at time t-τ. The process is described with Figure (2.3).

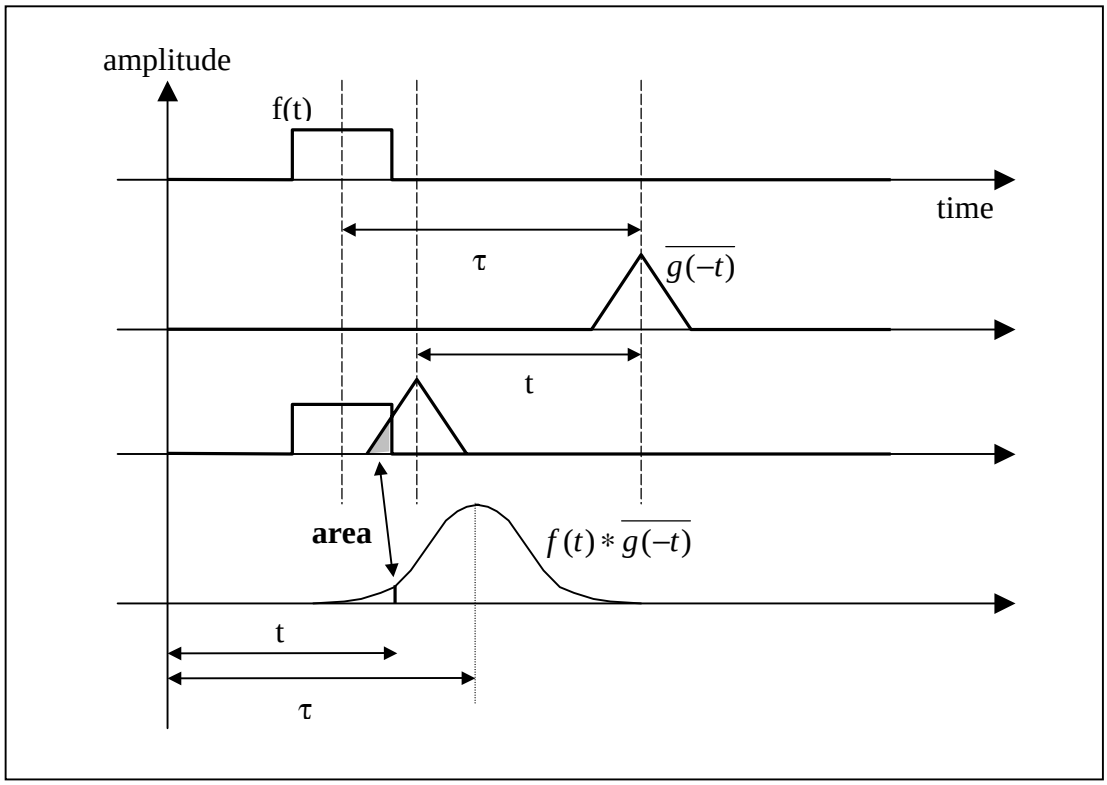

Figure 2-3 Graphical Explanation of the correlation process

Correlation can thus be understood as the following: the bigger the area delimited by the product between f(t) and g(t-τ) over the time domain, the higher the correlation. In other words, the more similar the shape of these two functions, one of which is delayed by τ,

the higher their correlation at time τ. This yields the conclusion that the correlation is a measure of the degree of similarity between f and g as a function of time delay. If two similar signals separated by a time delay τ are correlated, the result is a function whose maximum is reached at time t = τ. This explains why correlation is a tool for time delay measurement.

In the frequency domain, correlation corresponds to the multiplication of the Fourier transforms of the functions that are correlated, as given in equation (2.3).

$$C(f) = F(f).\overline{G(f)} \tag{2.2}$$

Where C(f) is the Fourier transform of the correlation function of equation (2.1), and $\overline{G(f)}$ denotes the complex conjugate of function G.

2.1.2 Correlation for synchronization problems

2.1.2.1 Wide Spectrum Signals and correlation

The property of measuring the degree of similarity between two signals has lots of applications, which justifies the use of correlation in many systems, like GPS, CDMA based systems, and even Radar systems through pulse compression. All of these systems use correlation as both a synchronization and detection technique. The concept is to shape the signal we wished to transmit with a certain modulation pattern that has a large cross-correlation peak and low sidelobes. This can be obtained by modulating the signal with a code. At the receiver, the signal is recovered by mixing the signal with the same code. This process is illustrated in Figure (2.2) in the case of a direct sequence system. It has to be noted that the demodulation process requires a carrier frequency recovery and synchronization of the process that is not illustrated in Figure (2.4).

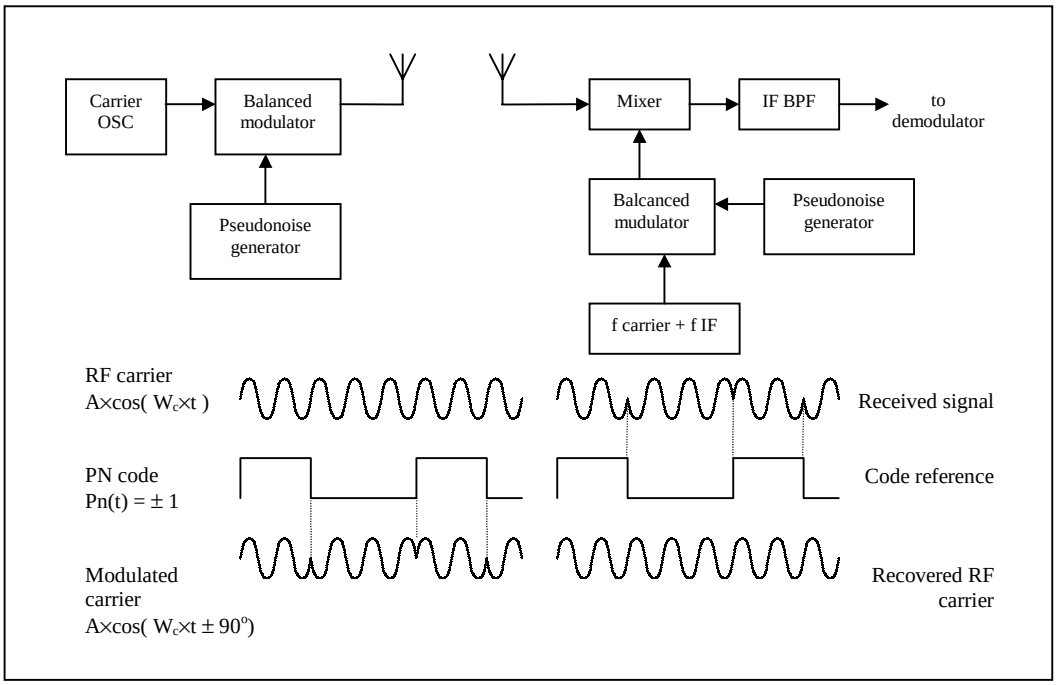

Figure 2-4 Direct sequence modulation and demodulation

Two considerations must be given to the choice of the code. The first point is that this code should be at a frequency higher than that of the signal. The modulation of the original message with this sequence results in a large bandwidth. De-spreading is accomplished in the receiver by correlating the spread spectrum signal with its original modulated code. As reported in [Dix84], the result of this process is that the information signal collapses to its original bandwidth prior to spreading, whereas any unmatched input signal like noise is spread over a bandwidth equal at least to that of the modulation code. Consequently, the SNR of the received signal after correlation is increased by a certain amount called the processing gain. This gain is reported in [Dix84] to be equal to the ratio between the information bandwidth and the actual RF bandwidth used to send this signal. The consequence is that signals with low SNR can still be processed, reducing the need for a high power transmitter, as it is the case in GPS systems.

The second consideration is to have different codes with high auto-correlation (code correlated with itself) and low cross-correlation (code correlated with a different one) in order to distinguish one single signal, and reject all the others. Pseudorandom codes, and more precisely Gold-codes in the case of GPS, fulfill this requirement. These codes are

implemented using feedback shift registers that are driven by the chipping frequency of the code. A particularly clear presentation on this subject is found in [Kap96]. Figure (2.5) illustrates a 4-bit pseudorandom code generator.

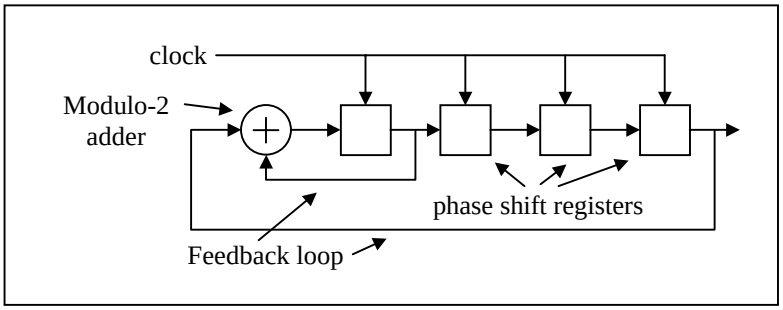

Figure 2-5 4-bit pseudorandom code generator

Consequently, correlating the received signal with different codes yields a high correlation peak when the correct code is used, and this peak therefore ensures the synchronization of the internal clock of the system: CDMA handset, or GPS receiver. This last example is actually a significant example to prove the accuracy of time measurement that can be obtained through correlation.

2.1.2.2 Example of GPS

The GPS approach for providing accurate 3D position consists in finding the distance of the receiver to at least four GPS satellites. The position solution is based on the resolution of a matrix system of equations through an iterative method. The clever idea of GPS is that it also resolves the receiver clock offset, which is a nice way to obtain an accurate knowledge of a standard time scale like the Coordinated Universal Time (UTC). The time difference between GPS time and UTC is guaranteed to be less than 100ns as reported in [Lev99]. Besides, the offset between these two times can also be obtained and is usually known within 25ns accuracy.

As a spread spectrum system, GPS uses pseudorandom codes. Yet, GPS receivers have to distinguish multiple signals coming from different satellites. Since two pseudorandom codes are often similar enough to appear correlated when in fact they are not, a subclass

of pseudorandom codes called Gold codes is used. These sequences are obtained from the addition of two specially chosen pseudorandom codes. The parent codes are generated using 10 bit feedback shift registers, then added together to produce the resultant code with a length of 1023 bits. The coarse acquisition code (C/A), one of the two codes used in GPS, is indeed a Gold code, and is thus 1023 bits long with a bit rate of 1.023 Mbps. The precise code on the other hand is rather more complex. A complete description of both sequences can be found in [Hof97].

The accuracy of GPS time suggests that an efficient synchronization and tracking method is used in its receiver. Detection and tracking of the peak of the correlation between the received message and the original modulation code achieves this. The initial synchronization is performed using a sliding correlator, which is in charge of testing all possible codes and searching for all possible leads and lags between the received signal and each code. Once the GPS receiver has synchronized on a received signal, that means when the correlation peak has been detected, the receiver continues to operate by maintaining synchronization. This function is performed using a delay lock-tracking system. Figure (2.6) presents the concept of this tracking system in block-form.

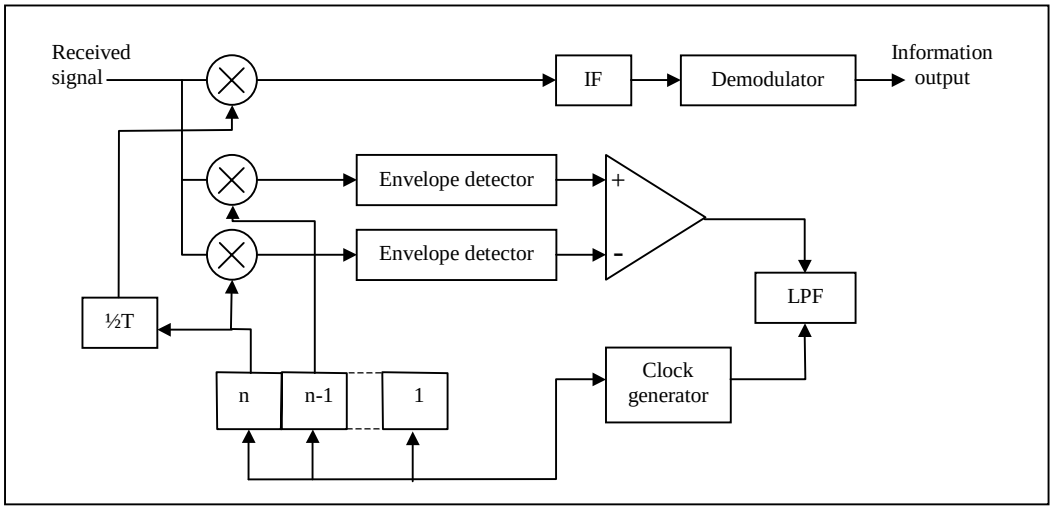

Figure 2-6 Delay-lock loop with half-chip-delayed correlator

The idea is to use two separate correlators driven by two code reference signals delayed by a chip length. One will be used as an early correlator, and the other one as a late

correlator, thus driving the clock to mid-point. The composite correlation function resulting from this configuration is represented on Figure (2.7). Appropriate filtering and the use of a VCO ensures the tracking of this halfway point. This is how a GPS receiver locks onto a desired signal.

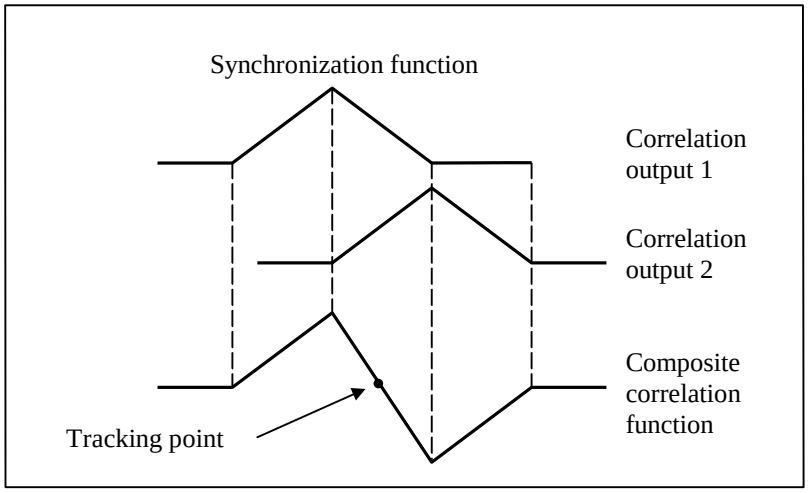

Figure 2-7 Correlation waveforms in delay-lock loop

Considering that the performance of GPS receivers has always exceeded the design requirements reinforces the idea that it is a highly accurate system. During the system testing and deployment period, GPS proved to provide a position solution with an rms error of 2.4m. This error is due mainly to the receiver thermal noise and correlation error. As a result, Selective Availability was adopted by the Department of Defense in order to degrade the accuracy of the GPS solution by dithering the satellite clock and altering the satellite ephemerides of the navigation message. This degradation process was removed from the GPS C/A signal on 05/02/2000. A 2.4m rms error corresponds to a time error of about a hundredth of GPS chip length, which is 10ns. This high accuracy results from the correlation synchronization process, which highlights the accurate time measurement property of the correlation method.

2.1.2.3 Example of Pulse compression radars

In order to complete the discussion on spread spectrum techniques, we need to mention that spread spectrum communication systems have their counterparts in Radar Systems called pulse compression radar. Yet, the use of spread spectrum techniques in radar is not restricted to that of communication systems. The latter needs this technique for diversity, rejection of interference, and sometimes provision for privacy, whereas the former needs it mainly for a range-resolution increase. However, several military radars can share a common bandwidth thanks to pulse compression, and also prevent jamming. Pulse compression combines the benefit of a long pulse, larger radiated energy, with that of a short pulse, increased range resolution. The more energy the radar can send through a pulse, the greater its range, which requires that the pulse be either of large amplitude, or large duration. If the pulse is short, then a high power is needed, but if the pulse is large, the time required to receive a returned pulse generates a proportional ambiguity in the measured distance. This ambiguity is given in equation (2.4) and can be found in any radar textbook such as [Sko80]:

$$\Delta R = \frac{c\tau}{2} \tag{2.4}$$

where ΔR is the range resolution, c is the speed of light, and τ is the pulse width.

Although there are many types of pulse-compression techniques, two have seen wide applications: linear frequency modulation, and phase-coded pulse. The first technique consists in sending a modulated signal with increasing frequency over time, also known as a chirp. Its origin and explanation can be found in [Dic45]. The second technique is directly related to our subject. A long pulse of length T that is sent is composed of N subpulses of length τ, each of them having a phase equal to either zero or pi radians. The matched filter used at the receiver is the correlation of the sent and received sequences. The output of this filter is a spike of width τ, of height N times greater than that of the long pulse, and with time sidelobes of length T apart from the peak. N is also referred to as pulse-compression ratio. This description is illustrated in Figure (2.8).

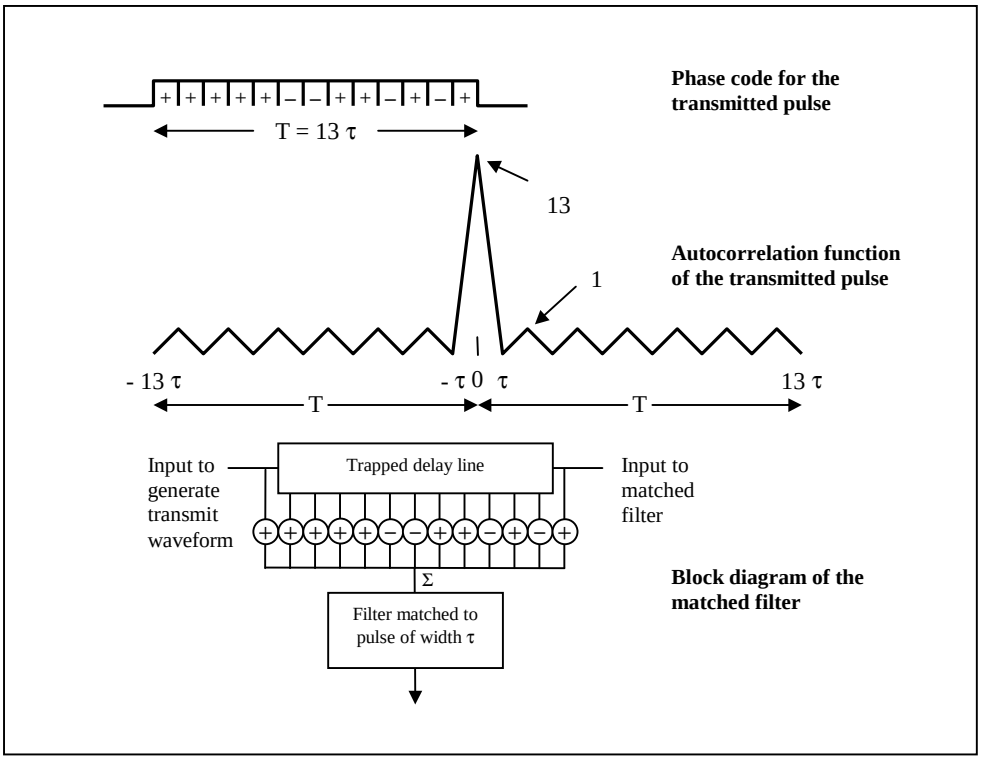

Figure 2-8 Example of a Barker code of length 13 with associated matched filter

The simple codes used to generate the sequence of phase of the subpulses belong to the Barker code. The property of these codes is that after passing through a matched filter, the sidelobes of the output are of equal amplitude. Their level was calculated and found equal to the code length, as presented in [Sko80]:

$$\text{Sidelobe level} = 20 \times \text{Log}_{10} (\text{Code length}) \qquad (2.5)$$

The longest Barker code is of length 23, which is a small code for pulse compression. However, pseudorandom codes are also used, which can yield increased pulse-compression ratio. A description of these sequences can be found in [Sko80].

In any case, the only matched filter used is correlation between the received waveform and the original code. This technique proves particularly interesting to determine accurately time delays between sent and received pulses although strong noise distortion is generated by jamming, for instance.

2.2 Matched filter theory

We have reported in the previous paragraph an interesting property of correlation in the time domain, which resulted in its use as a clever time measurement process. It is also important to review the properties of correlation in the frequency domain in order to understand why correlation is commonly used as a matched filter. The purpose of this part is thus to relate the concept of matched filter theory to cross-correlation detection, and to give some insight into its use in detection theory. This section follows the development of Merrill I. Skolnik in [Sko80].

It is widely known that a radar system detects a target from the echoes of the pulses that it has previously sent. It then extracts information from the received waveform. The capability of the radar to perform accurate detection is limited by noise. This capability thus depends on the signal-to-noise-ratio of the received waveform. The aim of a radar receiver is therefore to maximize this ratio, and the optimal filter for that criterion is called a matched filter. To be more precise, these filters have a frequency-function that maximizes the output peak-to-mean-noise (power) ratio R_f given in equation (2.6):

$$R_f = \frac{|s_0(t)|^2_{max}}{N} \tag{2.6}$$

where s_0 is the output signal of the filter, N is the noise power, and $|f|_{max}$ denotes the maximum of the absolute value of function f.
The above definition implies that the bandwidth of such filters is adapted so that it is neither too wide nor too narrow. The former case results in the introduction of extraneous noise to the signal, the latter results in the reduction of the signal energy. Both cases make the SNR decrease.

[Sko80] reports that the frequency-response function of the linear, time-invariant filter that maximizes the output peak-signal-to-mean-noise (power) ratio for a fixed input signal-to-noise (energy) ratio is given in equation (2.7). This matches Turin's statements

in [Tur60] which says that “the transfer function of a matched filter is the complex conjugate of the signal to which it is matched”.

$$H(f) = \frac{G_a.\overline{S(f)}.\exp(-j2\pi f t_1)}{[N_i(f)]^2} \tag{2.7}$$

S(f) is the Fourier transform of the input signal, while $\overline{S(f)}$ denotes its complex conjugate. G_a is the maximum filter gain, t_1 is a fixed value of time at which the signal is observed to be maximum, and N_i is the power spectrum of the interfering noise;

Two assumptions are made to establish the above result. The matched filter described by equation (2.7) is defined by the transfer function of the receiver at the output of the IF amplifier. The second assumption is that noise is stationary.

Skolnik showed that the maximum value for R_f defined by equation (2.6) and obtained with a matched filter does not depend upon the shape of the input-signal waveform, but is rather given by equation (2.8).

$$\text{Max}(R_f) = \frac{2E}{N_0} \tag{2.8}$$

E is the signal energy of the input signal and N_0 is the noise per hertz of bandwidth.

By taking the inverse Fourier transform of the frequency-response function H(f) provided in equation (2.7), the impulse response is derived and given in equation (2.9).

$$h(t) = G_a \times s(t_1 - t) \tag{2.9}$$

The output of a filter $y_{out}(t)$ is by definition the convolution of the input signal with its impulse response, hence:

$$y_{out}(t) = \int_{-\infty}^{+\infty} y_{in}(u).h(t-u)du \tag{2.10}$$

Considering that the input signal $y_{in}(t)$ of the matched filter is modeled by the noise-free signal s(t) embedded in noise n(t), then equations (2.9) and (2.10) yields:

$$y_{out}(t) = G_a . \int_{-\infty}^{+\infty} (s(u) + n(u)).s(u + t_1 - t)du \qquad (2.11)$$

Therefore, matched filters form the correlation of the received signal corrupted by noise and a replica of the noise-free transmitted signal translated in time. This ensures that the signal-to-noise ratio of the received signal is maximized at the output of the filter.

The above statement is a very important conclusion that is used throughout this thesis, because it proves that correlation can be used as a matched filter. Moreover it is important to note that matched filters that do not directly use correlation can be sometimes difficult to implement. Since correlating two versions of the same signal at high SNR approaches the matched filter specification, then correlation is an attractive solution as a nearly optimum filter.

2.3 Detection process

Detecting a signal has two meanings. The first idea is to find an intended signal that is buried in noise, and the second one is to avoid being fooled by signal-like noise peaks. Since noise implies a stochastic phenomenon, the two above ideas can only be conceived in a probabilistic way. This yields the concept of detection and false alarm probabilities. In other words, declaring that a signal is detected will always be known within a certain confidence defined by the two above quantities. The three following chapters present the definition of detection and false alarm probabilities, followed by the introduction of different detection methods used primarily in radar systems.

2.3.1 Detection and false alarm probabilities

To deal with noise quantitatively, one must assume some characteristics for the noise samples in which signals are buried. Noise is usually modeled by its probability density function, which gives the probability of noise values to be found within a certain amplitude band. This is illustrated in Figure (2.9).

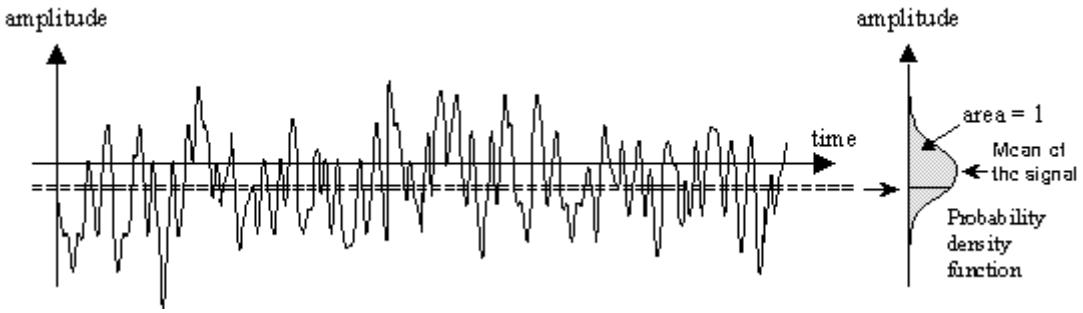

Figure 2-9 Noise distribution

Thanks to this distribution function, the probability that noise crosses a threshold level can be computed by integrating the probability density function over all the amplitude levels above threshold. The obtained value is called the probability of false alarm associated to a certain threshold level.

The probability of detection of a signal is the probability that this signal embedded in noise crosses a certain threshold level. It is therefore obtained by integrating the probability density function of the signal buried in noise from the threshold level considered to infinity, as illustrated in Figure (2.10).

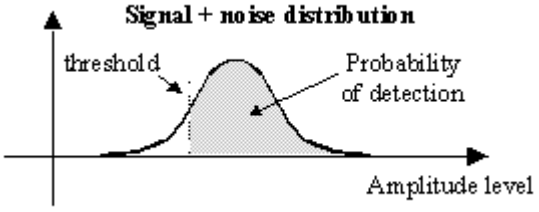

Figure 2-10 Probability of detection definition

These two quantities are important because they will be referred to all along this thesis.

2.3.2 Threshold detection and its derivative

The threshold technique is based on the simple criterion that consists in declaring a detection if the energy of the received signal exceeds a pre-established threshold. Adjusting the threshold level has a direct impact on the detection and probability of false alarm that are targeted. Too low a threshold results in a high probability of detection, but presents the inconvenience of a high probability of false alarm. A relatively large threshold on the other hand will make both the detection and false alarm probabilities decrease.

The Neyman-Pearson observer is an extension of the threshold detection. As reported in [Mid53], it is considered as “a uniformly most powerful and optimal test, no matter what the priori probabilities of signal and noise”. The idea behind this observer is simply to maximize the detection probability of a system for a fixed probability of false alarm.

Another type of detector is reported in [Sko80] and called “likelihood-ratio receiver”. This detection technique is based on the threshold detection of signals at the output of a filter that computes the ratio of the probability-density function of the signal plus noise, to that of the noise alone. The implementation of such a filter is difficult since the distributions involved may change over time. However it is reported to be equivalent to a matched filter, or a cross-correlation function as following the result presented on the matched filter theory.

Finally, another type of detector is based on the statistical approach of inverse probability. The inverse probability consists in finding the most likely cause of an observed event. Practically, a threshold crossing is considered as a detected target if it is more likely - in a probabilistic sense - that the threshold crossing was generated by the expected signal rather than noise. An a-posteriori filter has been derived to perform this detection and is presented in [Sko80]. This filter is practically implementable if the a-

priori probabilities can be specified. An important point to note however is that under the hypothesis that the a-priori probability of the signal plus noise is constant, this filter is equivalent to a cross-correlation receiver or matched filter. If the a-priori probabilities are not known, as it is usually the case, then the likelihood-ratio estimator should be employed. In other words, it is far more reliable and simpler in any case to implement an efficient detector by computing the cross-correlation function between the received signal and the noise-free version of this same signal.

2.3.3 M/N detection

The M-out-of-N detection is a method based on threshold detection. It consists in declaring target detection if a signal is reported to cross, at regular intervals, the same threshold M times out of N investigation periods. This is why the M-out-of-N detection is sometimes referred as double-threshold detector, as in [Wal71]. The probabilities of detection and false alarm can be mathematically derived ([Too82]), and will be presented in Chapter 6 of this thesis. The analytical result proves that if the pulse repetition of the signal is stable during the observation time, the false alarm and detection probabilities can be maintained over a wider range of signal ratio, or that these probabilities could be improved at fixed SNR.

2.3.4 Summary

Several detection methods have been reviewed, and all were based upon comparing the output of a receiver with some threshold level. Some of the presented methods need the a-priori knowledge of the signal and noise distributions in order to be implemented. While this can be applicable to certain problems, it might also prove completely inappropriate when the involved distributions vary in time. Yet, it is important to note that most of these methods were relying on a filter that could be implemented using a cross-correlation function of the received and expected signal. This proves again that

correlation presents not only the capability of performing accurate time measurements, but also essential filtering properties for detection issues.

2.4 The time difference of arrival problem

Finally we conclude our discussion by reviewing a practical problem where correlation is used for time delay measurements and compared to other estimation methods. The estimation of the time difference of arrival of a signal at two spatially separated receivers is a problem of considerable practical interest in disciplines ranging from underwater acoustics (Sonar), geophysics and radio-astronomy (VLBI), and GPS. The practical applications are, for instance, location and tracking in mobile telephony, indication of a transit time, or estimation of speed of waves in a medium. This area has been widely discussed in the literature: [Sle54], [Wei83], and [Wei84], and the best method needed for this estimation opposed several authors. [Wuu84] discusses some of the contradictory ideas that were raised. Consequently, a brief review of estimation theory is necessary in order to understand why correlation is a good estimator in the TDOA case, and to compare it to other methods.

2.4.1 Review of the estimation problem

Estimation is the process of extracting information concerning a parameter vector U from noise-corrupted observations x with a probability density function (PDF) depending on U: p(x, U). An estimator $\mathring{U}$ is a random variable that can be characterized by its bias:

$$b(\mathring{U}) = E\{\mathring{U}\} - U \tag{2.12}$$

and its variance:

$$\mathrm{cov}(\mathring{U}) = E\{ (\mathring{U} - E(\mathring{U})).(\mathring{U} - E(\mathring{U}))^T \} \tag{2.13}$$

where the operator E{x} defines the mean of the variable x.

The smaller the variance, the better the estimate. Therefore, the estimation problem focuses on finding the best estimator for a specific problem. The best estimator is the one whose variance is the lowest as compared to any other estimator for that specific case of study.

The absolute minimum variance that an estimator can reach is the Cramer-Rao Lower Bound (CRLB). The CRLB is an important concept since it is a reference for the study of any estimator. The theory of CRLB defines the cases when there is actually an estimator reaching the CRLB. If no such estimator exists, it does not necessarily mean that there is no estimator with minimum variance. Yet, when none of these estimators can be found, other estimators should still be sought. The alternative consists in other classes of estimators:

- the maximum likelihood estimator;
- the least square estimator;

These methods may not be optimum, yet they provide simple processes that can yield efficient estimators.

The overall approach of finding an estimator is summarized in Figure 2.11, as given in [Bes98]. This figure is given as an illustration of the different options when trying to find an estimator for a specific problem. The content of this diagram will not be discussed since some of the points are not relevant to our problem. However, some of the steps will be followed in the presentation of this chapter. The reader is encouraged to refer to [Nah69] for more details on the subject.

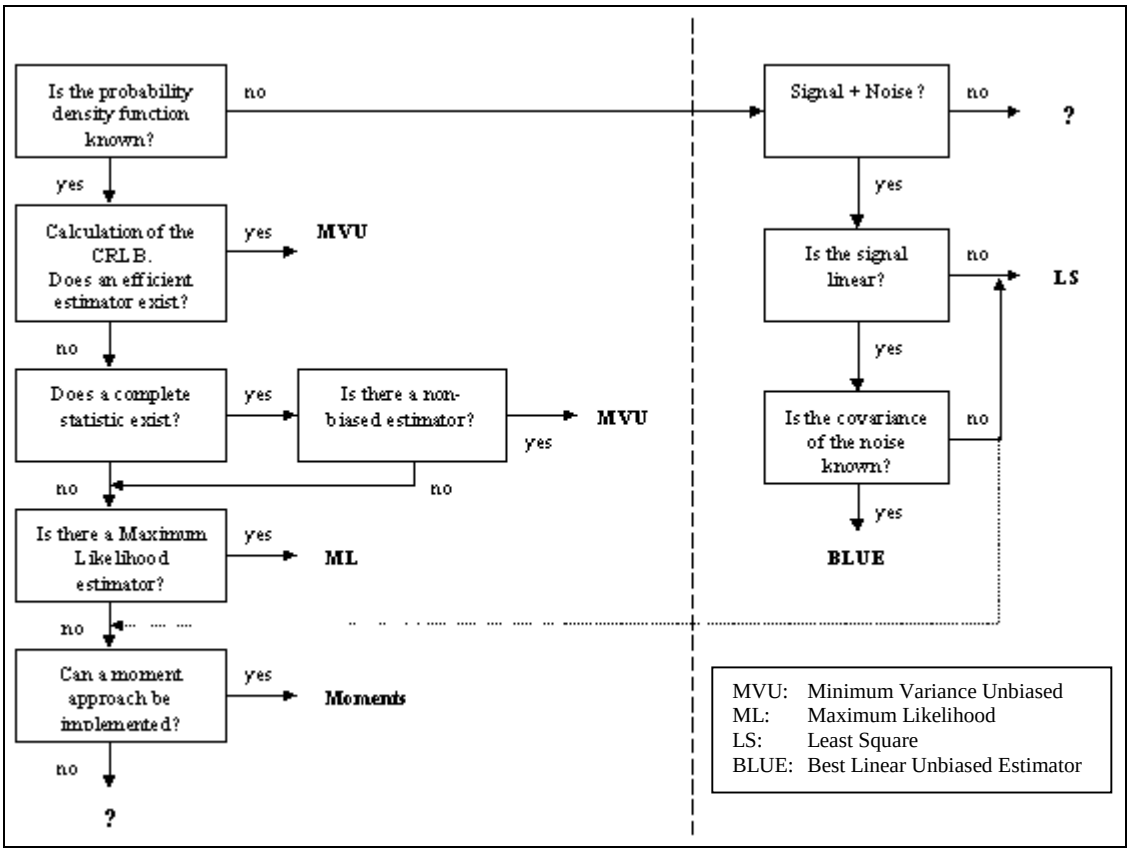

Figure 2-11 Estimation approach

2.4.1.1 Cramer-Rao Lower Bound

An important study to be performed when dealing with estimation problems is to determine the variance of the estimator as mentioned in Figure (2.11). The CRLB is defined as the lower bound on the variance of any estimator for a specific estimation problem. A rather interesting result is that this lower bound can be derived without any knowledge of the estimator itself, except that it is unbiased. The CRLB theorem is therefore presented below.

As given in [Bes98], if the PDF: p(x;U) of an estimator satisfies the regularity condition:

$$E\left(\frac{\partial \ln\left(p(x;U)\right)}{\partial U}\right) = 0 \qquad (2.14)$$

for any unknown parameter U, then the variance matrix of any unbiased estimator $\hat{U}$ satisfies:

$$\mathrm{var}(\hat{U}) \geq \frac{1}{E\left\{\left(\frac{\partial \ln(p(x;U))}{\partial U}\right)^2\right\}} \tag{2.15}$$

This lower bound can be reached for any parameter U if, and only if, there are two functions g and I that satisfy:

$$\frac{\partial \ln(p(x;U))}{\partial U} = I(U) \times (g(x) - U) \tag{2.16}$$

If that proved to be the case, the function g(x) is the Minimum Variance Unbiased (MVU) estimator, and its variance is 1/I(U).

If an unbiased estimator $\hat{U}$ reaches the CRLB for any U, then it is called an efficient estimator. An important point to note is that some estimators, especially the maximum likelihood estimator, can be asymptotically efficient when their expected square estimation error approaches the lower bound as the number of observations tends to infinity.

An application of the CRLB theorem is the case of signals buried in white noise b:

$$x[n] = s[n;U] + b[n] \tag{2.17}$$

where the noise b[n] is Gaussian. The probability density of the measure x is written as:

$$p(x,U) = \frac{1}{\left(2\pi\sigma^2\right)^{N/2}} \times \exp\left(\frac{-1}{2\sigma^2}\sum_{n=1}^{N}\left(x[n] - s[n,U]\right)^2\right) \tag{2.18}$$

where σ is the variance of the white noise, and N is the total number of observations.

As a consequence, the quantities: $\frac{\partial \ln(p(x;U))}{\partial U}$, and $\frac{\partial^2 \ln(p(x;U))}{\partial U^2}$ can be computed:

$$\frac{\partial \ln(p(x;U))}{\partial U} = \frac{1}{\sigma^2}\sum_{n=1}^{N}(x[n]-s[n,U])\frac{\partial s[n;U]}{\partial U} \tag{2.19}$$

$$\frac{\partial^2 \ln(p(x;U))}{\partial U^2} = \frac{1}{\sigma^2}\sum_{n=1}^{N}(x[n]-s[n,U])\frac{\partial^2 s[n;U]}{\partial U^2} - \left(\frac{\partial s[n;U]}{\partial U}\right)^2 \tag{2.20}$$

The expectation of equation (2.20) leads to equation (2.21).

$$\mathrm{E}\left(\frac{\partial^2 \ln(p(x;U))}{\partial U^2}\right) = -\frac{1}{\sigma^2}\sum_{n=1}^{N}\left(\frac{\partial s[n;U]}{\partial U}\right)^2 \tag{2.21}$$

According equations (2.15) and (2.21), the CRLB can be written as:

$$\mathrm{CRLB(U)} = \frac{\sigma^2}{\sum_{n=1}^{N}\left(\frac{\partial s[n;U]}{\partial U}\right)^2} \tag{2.22}$$

Although the lower bound can be calculated thanks to the above formula, this does not necessarily mean that an estimator reaching this bound can be found. The theorem suggests finding two functions g and I that satisfy:

$$\frac{\partial \ln(p(x;U))}{\partial U} = \mathrm{I(U)} \times (\mathrm{g(x)\text{-}U}) = \frac{1}{\sigma^2}\sum_{n=1}^{N}(x[n]-s[n,U])\frac{\partial s[n;U]}{\partial U} \tag{2.23}$$

The above equation cannot be met unless s[n,U] is a linear function of the unknown parameter U. In other words, in the case of a signal embedded in an additive Gaussian noise, there is no efficient estimator, except when s[n,U] is a linear function of U.

In the problem of this thesis however, the signals received are Gaussian pulses as given in equation (2.24).

$$s[n,U] = (A_1 \times \exp[-a \times n^2] + A_2 \times \exp[-a \times (n-U)^2]) \quad (2.24)$$

where A_i is the amplitude of the i^{th} pulse, and 'a' a constant in units of $time^{-2}$. Since there is non linear dependence between s[n,U] and U, no efficient estimator exists.

2.4.1.2 Minimum variance estimation

Although an efficient estimator may not exist, an estimator with minimum variance may still be found provided a sufficient statistic can be found. A statistic T(x) is sufficient for the unknown parameter U if, and only if, the probability: $p(x \mid T(x) = T_0 ; U)$ does not depend on U. The difficulty is then to find a sufficient statistic. The Neyman-Fisher theorem provides a way to find this statistic, and is given as follow:

If PDF p(x;U) of the observations x can be factored as:

$$p(x;U) = g(T(x),U) \times h(x) \quad (2.25)$$

then T(x) is a sufficient statistic for U. On the other hand, if T(x) is a sufficient statistic for the unknown parameter U, then the density function of the measurements x can be written as in equation (2.25).

Another definition is needed to find the minimum variance estimator. A statistic is said to be complete if the condition:

$$E\{f(T)\} = 0 \quad \text{for any U} \quad (2.26)$$

implies that f(T) = 0 with a probability equal to 1. In the above expression, T is the sufficient statistic identified previously, and E{.} is the mean.

The last theorem needed to find the MVU estimator is the Rao-Blackwell-Lehman-Scheffe theorem that states that: if $\tilde{U}$ is a non-biased estimator of U and T(x) is a sufficient statistic for U, then $\mathring{U} = E\{ \tilde{U} \mid T(x) \}$ is a non-biased estimator of U, and its variance is inferior to $\tilde{U}$ for any U. Besides, if the statistic T is complete, then $\mathring{U}$ is the minimum variance estimator.

As a consequence, two approaches can be used to calculate the MVU estimator. We can either calculate $E\{ \tilde{U} \mid T(x) \}$ where $\tilde{U}$ is any non-biased estimator of U, or try to find the unique function G that makes g(T(x)) an unbiased estimator of U.

The application of the above theorem to the case of signals buried in white noise is presented below. If the observations of a signal can be written as in equation (2.17), then the probability density of the observations is given by equation (2.18), which is rewritten in equation (2.27).

$$p(x,U) = \frac{1}{\left(2\pi\sigma^2\right)^{N/2}} \exp\left(\frac{-1}{2\sigma^2} \sum_{n=1}^{N} \left(x[n]\right)^2 \right) \times \ldots$$

$$\ldots \exp\left(\frac{1}{2\sigma^2} \sum_{n=1}^{N} \left(2x[n] \times s[n,U] - s[n,U]^2\right) \right) \quad (2.27)$$

The PDF p(x,U) as written in equation (2.27) is factored as in equation (2.25) with:

$$h(x) = \frac{1}{\left(2\pi\sigma^2\right)^{N/2}} \exp\left(\frac{-1}{2\sigma^2} \sum_{n=1}^{N} \left(x[n]\right)^2 \right) \quad (2.28)$$

$$T(x) = \frac{1}{2\sigma^2} \sum_{n=1}^{N} \left(2x[n] \times s[n,U]\right) \quad (2.29)$$

As a result, T(x) is a sufficient statistic for U. Yet since E(x[n]) = s[n;U], then it might be difficult to find a function f so that $E\{ f(T(x)) \} = U$ as in equation (2.26). Therefore, the minimum variance estimator is hard to find for the case of signal buried in Gaussian

noise, and may not exist. The literature review performed did not reveal any minimum variance estimator for this case of study. An alternative has thus to be found.

2.4.1.3 Maximum likelihood estimator

The idea behind the maximum likelihood estimator is simple. It consists in finding the parameter U that maximizes the probability density function p(x,U) with x fixed and equal to the observed data. It is proven in [Bes98] that if an estimator is efficient, then the maximum likelihood generates it.

A well-known theorem provided in [Wei83] asserts that the maximum likelihood estimator is asymptotically unbiased, and that its error variance approaches the CRLB arbitrarily closely for sufficiently long observation times.

In our case of study, that is when a signal is buried in Gaussian noise, the maximum likelihood estimator is obtained by equation (2.30).

$$\underset{U}{Max}\{\ \ln(\ p(x;U)\ )\ \} = \underset{U}{Min}\{\ \frac{1}{\sigma^2}\sum_{n=1}^{N}\left(x[n]-s[n,U]\right)^2\ \} \qquad (2.30)$$

In that case, the maximum likelihood estimator is asymptotically efficient, that is efficient for N tending toward infinity.

It has to be noted that according to equation (2.30), the maximum likelihood estimator corresponds to the least-square estimator in the non-linear case. The properties of this estimator are thus reviewed in the following section.

2.4.1.4 The non-linear least-square estimator

The least-square estimator consists in minimizing the equation:

$$J(U) = (x - s(U))^T \cdot (x - s(U)) \tag{2.31}$$

Two approaches can be used to solve this problem. The first one consists in finding a transformation that converts the problem into a linear one, for which a general solution has already been developed. A second method is to use an iterative approach to solve equation (2.31), as given by the Newton-Raphson method:

$$\theta_{k+1} = \theta_k - \left\{ \left[\frac{\partial^2 J}{\partial U \partial U^T} \right]^{-1} \times \frac{\partial J}{\partial U} \right\}_{U=U_k} \tag{2.32}$$

This method implies complex calculations.

2.4.1.5 Summary of the estimation approach

The above methods were studied in order to understand the issues in the literature associated with the TDOA measurement technique. However, it was shown that the best estimators might not always exist. Besides, even if a specific method can be implemented, a tradeoff between performance and computational complexity must be made in most cases. Finally, estimation theory relies on the hypothesis that a statistical law can model the measures, like the case of white noise. While this tends to simplify the calculation, it can sometimes yield an error in the model, so that the estimator that was calculated does not offer the expected performance in practical experiments. Therefore, we can already mention that a method like correlation that does not rely on the knowledge of signal distribution might be more robust.

2.4.2 The Time Delay Of Arrival problem

The problem of estimation of the TDOA is a recurrent issue in the literature, especially in the area of acoustic signal processing. Correlation has been mainly discussed in that literature too. Yet, as mentioned earlier, the practical cases studied were always the detection of wideband signals recorded at two spatially separated receivers. The signal is

always modeled as white noise, with the same bandwidth as the noise. An exception can be found in [Kum93] where the signals have a Gaussian autocorrelation function.
The purpose of the following chapters is to summarize the work that has been done in that field, while presenting the inherent differences that have to be considered in our case of study.

2.4.2.1 Summary of the results in the TDOA problem

The delay estimation between signals radiated from a common source and received at two spatially separated sensors is the subject of most of the literature dealing with the TDOA issue. Three common methods are usually used and compared: phase data, cross-correlation, and parameter estimation techniques. The last two approaches are usually compared since they seem to provide the best results. [Wuu84] refutes the claim that the parameter estimation method is superior to correlation for a simple delay problem with short data-lengths. He shows through extensive use of simulations that cross-correlation outperforms the parameter estimation method, especially at low SNR. He also reports that the estimation method requires far more computation, and can suffer from mis-estimation of the statistic of the signal and/or noise with a finite data set. Indeed, the use of parameter estimation is only suggested for the special case of difference in channel dynamics and sensor responses.

The superiority of one method as compared to another is contestable, and depends only on certain characteristics of the medium and channel dynamic of the receivers, which is irrelevant in our case of study since a single receiver is used. As a result, this discussion is avoided, and we now concentrate our study on the cross-correlation method discussed in the literature. It is well established ([Han75]) that the cross-correlator, with proper filtering, is the maximum likelihood estimator for time delay. Maximum likelihood estimators, however, only reach the CRLB for non-linear estimation problems, which is when estimation errors are small. Therefore, several papers treat the complex problem of estimating the SNR for which the variance of the time delay estimate begins to depart significantly from that given by the CRLB: [Ian83] and [Wei83]. It is shown using

simulations that a sudden increase in the variance of the delay estimation occurs at a certain SNR. Four regions of SNR are actually identified in [Wei83]. This is illustrated in Figure (2.12). What is reported as the Ziv-Zakai Lower Bound in [Ian83] and [Wei83] is the calculation of a lower bound that takes into account the ambiguity problem associated with the occurrence of large cross-correlation peaks, different than the one associated with real time delay.

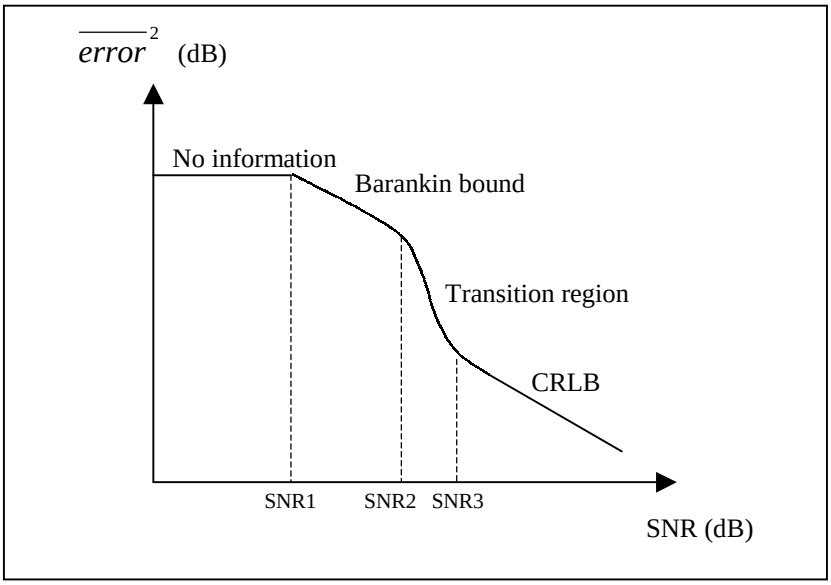

Figure 2-12 Mean square error behavior versus SNR

For SNR below SNR_1, observations are dominated by noise, which results in a mean square error (MSE) bounded by the a priori knowledge of the delay estimation. For SNR above SNR_3, the MSE is given by the CRLB. Finally, the region [SNR_1-SNR_2] corresponds to a region dominated by ambiguities, while [SNR_2-SNR_3] is the transition regime between the ambiguity-dominated and ambiguity-free regions. The analytical boundaries of the different SNRs identified above are given in [Wei83], and result in simple conclusions: the increase of SNR, the up-shifting of the signal in the frequency domain, and the increase of the observation interval all result in the decrease of the minimum MSE as given by the CRLB. These conclusions are also confirmed in [Ken84]. A similar discussion is reported in [Ian83], where experimental results show that cross-correlation simulations results are indeed close to the ZZLB. Consequently, it reinforces the idea that cross-correlation is nearly an optimal instrumentation in the MSE sense.

Another pertinent factor is that the un-gated mode of operation, which corresponds to avoiding the track of the true delay through a time window, results in a MSE that is higher than the gated mode of operation for any SNR. Consequently, the idea of precisely detecting the signal is important, not only to maintain a reasonable error at SNR lower than SNR_1, but also for the other SNR regions.

Finally, an important point mentioned in the discussion of the TDOA problem: [Kna76], [Wuu84] is that cross-correlation is sometimes improved by pre-filtering the signals. These methods are justified by the configuration of the problem that assumes that the noise-free signals received at each detector differ only by a multiplicative constant. [Kna76] compares different weighting functions reported in the literature: [Eck52], [Car73], [Han73], and [Rot71], and proves that one of them is the Maximum Likelihood estimation. Yet, two main comments can be given considering his ideas. The first one is that using a weighting function may require a parameter estimation depending on the a-priori knowledge that we have of the problem. The second thing is that the prefilters may need to be modified in time as the properties of the medium, or the signals, change.

2.4.2.2 Differences between the TDOA problem and our case of study

The literature review performed on the time delay measurements is bounded in its application to the TDOA problem. Noise and signals are most of the time modeled as white processes, or uncorrelated Gaussian random processes. Besides, the practical application of this theory implies that the signal samples be collected at two spatially separated receivers, which introduces the complex case of two non-perfectly similar filter responses. Then, the peak of the correlation process is directly used as the time delay estimator, since this peak is not wide enough to be estimated using a threshold method. Finally, no detection process is performed since an estimation of the TDOA is easily predicted thanks to the knowledge of the configuration of the receiver and the average speed of the signal in the medium.

The above hypotheses all differ from the case that we propose to study: Gaussian like pulses buried in Gaussian bandlimited noise and received at one single detector. However, this does not mean that the discussion was irrelevant. On the contrary, it addressed some important issues, and gave some intuitive insights about the problems that may arise with time delay measurements through correlation.

2.5 Summary on the dual problem of detection and accurate measurement

The literature review presented above shown that finding an estimator implies an optimization of a certain cost function. The common optimum performance criteria are:

- the maximum signal to noise ratio;
- the minimum mean-square-error;
- the minimum variance;
- the least-square.

It has been showed that optimizing the detection capabilities of a system implies maximizing the SNR of the received signal. Moreover, it is important to remember that the goal of this thesis involves the improvement of the accuracy of time delay measurements. Therefore, the objectives of our case of study naturally lead to correlation. Correlation is a matched filter but also corresponds to a maximum-likelihood estimator. Under certain circumstances, correlation approaches the CRLB, which suggests that it has good variance properties. As a result, correlation is a powerful and simple estimator. We will therefore avoid the discussion of finding a better estimator, which might result anyway in an increase of the computational complexity, as is usually the trade-off in estimation theory. On the other hand, we will compare correlation to the threshold process presented in Section 2.2 since this method is widely used in radar techniques due to its simplicity, and also because it allows a direct time localization of a pulse.

2.6 Conclusion

The literature review performed here leads us to understand why correlation is a useful solution for both the case of accurate time measurements and optimum detection process. This idea is confirmed by the wide use of correlation in the TDOA problem, in synchronization problems as in GPS receivers, and by its use as an important filter for detection. Yet, as mentioned previously, the literature discussion on the TDOA problem has only considered the case of noise-like random signals observed at two spatially separated receivers. This case of study is different from our subject, which consists in identifying the delays of several different pulses received at one detector. Besides, most of the literature discusses the problem of the time delay of wideband signals, and the problem of Gaussian pulses embedded in noise has therefore been neglected. The use of correlation for time measurements of Gaussian pulses buried in noise is therefore analyzed in the following chapters.

Chapter 3

3. Accuracy of Threshold Measurements

The theoretical accuracy of time measurements using threshold is a necessary study in this paper. The purpose is to determine theoretically the time delay between two received pulses. If reliable analytical results for threshold accuracy are obtained, then these results will be derived for the case of correlation accuracy. This analysis could result in the comparison of both methods from an analytical point of view, avoiding complex simulations and being able to directly gauge the influence of any parameter on the accuracy of each method.

Section 3.1 restates the case of signals that this thesis is covering, and introduces parameter notations. The mathematical results gathered in [Sko80] on the theoretical accuracy of radar measurements are presented in Section 3.2. They give a general limit on threshold accuracy that can be expected in an average sense. Yet a comparison between theoretical and experimental results will be performed in Section 3.3 in order to determine if these results do match, and to what extent.

A point has to be mentioned however. Time delay between two pulses is the focus of this thesis, but computing this quantity requires the time location of each pulse independently. This will not be the case with correlation that requires only one measurement for time delay estimation between two pulses.

3.1 Signal studied and notations

The mathematical developments that are performed throughout this thesis concern Gaussian pulses. A Gaussian pulse p(t) can be modeled by two parameters: its amplitude and time constant, as given by equation (3.1).

$$p(t) = A \times e^{-\left(\frac{t}{\tau}\right)^2} \tag{3.1}$$

A is the amplitude of the pulse, and τ is the time constant of the pulse.
However, another parameter will be used for the simplicity of the equations that will be derived later.

$$p(t) = A \times \exp(-at^2) \tag{3.2}$$

The dimension of the constant 'a' is the inverse of a time squared, and is related to the time constant τ_G of the Gaussian pulse by equation (3.3). A typical number for 'a' is 650×10^9 s^{-2} for pulses of approximately 3µs

$$a = \frac{1}{\tau_G^{\,2}} \tag{3.3}$$

Finally, two other quantities describing Gaussian pulses have to be introduced: the half-power bandwidth B_G and half-power pulse width τ_G of the pulse. These two parameters are linked to the constant 'a' by equations (3.4) and (3.5), and related to each other using equation (3.6).

$$a = \frac{4 \times \ln(\sqrt{2})}{\tau_G^{\,2}} \cong \frac{1.39}{\tau_G^{\,2}} \tag{3.4}$$

$$a = \frac{(\pi B_G)^2}{4 \times \ln(\sqrt{2})} \cong 7.12 \times B_G^{\,2} \tag{3.5}$$

$$B_G \times \tau_G \cong 0.44 \tag{3.6}$$

As mentioned in the introduction of this thesis, Gaussian pulses are studied for two reasons. The first is the simplicity of jumping from the time domain to the frequency domain, and vice versa. The second reason is that it will be shown that the slope of the pulse where the timing measurement is performed is an important parameter affecting the accuracy of the measurement. Most of the pulses used for time measurements, which are bandlimited rectangular pulses, bandlimited trapezoidal pulses, or sinc pulses, present slopes that can be approximated to a certain extent by exponential slopes. Hence, the Gaussian form is a logical choice for the comparison.

3.2 Theoretical accuracy

Skolnik has reported in [Sko80] the theoretical accuracy of radar time measurements of received pulses by two different methods. The first method is called the leading edge measurements, and the second is the gating signal and matched filter measurement. Both methods provide the same result for the case of rectangular pulses, but the second method was derived for Gaussian pulses. In the mathematical developments of Skolnik, noise is assumed to be an additive white Gaussian noise (AWGN), and the measurements are performed in the video detector part of the radar.

The gating method yields a general expression for the root-mean-square value (RMS) of the error: δT_R as given in equation (3.7).

$$\delta T_R = \frac{1}{\beta\sqrt{\frac{2E}{N_o}}} \tag{3.7}$$

E is the signal energy, N_0 is the noise power per unit bandwidth, and β is called the effective bandwidth. The effective bandwidth, as used in [Gab46] and [Woo53], is defined by Skolnik as the normalized second moment order of the signal spectrum about the mean. Mathematically, this quantity is defined by equation (3.8):

$$\beta^2 = \frac{\int_{-\infty}^{+\infty} (2\pi f)^2 |S(f)|^2 df}{\int_{-\infty}^{+\infty} |S(f)|^2 df} \tag{3.8}$$

where S(f) is the Fourier transform of the input signal of the matched filter.
The effective bandwidth is more a mathematical tool than a physical quantity. It cannot be simply related to either the half-power bandwidth or the noise bandwidth as reported in [Sko80]. However, the expression for the effective bandwidth can be simplified in the case of Gaussian pulses described by equation (3.2). The values of the numerator and denominator of equation (3.8) are provided in equations (3.9) and (3.10).

$$\int_{-\infty}^{+\infty} (2\pi f)^2 |S(f)|^2 df = A^2 \times \sqrt{\frac{\pi a}{2}} \tag{3.9}$$

$$\int_{-\infty}^{+\infty} |S(f)|^2 df = A^2 \times \sqrt{\frac{\pi}{2a}} \tag{3.10}$$

Hence, using equation (3.8), (3.9), and (3.10), the effective bandwidth in the case of Gaussian pulses is given in equation (3.10).

$$\beta^2 = a \tag{3.11}$$

where ‘a’ is given in equation (3.2).

Injecting this result in equation (3.6) yields the following formula for the rms time measurement error using threshold:

$$\delta T_R = \frac{1}{\sqrt{a \times \frac{2E}{N_o}}} \tag{3.12}$$

As seen with equation (3.12), the higher the signal to noise ratio, the less the distortion of the pulse, and thus the more accurate the measurement. Moreover, the steeper the slope

of the pulse, the larger the parameter a, and therefore the more accurate the time measurement. This can be interpreted by the fact that a noise peak occurring at the trailing or leading edge of the pulse will yield less distortion, and therefore has smaller negative impact on the measurement, if the pulse has a fast decay rather than a long decay time.

Yet, as mentioned in introduction, the focus of the study is the time delay between two pulses. Since equation (3.12) only applies to the rms error of the time position of one pulse, this equation has to be adapted. Let us called T_1 and T_2 the two random variables describing the error in the time position of each pulse given by a threshold measurement. The rms value of these two variables is given by equation (3.12). Let us assume that over the time of the observations, the average distance between the pulses does not vary, and the mean of T_1 and T_2 is null. Then, the random variable T_D associated with the error in time delay between the two pulses is given in equation (3.13), and its mean square value is derived and provided in equation (3.14).

$$T_D = T_2 - T_1 \tag{3.13}$$

$$\overline{T_D^2} = \overline{T_2^2} + \overline{T_1^2} - 2\overline{T_1 T_2} \tag{3.14}$$

$\bar{x}$ denotes the mean of the random variable x. Assuming independence between the noise samples that corrupt the time measurement associated with each pulse, then the average of the product of the two variables T_1 and T_2 is null. Equation (3.14) therefore leads to equation (3.15).

$$\overline{T_D^2} = \overline{T_2^2} + \overline{T_1^2} = 2 \times \delta T_R^2 \tag{3.15}$$

δT_R corresponds to the rms error of a single time location using threshold, as given by equation (3.12). As a result, the rms error of the time delay measurement associated with two similar Gaussian pulses and performed with threshold detection is given by equation (3.16).

$$\sqrt{\overline{T_D^2}} = \frac{1}{\sqrt{a \times \frac{E}{N_o}}} \tag{3.16}$$

Equations (3.12) and (3.16) are simple formulas, yet it is practically difficult to measure or express the signal-to-noise ratio (SNR) of a signal as the input signal energy divided by the noise power per cycle of bandwidth. This definition will be referred to as definition 1. It would be easier to use another definition for SNR that is the output signal voltage squared divided by the mean noise power. This definition will be referred as definition 2. Skolnik states in [Sko80] that the peak signal-to-noise ratio from a non-matched filter, which is given by definition 2, is equal to the signal-to-noise ratio from a matched filter given by definition 1, minus a loss ρ_f.

Equations (3.12) and (3.16) can be derived using matched filter theory, that is assuming a perfect Gaussian filter is used. The bandwidth of this filter is equal to the bandwidth of the Gaussian pulse studied, which practically means that the bandwidth of the filter can be linked to the pulse width using equation (3.6). In the matched filter case, the loss ρ_f is zero as reported in [Sko80]. As a result, the SNR given by definitions 1 and 2 are related by equation (3.17) in a Gaussian matched filter case.

$$\frac{2E}{N_o} = \frac{A^2}{N} \tag{3.17}$$

E is the received signal energy, N_o is the noise power per unit bandwidth, N is the noise power, and A is the maximum amplitude of the input signal.

In the case of a rectangular filter, Skolnik reports that the optimum bandwidth B_R for which the SNR of the received signal is maximized is 0.72 times the inverse half power width of the Gaussian pulse tested, or 1.64 times the half-power bandwidth of the Gaussian pulse, B_G, relying on equation (3.6). This result is provided in equation (3.19). He states that the loss is 0.49 dB, or mathematically:

$$\frac{2E}{N_o} = 0.9 \times \frac{\left|s_0(t)\right|^2_{\max}}{N} = 0.9 \times \frac{A^2}{N} \tag{3.18}$$

$$B_R = 1.64 \times B_G \tag{3.19}$$

The conclusion of this discussion is that the SNR in simulations can easily be fixed using the relative voltage levels of the signal and noise, and by comparing the results to equation (3.12) and (3.16) using equation (3.17) or (3.18).

3.3 Comparison between theory and practice

Since the theoretical accuracy of a threshold time measurement will be derived for the case of a correlation measurement, equation (3.12) or (3.16) needs to be validated practically. Yet one threshold measurement is needed to compute the time delay between two correlated pulses, therefore only the experiment concerning the validation of equation (3.12) will be presented although both equations (3.12) and (3.16) were indeed verified.

The parameters that are tested in the simulation are introduced in Section 3.3.1. Section 3.3.2 describes the experiment itself, and Section 3.3.3 presents the results and conclusions of the experiment.

3.3.1 Parameters involved in the experiment

According to equation (3.12), the parameters influencing the rms error of time delay measurements using threshold are:

- the constant ‘a’, related to a Gaussian pulse by equation (3.2);
- the signal to noise ratio as given in equation (3.17) or (3.18) depending on the type of filter used;
- the type of filter that is used: Gaussian or rectangular;

The set of simulations performed involve the test of each of the above parameters.

3.3.2 Description of the experiment

Practically, the simulation consists in generating a Gaussian pulse with a certain time constant, and adding Gaussian noise to it. Noise is obtained from a matrix that is computed by summing a thousand random points contained between –0.5 and 0.5V for each value of the sample. This generates a Gaussian distribution according to the Central Limit Theorem. This matrix of noise is then filtered by convolution in the time domain with a sinx/x function for optimum rectangular filtering, or with the noise-free Gaussian pulse for Gaussian matched filtering. This is justified by considering that filtering in the frequency domain is equivalent and much simpler to perform in the time domain using convolution, as reported in [Cou01].

The rms value of the noise is then adjusted to accommodate different SNRs. Finally, the pulse and noise are added together, and a threshold measurement is performed. The time occurrences of the two threshold crossings at both edges of the pulse are recorded, and their mean gives the time center of the pulse. The simulation is repeated 500 times for each SNR point, and the rms value of the error of the time measurements is calculated over all these repetitions. Several filter bandwidths are accommodated: 300, 600 and 900kHz. The experiment is conducted for different constants ‘a’ given in equation (3.2).

It has to be noted that to tackle the problem of false alarms at low SNR, the measurement was performed in a window of time corresponding to the expected occurrence of the signal. The maximum error will therefore be bounded by the time window size.

3.3.3 Results of the experiment

The results of the simulation described in Section 3.3.2 are presented in Section 3.3.3.1 for the Gaussian filter case, and in Section 3.3.3.2 for the rectangular case. Finally, Section 3.3.3.3 discusses the results.

3.3.3.1 Use of a Gaussian filter

Figure 3.1 presents the results of the simulation for a Gaussian pulse with a constant 'a' equal to 650×10^{9} s^{-2}, leading to half-power bandwidth of 300kHz as given in equation (3.5). The curve called "Skolnik" is the theoretical error as given by equation (3.12).

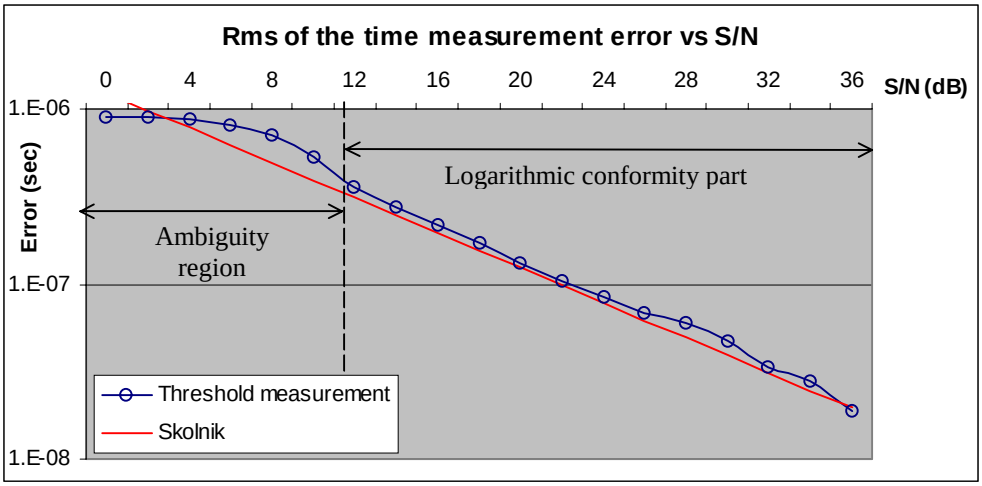

Figure 3-1 RMS error of time measurements using threshold versus SNR with a 300kHz half power Gaussian filter

This graph clearly shows a good match between the practical rms time error using threshold and the theoretical result predicted by equation (3.12) at high SNR. This match part is referred to as the logarithmic conformity part. At low SNR however, the difference between the experimental curve and equation (3.12) becomes quite appreciable. This part is referred to as the ambiguity region. The shape of the result in each region is explained in Section 3.3.3.3.

3.3.3.2 Use of a rectangular filter

Figure 3.2 presents the results of the simulation for a Gaussian pulse with a constant 'a' equal to 240×10^{9} s^{-2}, leading to an optimum rectangular filter which bandwidth is set at 300kHz according to equations (3.5) and (3.19). The curve called "Skolnik" is the theoretical error as given by equation (3.12).

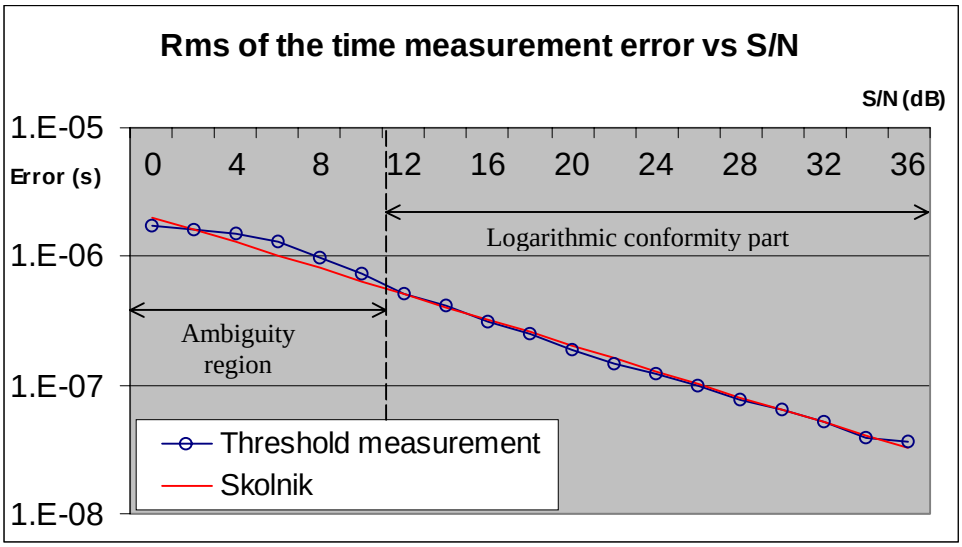

Figure 3-2 RMS error of time measurements using threshold versus SNR with a 300kHz rectangular filter

This graph also shows a good match between the practical rms time error using threshold and the theoretical result predicted by equation (3.12) at high SNR. This match part is referred to as the logarithmic conformity part. In the ambiguity region however, the difference between the experimental curve and equation (3.12) becomes quite appreciable.

3.3.3.3 Analysis and discussion

In both filter cases, the results of the simulations demonstrate that the rms error of the time measurement is correctly estimated by equation (3.12). Yet, remarks concerning the shape of the curves obtained at low SNR need to be made.

In both filter cases and at SNRs below 12dB, the accuracy of the measurement is quite different from the theoretical result. Two parts can be distinguished, an increase of the slope for the SNRs between 7 and 12dB, followed by a decrease at SNR below 7dB. This difference can be explained by the limitations in Skolnik's development due to the non-consideration of false alarms. Since noise bandwidth is fixed by the bandwidth of the filter matched to the Gaussian pulses, noise peaks are similar in shape to these expected

pulses. At low SNR, noise peaks are also more and more similar to signal pulses in amplitude, leading to an increasing difficulty to distinguish noise and signal peaks. This yields ambiguities within the time window in which the signal is processed, leading to an increase of the rms error measured as compared to the theoretical result.
The flat part of the error curve at SNR below 7dB seems to contradict what was said above. It is actually a direct consequence of the method used to avoid false alarms, that is windowing the expected pulse, and trying to perform timing measurement over that window. The error in timing measurement is limited in its extent to a fixed value set by the length of the time window. This behavior results in a curve that flattens at SNR close to 0dB.

The shapes of the curves obtained in Figure (3.1), and (3.2) are actually very similar to the results of the ambiguities noticed in the TDOA estimation problem mentioned in the literature review of this thesis. As reported [Wei83], time delay measurements using estimation methods can depart significantly from the lowest rms error given by the Cramer Rao Lower Bound (CRLB). Using extensive simulations, this paper shows that a sudden increase in the rms value of the delay estimation occurs below a certain SNR. Four regions of SNR are actually identified in [Wei83] as illustrated in Figure (3.3).

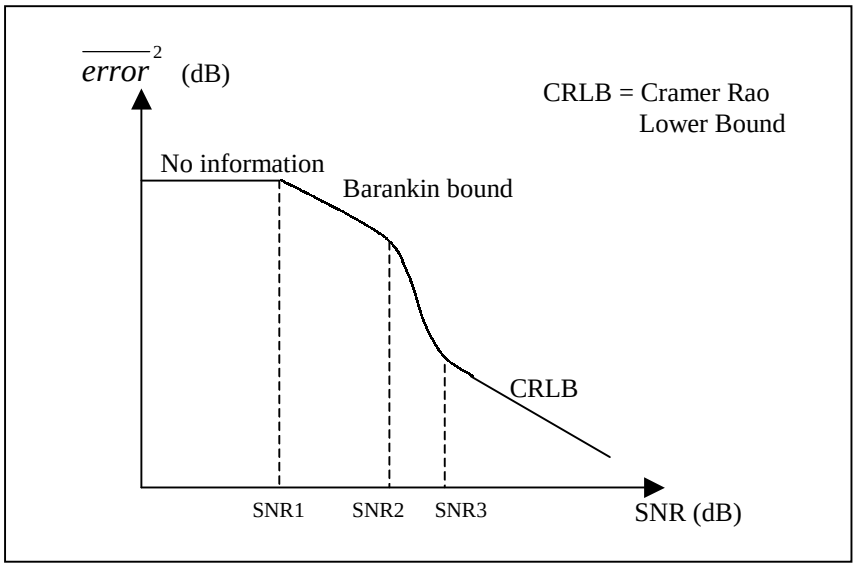

Figure 3-3 Observed mean square measurement errors versus SNR for estimation methods in the TDOA problem

For SNR below SNR_1, observations are dominated by noise, which results in a mean square error (MSE) bounded by the a priori knowledge of the delay estimation. For SNR above SNR_3, the MSE is given by the CRLB. Finally, the region [SNR_1-SNR_2] corresponds to a region dominated by ambiguities, while [SNR_2-SNR_3] is the transition regime between the ambiguity-dominated and ambiguity-free regions.

The comparison between the errors obtained in the TDOA approach using estimation techniques and our results therefore shows similar behaviors. Below a certain SNR, ambiguities due to the increasing similarity between noise peaks and signal pulses in shape and amplitude yield difficulties in performing a time measurement on the expected pulses. This problem is illustrated in Figure (3.4).

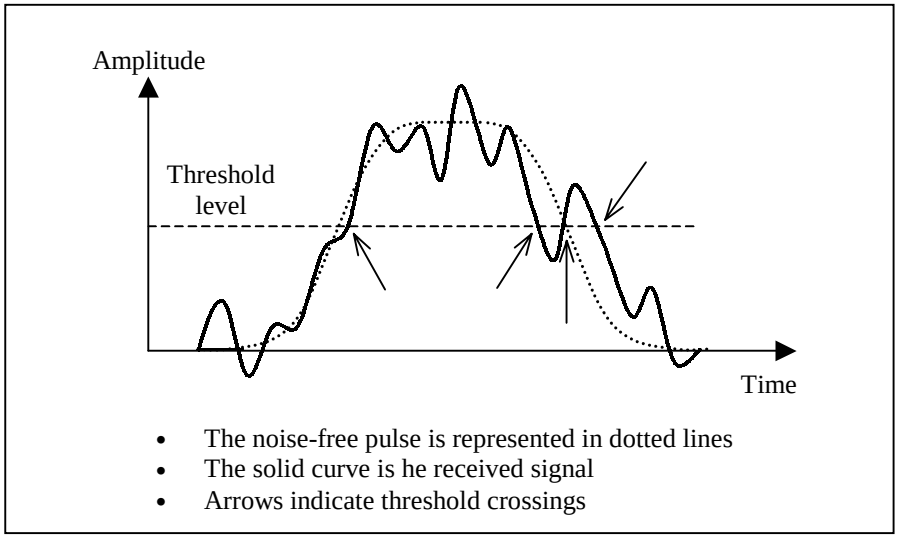

Figure 3-4 Ambiguity of the time measurement method

In Figure 3.4, it is quite difficult to determine what should be considered as the pulse, since there are four threshold crossings, which the current processing system will interpret as two separate, but closely spaced pulses. Anyway, it is easy to see that whether the system uses the inner threshold crossings or the outer crossings, both cases will yield an error.

Predicting a timing error is thus difficult with a threshold crossing system when the SNR is low.

3.4 Conclusion

This first analysis of the theoretical accuracy of a threshold measurement leads to analytical results given by equations (3.12) and (3.16) that are reliable at high SNR. This law depends on the slope of the Gaussian pulse, and the relative voltage squared ratio between the signal and noise. As the slope of the Gaussian pulse is made steeper, the rms noise error of a threshold measurement is decreased. The same conclusion is reached when the SNR of the received signal is increased. The theoretical law modeling the rms error for threshold measurements can therefore be derived for correlation at high SNR. This is the focus of Chapter 4.

On the other hand, at low SNR, time measurement errors depart significantly from theoretical results due to increasing numbers of ambiguities that make threshold measurements miss the expected pulses. These ambiguities are the result of noise peaks that are closer in amplitude to the measured pulses as the SNR is decreased. Consequently, a system decreasing the noise level as compared to the noise-free signal is needed prior to threshold measurements. Integration has this property and is presented in Chapter 6.

Chapter 4

4. Correlation Accuracy

The study presented in Chapter 3 of this thesis led to the theoretical accuracy of threshold measurements on Gaussian pulses. Chapter 2 introduced correlation and showed that the output of correlation yields a peak centered on the time delay between the two correlated pulses. Using a threshold technique on the output of correlation therefore provides the time delay between the two correlated Gaussian pulses. The key idea of this chapter lies in the fact that the correlation of two Gaussian pulses embedded in noise leads to a Gaussian pulse embedded in noise, for which the analytical study performed in Chapter 3 applies. The accuracy of a correlation measurement can therefore be derived from the analytical result on threshold measurements. The goal of this chapter is therefore to proceed to the derivation of the threshold accuracy, and determine if there is a match between theoretical and practical results.
Section 4.1 presents the analytical developments, whereas Section 4.2 is focused on the simulations used to validate the analytical results.

4.1 Theoretical accuracy

The derivation of threshold analytical accuracy is an uneasy task when applied to correlation of signals of finite lengths, as it is practically always performed. Section 4.1.1 therefore presents the methodology that is used for the derivation, and addresses issues linked to the developments. Section 4.1.2 summarizes the notations used throughout the chapter. Finally, Section 4.1.3 is dedicated to the mathematical calculations.

4.1.1 Preliminary comments

The key idea the mathematical developments are going to rely on is the application of threshold theoretical accuracy to the output of the correlation of two Gaussian pulses embedded in noise. This idea is justified in Section 4.1.1.1. However, comments concerning the practical use of this approach are presented in Section 4.1.1.2.

4.1.1.1 Justification of the use of threshold theoretical accuracy

The notation for the correlation operation is identical to Chapter 2. If u and v are two functions modeling real signals, the correlation of these two quantities is written as in equation (4.1).

$$\text{Corr(u,v)}\ (\tau) = u(t) * \overline{v(-t)} = \int_{-\infty}^{+\infty} u(t) \times \overline{v(t-\tau)} dt \qquad (4.1)$$

where $*$ is the convolution operator, and $\overline{v(t)}$ denotes the complex conjugate of function v.

The correlation operation is linear since integration is linear, so that if two pulses, p_1 and p_2, are embedded in noise, n_1 and n_2, the result of cross-correlation operation is given by equation (4.2).

$$\begin{aligned} &\text{Corr}\ [\ p_1(t) + n_1(t)\ ,\ p_2(t) + n_2(t)\ ] = \ldots \\ &\quad \ldots = p_1(t) * \overline{p_2(-t)} + p_1(t) * \overline{n_2(-t)} + p_2(t) * \overline{n_1(-t)} + n_1(t) * \overline{n_2(-t)} \end{aligned} \qquad (4.2)$$

Equation (4.2) shows that correlation of two pulses embedded in noise is composed of a pulse p_c given in equation (4.3), embedded in a noise n_c provided in equation (4.4).

$$p_c(\tau) = p_1(t) * \overline{p_2(-t)} \qquad (4.3)$$

$$n_c(\tau) = p_1(t) * \overline{n_2(-t)} + p_2(t) * \overline{n_1(-t)} + n_1(t) * \overline{n_2(-t)} \qquad (4.4)$$

If now we consider that the pulses are identical, so that $p_1 = p_2 = p$, then equation (4.3) and (4.4) can be simplified.

$$p_c(\tau) = p(t) * \overline{p(-t)} \tag{4.5}$$

$$n_c(\tau) = p(t) * \overline{n_2(-t)} + p(t) * \overline{n_1(-t)} + n_1(t) * \overline{n_2(-t)} \tag{4.6}$$

To apply the analytical accuracy of a threshold measurement to the correlation of two Gaussian pulses embedded in an additive white Gaussian noise (AWGN), two things have to be checked: first that the pulse is Gaussian, and second that the noise is AWGN.

Mathematically, the correlation of two Gaussian pulses is a Gaussian pulse:

$$\text{Corr}\left[A\times\exp(-at^2) , B\times\exp(-bt^2) \right] = AB \times \sqrt{\frac{\pi}{a+b}} \times \exp\left(-\frac{ab}{a+b} t^2 \right) \tag{4.7}$$

The correlation noise $n_c(\tau)$ as described by equation 4.6 is additive. Moreover, at low signal-to-noise ratio noise is predominant, so that $n_c(\tau)$ can be approximated by equation (4.8).

$$n_c(\tau) = n_1(t) * \overline{n_2(-t)} \tag{4.8}$$

Correlating signals in the time domain corresponds to multiplying the Fourier transforms of these signals in the frequency domain as reported in [Cou01]. An AWGN is a signal having a frequency spectrum that is continuous and uniform over a specified frequency band ([Cou01]). Therefore, the multiplication of two continuous and uniform spectra yields also a continuous and uniform spectrum, leading to the conclusion that the correlation of two AWGN noise samples is an AWGN noise sample. As a result, the correlation noise $n_c(\tau)$ has a Gaussian distribution at low SNR. On the other hand, noise cannot be strictly speaking considered as AWGN at high signal-to-noise ratio because of the presence of Gaussian pulse in equation (4.6). Yet, AWGN is an ideal mathematical form that only approximates real noise distributions. The use of an approximated AWGN

in the experiment of Chapter 3 did not prevent us from observing the expected analytical results. It will therefore be assumed that this condition is valid.

Consequently, Skolnik's results on threshold theoretical accuracy can be applied to correlation time measurements in the case of Gaussian pulses embedded in AWGN.

4.1.1.2 Comments concerning the mathematical developments

The idea of applying threshold theoretical accuracy to correlation has been justified in Section 4.1.1.1. However, there is a problem with this approach when considering what is happening practically. First of all, correlation is always practically applied to finite samples of signals, whereas the usual analytical results that are known for correlation assume integration over infinite lengths of time. Equation (4.7) for instance was written assuming that two Gaussian pulses defined over infinite lengths of time were correlated, whereas practical correlation of Gaussian samples of finite lengths is not strictly speaking represented by equation (4.7). Yet, the difference will be negligible since exponential functions are quasi null at a certain distance from the peak of the function. This approximation can not be performed in the case of AWGN since energy is lost when the signal is truncated.

As a result, the mathematical developments that we are proposing are going to assume infinite time duration for the signals in order to rely on existing analytical solutions. However, practical tests will be performed on the results in order to correct factors that may have appeared due to this incorrect assumption. The presented approach will therefore be empirical, and the reader should not be surprised to see such corrections.

4.1.2 Mathematical developments

The model of a Gaussian pulse is a function p(t) given by equation (4.9).

$$p(t) = A \times \exp(-at^2) \tag{4.9}$$

where A is the amplitude of the pulse, and a its inverse time constant squared.
The analytical solution for the accuracy of a time measurement using threshold applied to a Gaussian pulse modeled by equation (4.9) is provided in equation (4.10).

$$\delta T_R = \frac{1}{\sqrt{a \times \frac{A^2}{N}}} \tag{4.10}$$

N is the noise power of the noise.

Equation (4.10) is valid in a Gaussian matched filter case, however, a factor equal to 0.9 should be considered as given in equation (4.11) when a rectangular filter is used instead of the Gaussian filter, as reported in [Sko80].

$$\delta T_R = \frac{1}{\sqrt{a \times 0.9 \times \frac{A^2}{N}}} \tag{4.11}$$

As mentioned in the literature review ([Sko80]), correlating a signal with its noise-free replica performs a matched filter. Consequently, correlating two similar signals embedded in noise samples at high SNR approximate a matched filter, so that equation (4.10) can be used in our developments. According to equation (4.10), the accuracy of a time measurement using a threshold involves finding three parameters: the two parameters modeling the Gaussian correlation pulse (equation (4.5)), in other words its amplitude and bandwidth, and the correlation noise power (equation (4.6)). These parameters are calculated in Sections 4.1.2.1 and 4.1.2.2.

4.1.2.1 Calculation of the correlation pulse power

In Chapter 3, the practical definition used for the signal to noise ratio (SNR) is the ratio between the pulse peak voltage squared and the noise rms squared. It is assumed that the

pulses that are correlated do have the same SNR, which is a good approximation in most cases where the samples are close in time. A practical correlation operation performed on two finite samples produces a signal over a length of time equal to the sum of the duration of each sample. Therefore, if the ratio: $\frac{A^2}{N}$ needs to be related to the value of the SNR found for the exponential pulse defined on a half time length, then this SNR has to be divided by two. This factor is taken into account in equation (4.13).

The autocorrelation $p_c(\tau)$ of a Gaussian pulse is derived from equation (4.7), and provided in equation (4.12).

$$p_c(\tau) = \text{Corr}(A\times\exp(-at^2)) = A^2\sqrt{\frac{\pi}{2a}}\exp\left(-\frac{a}{2}t^2\right) \qquad (4.12)$$

Hence, equation (4.10) adapted to the Gaussian pulse given in (4.12) becomes:

$$\delta T_R = \frac{1}{\sqrt{\frac{1}{2}\times\frac{a}{2}\times\frac{\frac{\pi}{2a}A^4}{N}}} = \frac{1}{\sqrt{\frac{\pi}{8}\frac{A^4}{N}}} \qquad (4.13)$$

4.1.2.2 Calculation of the noise power of the correlation noise

To calculate the noise power associated with the correlation noise of equation (4.6), mathematical developments will be performed in the frequency domain for ease of the manipulations of the expressions.

The Fourier transform of the correlation noise $n_c(\tau)$ (equation (4.6)) is given in equation (4.14).

$$N_C(f) = P(f)\times\left(\overline{N_1(f)} + \overline{N_2(f)}\right) + N_1(f)\times\overline{N_2(f)} \qquad (4.14)$$

P(f) is the Fourier transform of the noise-free Gaussian pulse. $N_1(f)$and $N_2(f)$ are the Fourier transforms of the noise samples. $\overline{N(f)}$ denotes the complex conjugate of function N(f).

The case of study of our thesis specifies that the processed signals be received at a unique detector, which is different from the TDOA approach as mentioned in the literature review of this thesis. As a result, the noise distributions of n_1 and n_2 (equation (4.7)) are similar, along with their spectrum. We can therefore write equation (4.15). Equation (4.16) is derived from equation (4.14) and (4.15), with the supplemental assumption that the signals we are using are non-complex.

$$N_1(f) \cong N_2(f) = N(f) \tag{4.15}$$

$$N_C(f) \cong N(f) \times (2 \times P(f) + N(f)) \tag{4.16}$$

To proceed to our derivation, we need to consider two cases: a high SNR where the contribution of noise is insignificant as compared to the pulse, and a low SNR where the situation is reversed.

4.1.2.2.1 Noise power of the correlation noise at high SNR

Equation (4.16), which represents the correlation noise power, is composed of two factors: the Fourier transform of the noise N(f) and the sum of the Fourier transforms of the noise and noise-free signals: N(f) + 2×P(f). This second factor can be simplified depending on the relative levels of the noise and noise-free signal, in other words the SNR. At high SNR, the Gaussian pulse is predominant in the correlation noise spectrum, whereas the contribution of noise is insignificant, and can be dropped. Equation (4.16) can therefore be simplified as given in equation (4.17) for high SNRs.

$$N_C(f) \cong 2 \times P(f) \times N(f) \tag{4.17}$$

We now need to be careful in order to calculate the power of the correlation noise. Noise is of finite power, but infinite energy, whereas a Gaussian pulse is both of finite power and energy. Therefore, Nc(f) has the same properties as the Gaussian pulse, which means that $n_c(t)$ it is both of finite energy and finite power.
As reported in [Cou01], the power spectral density of a power type signal is equal to the Fourier transform of the autocorrelation of that waveform.

$$PSD\{ g(t) \} = F\{ g(t) * \overline{g(-t)} \} = |G(f)|^2 \quad (4.18)$$

F{.} denotes the Fourier transform operator, while |.| returns an absolute value. G is the Fourier transform of function g(t).

As a result, the power spectral density of the correlation noise $n_c(t)$ is given by equation (4.19).

$$PSD\{ n_c(t) \} = | 2 \times P(f) \times N(f) |^2 \quad (4.19)$$

The Fourier transform of AWGN noise is presented in [Cou01], and modeled in the frequency domain by a flat spectrum over its bandwidth as given in equation (4.20). The Fourier transform of a Gaussian pulse is provided in equation (4.21), and can be found in any electronic textbook.

$$N(f) = F\{ n(t) \} = \sqrt{(½ N_o)} \times rect_{[-B_N, B_N]}(f) \quad (4.20)$$

$$P(f) = F\{ A \times \exp(-at^2) \} = A \times \sqrt{\frac{\pi}{a}} \times \exp\left(-\frac{\pi^2}{a} f^2 \right) \quad (4.21)$$

The function $rect_{[-B_N, B_N]}(f)$ represents the two-sided noise bandwidth of the receiver filter.

The power of the correlation noise is obtained by integration of the power spectral density of the correlation noise given in equation (4.19) over all frequencies. Equation (4.23) is obtained from equation (4.22) using equations (4.20) and (4.21).

$$\text{Power } \{ n_c(t) \} = 2\times\int_0^{+\infty} | 2\times P(f)\times N(f) |^2 \, df \tag{4.22}$$

$$\text{Power } \{ n_c(t) \} = 2\times(½N_o)\times 4A^2\frac{\pi}{a}\times\int_0^{B_N}\exp\left(-\frac{2\pi^2}{a}f^2\right)df \tag{4.23}$$

The integral of a Gaussian signal is given by a function called error function, erf, and is used in radar and telecommunication theories. A table of the values for this function can be found in [Rap99]. An important result concerning this function is given in equation (4.24).

$$\int_0^X \exp(-af^2)df \;=\; \frac{1}{2}\sqrt{\frac{\pi}{a}}\times erf\left(\sqrt{a}\times X\right) \tag{4.24}$$

Hence:

$$\text{Power } \{ n_c(t) \} = \; N_O\times 4A^2\frac{\pi}{a}\,\frac{1}{2}\sqrt{\frac{\pi a}{2\pi^2}}\times erf\left(\sqrt{\frac{2}{a}}\times\pi\times B_N\right) \tag{4.25}$$

$$\text{Power } \{ n_c(t) \} = \; N_O\times A^2\sqrt{\frac{2\pi}{a}}\times erf\left(\sqrt{\frac{2}{a}}\times\pi\times B_N\right) \tag{4.26}$$

Finally, the noise power per unit bandwidth N_O is equal to the noise power of the noise divided by its bandwidth. This leads to equation (4.27).

$$\text{Power } \{ n_c(t) \} = \; \frac{N}{B_N}\times A^2\times\sqrt{\frac{2\pi}{a}}\times erf\left(\sqrt{\frac{2}{a}}\times\pi\times B_N\right) \tag{4.27}$$

N is the noise power and B_N its bandwidth. A is the amplitude of the Gaussian pulse, and a models this pulse, as given in equation (4.10). erf{.} is the error function, which is defined in any radar textbook, and whose values can be obtained in any mathematical software like MATLAB, Mathematica, and Maple.

4.1.2.2.2 Noise power of the correlation noise at low SNR

At low SNR, meaning at SNR for which the correlation of both noise samples prevails in equation (4.16), equation (4.16) can be simplified as given in equation (4.28).

$$N_C(f) \cong |N(f)|^2 \tag{4.28}$$

Noise is a power type signal. The power spectral density of a power type signal is equal to the Fourier transform of the autocorrelation of that waveform, as given in equation (4.18). As a result, the power spectral density of the correlation noise $n_c(t)$ is given by equation (4.29).

$$PSD\{ n_c(t) \} = |N(f)|^4 \tag{4.29}$$

The power of the correlation noise is obtained by integration of the power spectral density of the correlation noise given in equation (4.29) over all frequencies, as provided in equation (4.30). Equation (4.31) is obtained from equation (4.30) using equations (4.20).

$$\text{Power } \{ n_c(t) \} = 2\times\int_0^{+\infty} | N(f) |^4 \, df \tag{4.30}$$

$$\text{Power } \{ n_c(t) \} = 2\times\int_0^{+B_N} \left|\sqrt{N_O/2}\right|^4 \, df \tag{4.31}$$

$$\text{Power } \{ n_c(t) \} = \frac{1}{2} B_N\times N_O \tag{4.32}$$

$$\text{Power } \{ n_c(t) \} = \frac{1}{2}\times\frac{N_2}{B_N} \tag{4.33}$$

N is the power of the noise and B_N its bandwidth.

4.1.2.3 Comments and correction factors

We have calculated in Section 4.1.2.1 and 4.1.2.2 what we defined as the correlation noise, which is the noisy signal added to the correlation of the two noise-free Gaussian pulses. Considering equations (4.13), (4.27), and (4.33), we have now the different elements needed to compute the accuracy of a correlation measurement. Yet, it was mentioned in Section 4.1.1.2 that an incorrect assumption was made in order to perform simpler mathematical developments. We assumed that the signals that were correlated were of finite lengths, although finite samples of signals are always processed. Besides, signals of infinite energy, the noise, and of both finite energy and power, Gaussian pulses, were mixed through correlation, and integration during the mathematical developments. This suggests that errors may have arisen between mathematical developments and what we would like to model: the correlation noise power of finite lengths of signals. Consequently, comparison between the mathematical developments and practical results are needed.

4.1.2.3.1 Correction of the correlation noise at high and low SNR

Equations (4.27) and (4.33) provide the correlation noise power at low and high SNR. The parameters that are involved in the formulas are the noise bandwidth, the noise power, the amplitude and the constant ‘a’ modeling the Gaussian pulse as given in equation (4.10).

In order to check the validity of the equation representing the accuracy of correlation at high SNR case (equation (4.27)), repetitive simulations consisting in generating a Gaussian pulse with a certain amplitude and width, and correlating it with two noise samples obtained from the same matrix of noise as generated in Chapter 3 were performed. The rms value of the obtained signal was computed. This value was then multiplied by the sampling period squared of the simulations so as to take account for the fact that simulations were performed with discrete samples of signals. In order to understand this point, we should remember that integration in the continuous domain is

approximated in the discrete domain by a summation times the period of the sampling. Since both correlation and noise power calculations imply integration (equations (4.1) and (4.22)), then the period squared has to be considered as a factor. Finally, the ratio of the mentioned quantity – the practical rms value of the noise correlation multiplied by the sampling frequency squared – and the analytical result of equation (4.27) was computed. This ratio is called R_1, and is given in equation (4.34).

$$R_1 = \frac{rms\left(p(t)*\overline{n_1(-t)}+p(t)*\overline{n_2(-t)}\right)\Big/F_S^2}{A^2\times\frac{N}{B_N}\times\sqrt{\frac{2\pi}{a}}\times erf\left(\sqrt{\frac{2}{a}}\times\pi\times B_N\right)} \tag{4.34}$$

F_S is the sampling frequency used in the experiment, while A and ‘a’ are the parameters of the Gaussian pulse p(t) as in equation (4.10). N is the power of the noise samples n_1 and n_2, and B_N the noise bandwidth. erf{.} is the error function.

The above experiment was repeated 500 times, for different sampling frequencies, 10 and 20 MHz, different number of points for the samples, 250 and 500, and different noise levels. Table (4.1) summarizes the result of these simulations.

A similar simulation was performed for equation (4.33) representing the correlation noise power in a low SNR case. In this case, two samples of noise obtained from the same matrix of noise as in the experiments of Chapter 3 were correlated, and the result was divided by the sampling frequency squared of the experiment for the same reason as above. The ratio of this quantity and the analytical result given in equation (4.33) was computed, and the experiment was repeated 500 times, with different sampling frequencies, number of points of the samples, and noise level. The ratio R_2 obtained in these simulations is summarized in equation (4.35).

$$R_2 = \frac{rms\left(n_1(t)*\overline{n_2(-t)}\right)\Big/F_S^2}{\frac{N^2}{2B_N}} \tag{4.35}$$

where N is the power of the noise samples n_1 and n_2, and B_N the noise bandwidth.

4.1.2.3.2 Results of the experiment

The results of the simulations described in Section 4.1.2.3.1 are summarized in Table (4.1). The Gaussian pulse used in this experiment has constant 'a' equal to 400×10^9 s^{-2}, and a half power bandwidth of 237kHz.

Sampling frequency	noise bandwidth	Number of points of the samples / duration of sample	SNR (dB)	R_1	R_2	R_2 divided by the duration of sample
10 MHz	**300kHz**	**250 pts 25ms**	**0**	0.23	123.0	0.49
			10	0.23	123.9	0.49
			20	0.24	125.3	0.49
			30	0.25	125.0	0.51
		500 pts 50ms	**0**	0.24	248.2	0.52
			10	0.27	252.0	0.51
			20	0.26	255.9	0.52
			30	0.25	265.6	0.51
	600kHz	**250 pts 25ms**	**0**	0.23	124.1	0.50
			10	0.24	126.6	0.50
			20	0.24	124.5	0.52
			30	0.26	125.8	0.50
		500 pts 50ms	**0**	0.24	253.7	0.51
			10	0.25	257.9	0.51
			20	0.27	259.6	0.52
			30	0.26	256.1	0.51
20 MHz	**300kHz**	**250 pts 50ms**	**0**	0.22	115.6	0.46
			10	0.23	116.5	0.46
			20	0.23	116.1	0.46
			30	0.25	114.5	0.46
		500 pts 100ms	**0**	0.24	241.4	0.48
			10	0.22	237.7	0.48
			20	0.23	238.4	0.49
			30	0.25	239.9	0.49
	600kHz	**250 pts 50ms**	**0**	0.22	120.9	0.48
			10	0.23	122.2	0.49
			20	0.22	120.8	0.49
			30	0.22	121.7	0.48
		500 pts 100ms	**0**	0.24	244.5	0.50
			10	0.24	252.2	0.50
			20	0.25	243.5	0.50
			30	0.26	245.0	0.49

Table 4-1 Ratios for the correlation noise power corrections

The results for R_1 are constant although the time duration of the samples, the sampling frequency, the noise level, and the noise bandwidths vary. The average value of R_1 proves to be approximately 0.25. This result is given in equation (4.36).

$$\left[\frac{Power(\text{exp}erimental)}{Power(theory)}\right]_{\text{High SNR case}} \cong \frac{1}{4} \tag{4.36}$$

To model the practical noise power obtained at high SNR, we therefore need to consider this factor in equation (4.27), which yields equation (4.37).

$$\text{Power } \{ n_c(t) \}_{\text{High SNR case}} = \frac{N}{B_N} \times \frac{A^2}{4} \times \sqrt{\frac{2\pi}{a}} \times erf\left(\sqrt{\frac{2}{a}} \times \pi \times B_N\right) \tag{4.37}$$

For the low SNR case designated by ratio R_2, the result seems to vary with both the number of points and the sampling frequency, or with the duration of the samples only. This conclusion is confirmed in column 7 of this table where ratio R_2 was computed and divided by the duration of the samples: Ds. The result is constant and equal to 0.5 on average. This result is summarized in equation (4.38).

$$\left[\frac{Power(\text{exp}erimental)}{Power(theory)}\right]_{\text{Low SNR case}} \cong \frac{1}{2} \times D_s \tag{4.38}$$

To model the practical noise power obtained at high SNR, we therefore need to consider this factor in equation (4.33), which yields equation (4.39).

$$\text{Power } \{ n_c(t) \} = \frac{D_S}{2} \times \frac{N_2}{B_N} \tag{4.39}$$

4.1.2.3.3 Comments

Comparing analytical developments and practical results of simulations concerning the evaluation of the correlation noise power was motivated by the assumption we made of having signals of infinite duration. This is not the case in practical experiments where finite samples of signals are processed. Yet, the practical case is actually what we tried to model in the mathematical part of Section 4.1.2.3. By the use of simulations, we intended to evaluate the differences of which we could not take account in the mathematical developments due to our incorrect assumption. It was shown that when correlation noise is mainly due to the correlation of the Gaussian pulse and the two samples of noise, then a correction factor of 0.25 is taken into account. When correlation noise is mainly due to the correlation of two samples of noise, then a correction factor equal to half the time duration of the samples emerges.

The duration of the sample that appears is directly due to the assumption mentioned above. A Gaussian pulse is of finite energy and finite power, no matter what the duration of the signal is: finite or infinite duration. Noise, however, is theoretically of infinite energy and finite power, but it is of finite power and energy when a sample of noise is taken. To account for this difference, the duration of the sample is expected, as given in equation (4.37).

The theoretical analysis, although developed thoroughly, still does not agree by two constant factors: 0.25 and 0.5 with the simulations that were done with care. It therefore seems to be an artifact of the numerical integration.

4.1.2.4 Final results for the accuracy of correlation

At high SNR, in other words when correlation noise is mainly due to the correlation of the Gaussian pulse and the two samples of noise, then the accuracy of a time measurement using correlation is provided in equation (4.40) using equations (4.13), and (4.36).

$$\delta T_{R-\text{High SNR}} = \frac{1}{\sqrt{\frac{\sqrt{a}}{K_1} \times B_N \times \frac{A^2}{N}}} \tag{4.40}$$

'a' is a constant in units of Hertz squared modeling the Gaussian pulse of amplitude A, as given in equation (4.10). B_N is the noise bandwidth, and N the noise power. The constant K_1 is given in equation (4.41), and can be simplified as given in equation (4.42).

$$K_1 = 2\sqrt{\frac{2}{\pi}} \times erf\left(\sqrt{\frac{2}{a}}\pi \times B_N\right) \tag{4.41}$$

$$K_1 \cong 2\sqrt{\frac{2}{\pi}} \cong 1.60 \quad \text{for values of } \frac{B_N}{\sqrt{a}} \geq 0.4 \tag{4.42}$$

At low SNR, in other words when the correlation of two samples of noise prevails in the correlation noise quantity, then the accuracy of a time measurement using correlation is provided in equation (4.43) using equations (4.13), and (4.39).

$$\delta T_{R-\text{Low SNR}} = \frac{1}{\sqrt{\frac{\pi}{4} \times \frac{B_N}{D_S} \times \left(\frac{A^2}{N}\right)^2}} \tag{4.43}$$

D_S is the sample duration is units of seconds.

4.2 Comparison between theory and practice

The theoretical accuracy of a time measurement using correlation for two Gaussian pulses has been derived, and given as two asymptotical laws: one for high SNRs, and the other one for low SNRs. High SNR denotes SNRs for which correlation noise is mainly due to correlation between the Gaussian pulse and each of the noise samples in which pulses are embedded, whereas low SNR concerns SNRs for which correlation of two samples of noise prevails. The limit between these two asymptotes is not quantified

though, and the derivation was based on a simplistic assumption that implied the computation of correction factors. As a result, a comparison between theoretical and practical results is needed in order to corroborate the validity of the developments.
Section 4.2.1 lists the parameters that are tested in the experiment while Section 4.2.2 describes the conditions of the experiment. Section 4.2.3 presents the results of the experiment, and Section 4.2.4 analyzes the results.

4.2.1 Parameters involved in the experiment

The parameters that need to be tested in the experiment are those given in equations (4.40) and (4.43): the noise bandwidth, the amplitude and constant ‘a’ of the Gaussian pulse, the duration of the sample, and the signal-to-noise-ratio.

4.2.2 Description of the simulation

As in Chapter 3 of this thesis, the simulation consists in generating a Gaussian pulse with a certain time constant, and adding noise with a Gaussian distribution and bandlimited to a certain frequency. Noise is obtained from a matrix which points are computed by summing a thousand random values contained between –0.5 and 0.5V. This yields a Gaussian distribution according to the central limit theorem. This matrix of noise is then filtered by convolution in the time domain with a sinx/x function for optimum rectangular filtering, or with the noise-free Gaussian pulse for Gaussian matched filtering. The rms value of the noise is adjusted to accommodate different SNRs. A time delay measurement is then performed by correlating two samples of a Gaussian pulse buried in noise, and the peak of the correlation is calculated using a threshold measurement at half the amplitude of the peak.
The simulation is repeated 500 times for each SNR point, and the rms value of the error of the time measurements is calculated over all these repetitions. Several filter bandwidths are accommodated and the experiment is conducted for different constants ‘a’ of the Gaussian pulse.

It has to be noted that to tackle the problem of false alarms at low SNR, the measurement was performed in a window of time corresponding to the expected occurrence of the pulses. The maximum error is therefore bounded by the time window size.

4.2.3 Results and comments

Figure 4.1 shows the result of correlation for two Gaussian pulses with a constant 'a' equal to 400×10^9 s^{-2} and 650×10^9 s^{-2}. The corresponding half power bandwidths are 237 and 300kHz respectively. The noise bandwidths simulated are 300kHz and 600kHz. The two other curves presented on Figure (4.1) are the theoretical formula given in Section 4.1.

The graphs of Figure (4.1) all show that the experimental error has a shape that can be divided into three parts:

- a linear part at high SNR – above 16dB – matched closely with the theoretical formula at high SNR given by equation (4.40);
- an intermediate part at SNR around 12 to 14dB which starts by approaching slowly the expected formula at low SNR given by equation (4.43);
- a decrease and stabilization of the error at SNR lower than 7dB.

Similar results were obtained when varying the other parameters, like the constant 'a' of the Gaussian pulse.

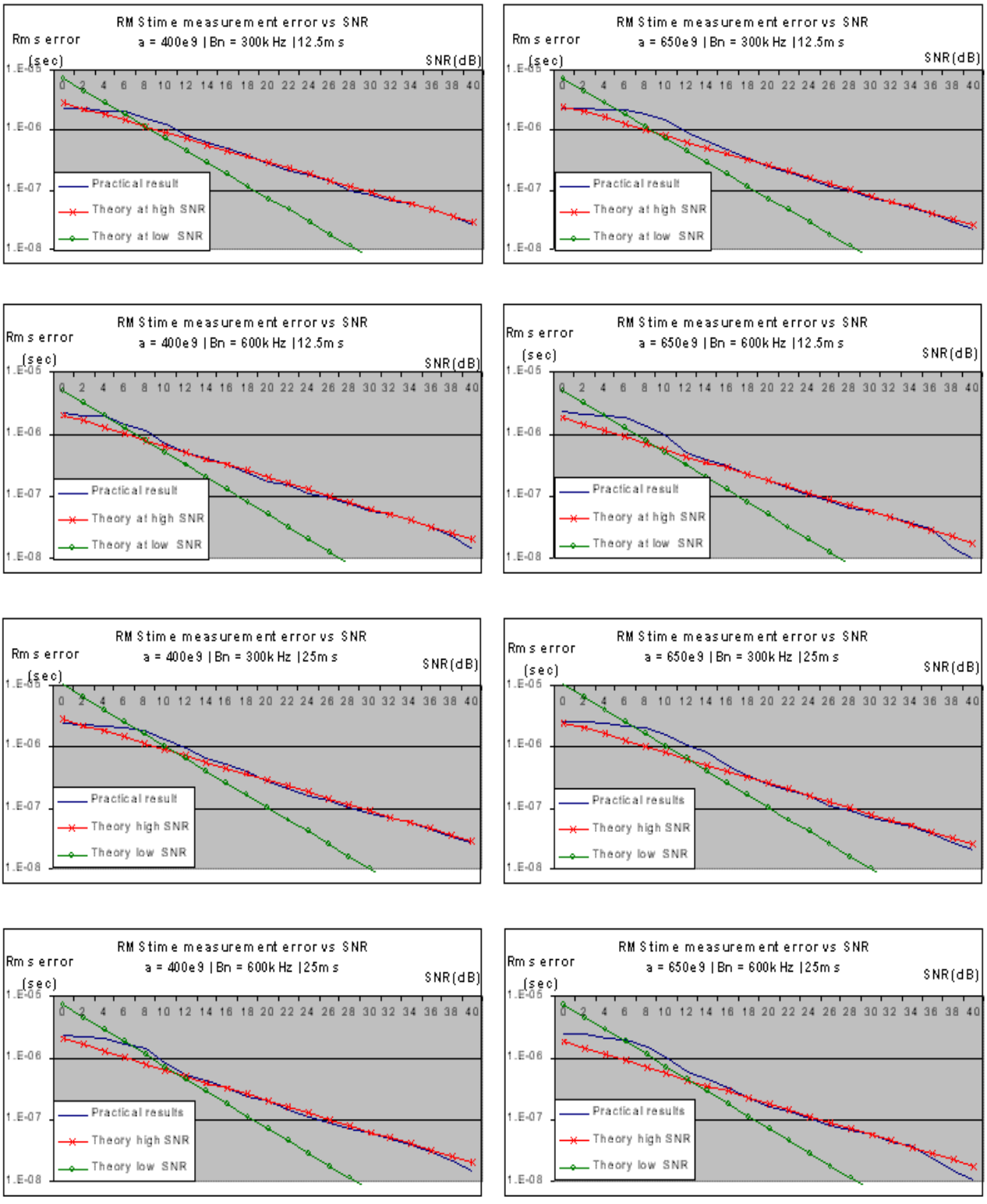

Figure 4-1 Rms value of the time measurement error using correlation

4.2.4 Analysis and discussion

The simulations performed in Section 4.2.3 presented the results of the accuracy of time measurements using correlation on Gaussian pulses. The practical results obtained at SNR above 14dB validated equation (4.40), corresponding to the high SNR case. Equation (4.43) seemed to correspond to the trend of the experimental accuracy at low SNR, unfortunately the window used to tackle the problem of false alarms artificially decreased the time measurement error. As explained in Chapter 3 of this thesis where threshold accuracy was presented and tested experimentally, ambiguities are raised in measurements because noise peaks are closer and closer to Gaussian pulses in terms of amplitude. As a result, the time accuracy is in average given by the length of the a-priori knowledge that we have of the position of the pulses, in other words the duration of the time window. Consequently, the only equation that can be relied on is the one for high SNRs.

4.3 Conclusion

We have determined two formulas that give the asymptotic accuracy of time measurements using correlation. These mathematical developments were based on the derivation of the threshold measurement accuracy. The theoretical results were then tested using simulations and different values for the parameters involved in the obtained equations. Section 4.2 proved there was a good match between theoretical and practical results. However, it was noticed again that at low SNR, usually in the range 0 to 6dB, practical results diverged from theoretical ones due to an increase of ambiguities in the measurements process, related to the increase of noise level. This conclusion suggests as in Chapter 3 that a method is needed to ensure that the expected pulses are indeed processed, and to ensure signal processing at high SNR. This will be the focus of Chapter 6. However, since theoretical laws modeling the accuracy of correlation and threshold time measurements are known, it is possible to proceed to a comparison between both methods, which is the focus of Chapter 5.

Chapter 5

5. Comparison of Threshold and Correlation Measurement Techniques

Chapter 2 of this thesis summarized the analytical study of the accuracy of a time measurement using a threshold detector. Chapter 3 consisted in a derivation of the theory of Chapter 2, and resulted in the analytical accuracy of time measurements via correlation. Based on these two chapters, an analytical comparison of both methods is possible, although restricted to simple cases where pulses are symmetrical and of same amplitude. It is therefore necessary to perform this comparison in both ideal and non-ideal cases. In the non-ideal cases where analytical results are difficult to obtain, conclusions will be based on simulations.

Section 5.1 presents the analytical comparison between correlation and threshold measurements for symmetrical pulses in both matched filter and non-perfect filtering cases.

In a practical cases however, pulses may be distorted, so that the model of perfect symmetrical Gaussian pulses may not be appropriate. Consequently, the pulses that are compared in Section 5.2 are asymmetrical, or present different shapes: different amplitudes, and different symmetries. Simulation will be the main tool to compare these methods.

Finally, Section 5.3 summarizes the above developments.

5.1 Comparison of analytical results

5.1.1 Summary of the analytical developments

Based on the theory presented in [Sko80], Chapter 2 of this thesis yields the following accuracy for the rms time delay error evaluated using a threshold detector:

$$\delta T_R = \frac{1}{\sqrt{\frac{a}{2} \times \frac{A^2}{N}}} \tag{5.1}$$

where 'a' is the inverse time constant of the Gaussian pulse, A is the amplitude of the same pulse, and N is the noise power. A typical value for 'a' is 650×10^9 s^{-2} since the time constant of the Gaussian pulse $\tau = a^{-½}$ is in the order of the microsecond.

At relatively high SNR, Chapter 3 reported that the rms error for correlation measurements was:

$$\delta T_R = \frac{1}{\left(\sqrt{\frac{\pi a}{8}} B_N \frac{A_2}{N}\right)^{\frac{1}{2}}} \tag{5.2}$$

where B_N is the noise bandwidth.

Finally, at low SNR, the correlation error was determined to be:

$$\delta T_R = \frac{1}{\left(\frac{\pi}{4} \frac{B_N}{D_s} \left(\frac{A_2}{N}\right)^2\right)^{\frac{1}{2}}} \tag{5.3}$$

where D_S is the duration of the sample in seconds.

The cross over point between high and low SNR is reached for a SNR approximately equal to:

$$\frac{A^2}{N} = \sqrt{\left(\frac{2a}{\pi}\right)} \times D_S \cong 0.8 \times \sqrt{a} \times D_S \tag{5.4}$$

5.1.2 Analytical comparison

Chapter 4 will address the issue of detecting the signals with better accuracy and improving the SNR of the received signal. Let us therefore compare the threshold and correlation processes at large SNR in order to determine which is more accurate.

According to equation (5.1) and (5.2), correlation will be more accurate if:

$$\sqrt{\frac{\pi a}{8}} B_N \geq \frac{a}{2} \tag{5.5}$$

that is:

$$B_N \geq \sqrt{\frac{2a}{\pi}} \tag{5.6}$$

The inverse time constant ‘a’ is related to the halfpower bandwidth of the Gaussian pulse: B_{Gauss} by:

$$a = \frac{(\pi B_{Gauss})^2}{4 \times \ln(\sqrt{2})} \tag{5.7}$$

Hence, equation (5.6) becomes:

$$B_N \geq \sqrt{\left(\frac{\pi}{2\ln(\sqrt{2})}\right)} \times B_{Gauss} \cong 2.13 \times B_{Gauss} \tag{5.8}$$

In the case of a perfect matched filter, the bandwidth of the noise at the output of the filter will be equal to B_{Gauss}. This means that the inequality given by equation (5.8) cannot be satisfied.

Yet, a matched filter is practically hard to implement. If the near-matched filter case modeled by a rectangular filter is used, then Table 10.1 in [Sko80] relates the optimum rectangular bandwidth B_{rect} to the Gaussian bandwidth B_{Gauss} by:

$$B_{rect} = \frac{0.72}{0.44} \times B_{Gauss} = 1.64 \times B_{Gauss} \tag{5.9}$$

Equation (5.8) and (5.9) yield:

$$B_N \geq 1.30 \times B_{rect} \tag{5.10}$$

Therefore, in both the matched filter and near-matched filter cases, the threshold measurement will provide more accurate results than the correlation method. A discussion concerning this theoretical result will be conducted after presenting the simulation dedicated to that specific case.

5.1.3 Practical comparison

In both a matched filter and near-matched filter case, correlation proves to be not as accurate as a threshold measurement in the ideal case of symmetrical bandlimited pulses. However, the bandwidth limit was analytically determined to be 1.30 times the optimal rectangular filter bandwidth according to equation (5.10). This can be checked experimentally by taking a Gaussian pulse with a certain half-power bandwidth, and adding to it noise samples filtered at different bandwidths: the rectangular optimum bandwidth, the bandwidth given by equation (5.10), and a higher bandwidth.

The Gaussian pulse considered has a half-power bandwidth of 184kHz. The optimum bandwidth of a rectangular filter is 1.64 times this value (equation 5.9), which is about

300kHz. According to equation (5.10), the bandwidth providing the same accuracy for the threshold and correlation accuracy is 390kHz. Consequently, the noise bandwidths that were applied to the noise-free pulse had values of: 300, 390 and 460kHz. The results of these simulations are presented on Figure (5.1). These graphs present the rms value of the obtained errors limited to SNR ranging from 12 to 28dB in order observe the differences between the curves.

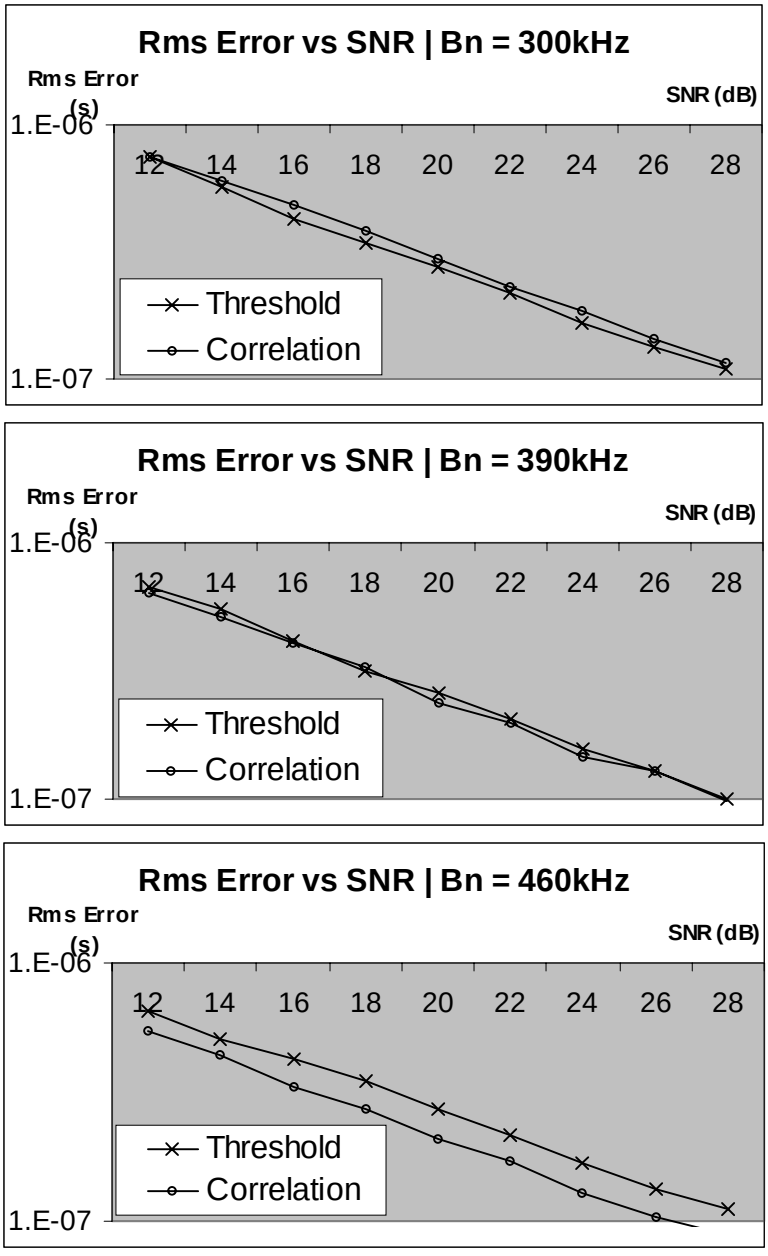

Figure 5-1 Threshold and correlation rms error with different noise bandwidth

The graphs of Figure 5.1 clearly show that the rms timing error generated by a correlation measurement is reduced as compared to a threshold measurement when the noise bandwidth is increased.

5.1.4 Discussion

The threshold time measurement was proved to be more accurate in the case of symmetrical pulses embedded in noise bandlimited at the bandwidth of the matched filter. Correlation proves important only above a certain bandwidth, which is 2.13 times that of the Gaussian matched filter, or 1.3 times that of the optimum rectangular filter. This suggests that one way to do low pass filtering of the signal and avoid problems with the phase response of the filter is to use a wide bandwidth pre-filter (to limit total noise power) and correlation.
Two questions however are raised:

- Why does the correlation process provide more accurate results than the threshold method at non-optimal bandwidths?
- Is not there a paradox when stating that the correlation method yields more accurate results at higher bandwidths than that of the matched filter, which is supposed to yield the optimum SNR of the signal, and therefore the optimum condition to perform a time measurement?

The answers to these questions are the focus of Sections 5.1.4.1 and 5.1.4.2.

5.1.4.1 Correlation improvement

As mentioned in the literature review of this thesis, correlating a signal embedded in noise with its noise-free version corresponds to a matched filter. In other words, correlation is a filter. In the case of baseband signals, like the Gaussian pulses we are considering, correlation is equivalent to a low-pass filter. This is illustrated in chapter 2.3 of this section although the signals that are correlated are both embedded in noise. The threshold correlation proves more robust than a threshold technique to an increase of the bandwidth of the noise because it has filtering properties that the latter process lacks.

One can however make the comment that correlation is important only in the case of bad filtering. Before discussing this point, it is important to recall that a Gaussian filter does not exist practically. There are however filters of a Gaussian type, but as mentioned in [Wil88] (page 2-56), these filters suffer from non-linear phase responses. A phase problem generates signal distortion, which is exactly the type of problem that causes biased time measurements. Consequently, the best practical filter to use in our case of study is an approximate rectangular filter, leading to the boundary given by equation (5.10). Therefore, the bandwidth for which correlation starts to be interesting is really close to that of the optimum practical bandwidth. Even if an optimum rectangular filtering is used, the gain in accuracy of the threshold measurement is only 20ns in an average case, as given in Figure (5.1). This difference vanishes if the bandwidth of the filter becomes 1.3 times that of the optimum rectangular filter, and correlation is 80ns more accurate as given in the third graph of Figure (5.1) when the noise bandwidth reaches 460kHz.

5.1.4.2 The interpretation of the SNR

Figure (5.2) gives the accuracy obtained by the correlation method for the different bandwidths used previously.

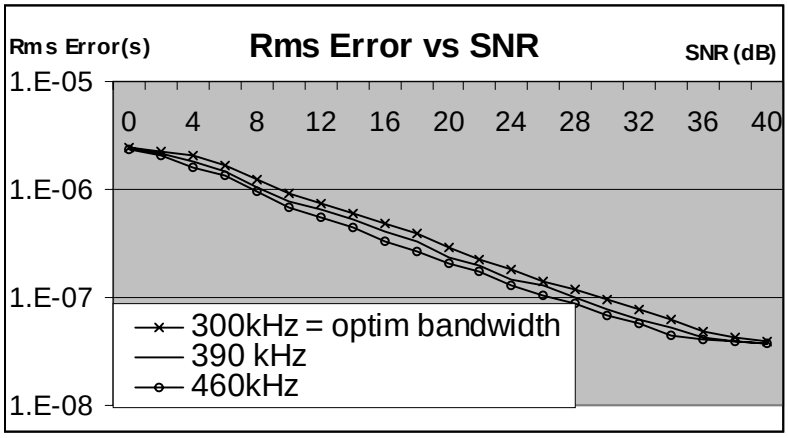

Figure 5-2 Rms error for the correlation process with different noise bandwidth

According to the above figure, one may be tempted to say that the time measurement obtained via correlation can be made more accurate by accepting more and more noise bandwidth. In order to obtain the same SNR between noise samples at 300 and 390kHz, the power spectral density is decreased for the latter sample. This reduces the noise spectral components within the optimum bandwidth, which is illustrated in Figure (5.3). Therefore, the negative influence of the noise spectral components affecting the measurement method is reduced, although at the same SNR. This explains why Figure (5.2) can be misleading.

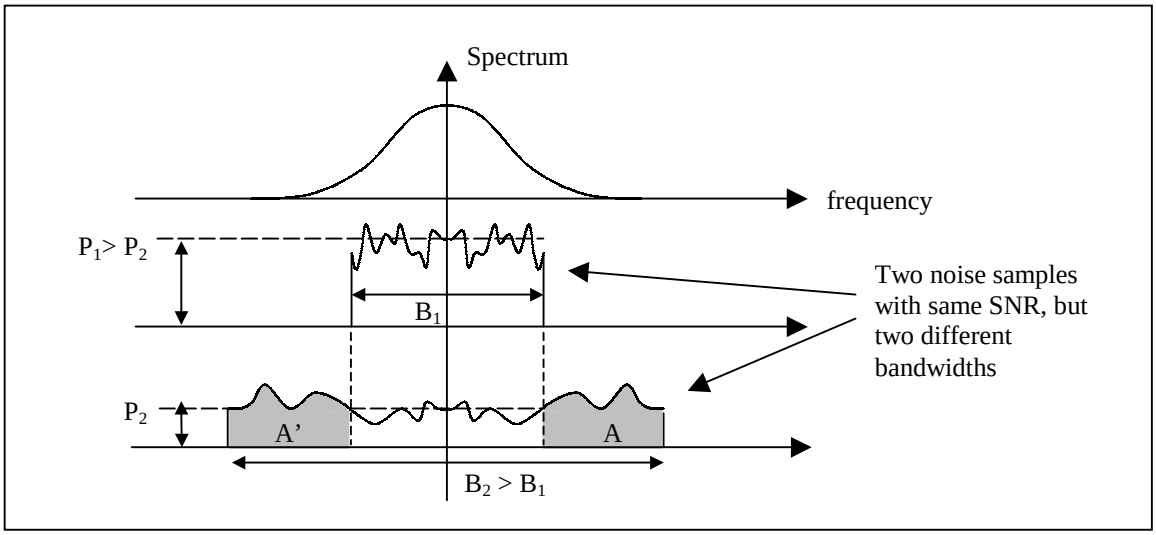

Figure 5-3 Two AWGN noise with same SNR, but different bandwidths

As a result, a more appropriate comparison between the correlation and the threshold processes can be illustrated by plotting the same graphs as Figure (5.1), but with a SNR in the abscissa referred to the same bandwidth of the optimum rectangular filter. This study is presented in Figure (5.4). The noise power taken into account in the SNR is obtained by integrating only the noise spectral components within the optimum rectangular bandwidth. Consequently, presenting the accuracy result for different bandwidths directly shows the robustness of the method to out-of-optimum-bandwidth noise spectral components.

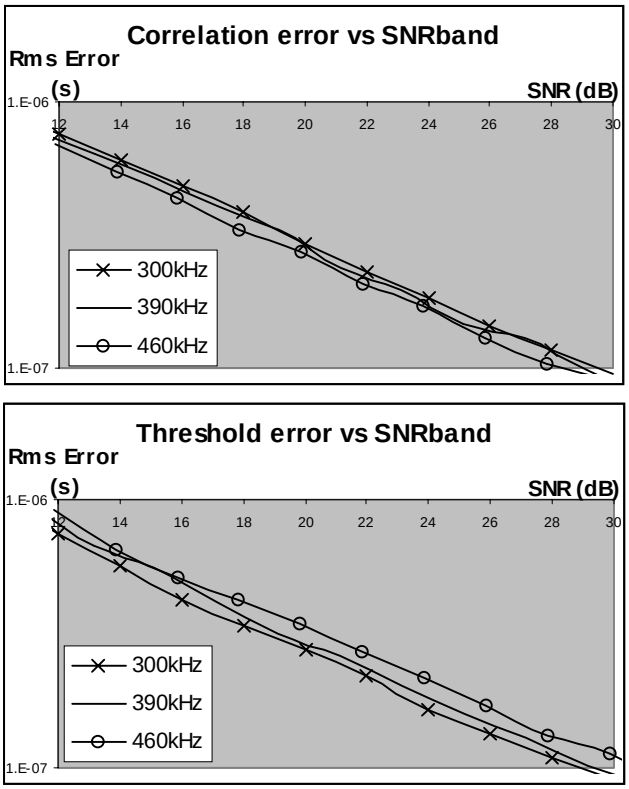

'SNRband' refers to the SNR of the signal established over a fixed bandwidth of 300kHz, not taking into account the noise spectral components falling out of this band.

Figure 5-4 Rms measurement error versus SNR referred to same noise bandwidth

As seen on these two graphs, whatever the amount of the non-optimum-band noise power is, correlation provides approximately the same accuracy. On the other hand, the higher the bandwidth, the less accurate the threshold measurement.

The conclusion is that correlation is able to filter the spectral components represented in Figure (5.3) by the two areas A and A', whereas the threshold process is hindered by these components that it cannot filter. Correlation therefore proves more robust to noise.

5.2 Comparison of non-perfect shaped pulses

The previous section presented the case of time measurements performed on equal amplitude and symmetrical Gaussian pulses. This is a simplistic case, although it proved interesting in the analysis of the differences between threshold and correlation methods. The focus of this section is to consider pairs of non-perfect pulses, which may have different amplitude, be either asymmetrical, or present symmetry for one of the pulses and asymmetry for the other pulse. The goal of this comparison is to go deeply into the analysis of the differences that arise between these two methods, and determine if one may be more valuable than the other for a specific case. Since analytical developments are difficult for these cases, a practical approach based on simulations is adopted. The following study will therefore be more qualitative than quantitative.

5.2.1 Asymmetrical pulses

In this section, both pulses will be of equal amplitude but of asymmetrical shape. This case of study is justified by the fact that some receivers may not respond to incoming symmetrical pulses with a symmetrical output due to capacitance effects, or non-linear phase filtering. Such a problem is illustrated in Figure (5.5).

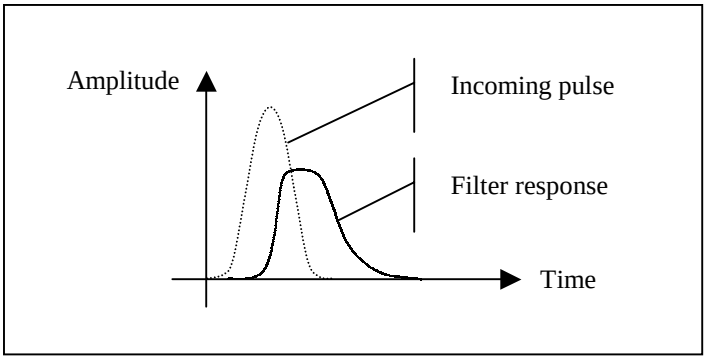

Figure 5-5 Imperfect time response of a filter to a symmetrical pulse

The simulations were performed in this special case. One important point to note is that the time measurement should not be biased since both pulses are asymmetrical, with the same degree of asymmetry.

5.2.1.1 Notation

All the pulses that are used in this part are referenced to a symmetrical pulse of same amplitude and energy. If the reference symmetrical pulse is modeled by the function:

$$p_{symm}(t) = A \times \exp(-a^2 t) \tag{5.11}$$

and has a constant 'a' equal to 650e9 s^{-2}, where 'a' is the inverse time constant squared of the Gaussian pulse, two ratios quantifying the asymmetry of the pulse as compared to the symmetrical pulse are derived.

$$\begin{aligned} r_1 &= a / a_1 \\ r_2 &= a / a_2 \end{aligned} \tag{5.12}$$

The asymmetrical pulse $p_{asymm}(t)$ is of the form:

$$\begin{aligned} p_{asymm}(t) &= A \times \exp(-a_1^2 t) \qquad \text{for } t \in [\, -\infty , 0 \,] \\ p_{asymm}(t) &= A \times \exp(-a_2^2 t) \qquad \text{for } t \in [\, 0, +\infty \,] \end{aligned} \tag{5.13}$$

We choose $r_1 < 1$, resulting in $r_2 > 1$ since p_{symm} and p_{asymm} have the same energy. The relationship between r_1 and r_2 is straightforward, and given as a result in equation (5.14):

$$\sqrt{r_1} + \sqrt{r_2} = 2 \tag{5.14}$$

5.2.1.2 Simulation

Three cases were tested, with increasing asymmetry of the pulse as compared to the reference symmetrical pulse. The three values of r_2 are: 1.5, 1.8, and 2.2, and the respective values of r_1 are: 0.6, 0.4, 0.3 according to equation (5.14). The noise bandwidth was restricted to that given by the steepest slope of the pulse (a_1 in our case), which is the highest frequency component of the pulse that passes the filter. If we recall that the constant 'a' of the Gaussian pulse is linked to the half-power bandwidth by:

$$a = \frac{(\pi B)^2}{4 \times \ln(\sqrt{2})} = 7.12 \times B^2 \qquad (5.14)$$

then the noise bandwidths used for the three simulations are respectively: 318, 390, and 460kHz. The results of the simulation are presented in Figure (5.6).

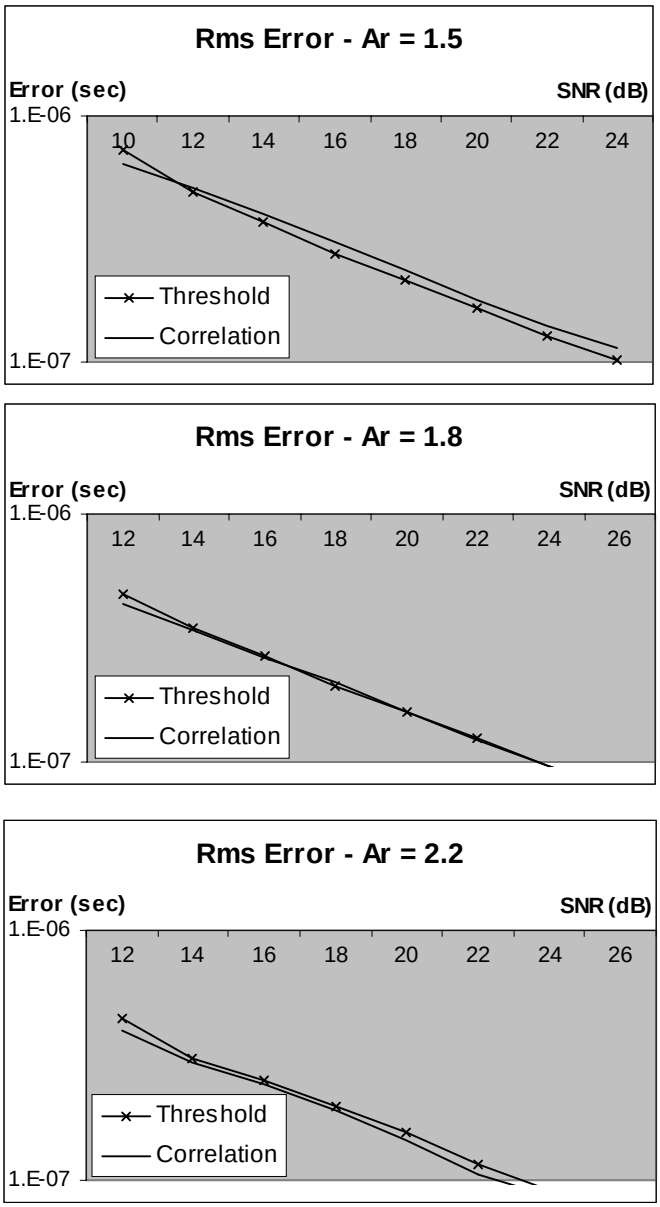

Figure 5-6 Rms error of the time measurement for asymmetrical pulses

Ar corresponds to r_2

5.2.1.3 Comments

According to Figure (5.6), the more the pulses are made asymmetrical, the closer the correlation result is to the threshold curve, till it goes below the threshold law. This means that correlation provides more and more accurate results as compared to the threshold method as the asymmetry of the pulse is increased. The reason for such an observation is given in the following part.

5.2.1.4 Discussion

There are two reasons for the correlation method to be more and more accurate as the asymmetry of the pulse is increased. The first one follows the time domain property of correlation introduced in the literature review of this thesis: correlation is a measure of similarity between signals as a function of their time delay. The more asymmetrical the pulse, the less similarity there is between a noise peak and the noise-free pulse.

The second reason is that as the asymmetry of the pulse is increased, the filter that needs to be used will have a larger bandwidth in order not to distort the pulse, resulting in a higher noise bandwidth. Hence, the graphs confirm again the discussion of paragraph 2.4.2, which concluded that correlation was important for its filtering properties.

5.2.2 Symmetrical and asymmetrical pulses

The case of two pulses received, one of which is symmetrical and the other one asymmetrical can be encountered in systems where several pulses are sent. One of the pulses is a reference pulse generated by the transmitter, and the other ones are all of the same shape, and generated by the receiving system.. If the time delay information between this reference pulse and the pulses of the other kind is needed, then a bias problem is generated. The goal of this chapter is to illustrate this result, and determine how the threshold and correlation methods react to this problem.

5.2.2.1 Simulation

Using the notation of paragraph 3.1.1, the symmetrical pulse of the previous chapter was considered as the reference pulse. The asymmetrical pulse was described by the ratio r_1 equal to 1.2, 1.5 and 1.8. Both pulses have the same energy. The resulting noise bandwidths are 318, 390 and 459kHz. Figure 5.7 presents the results of these simulations.

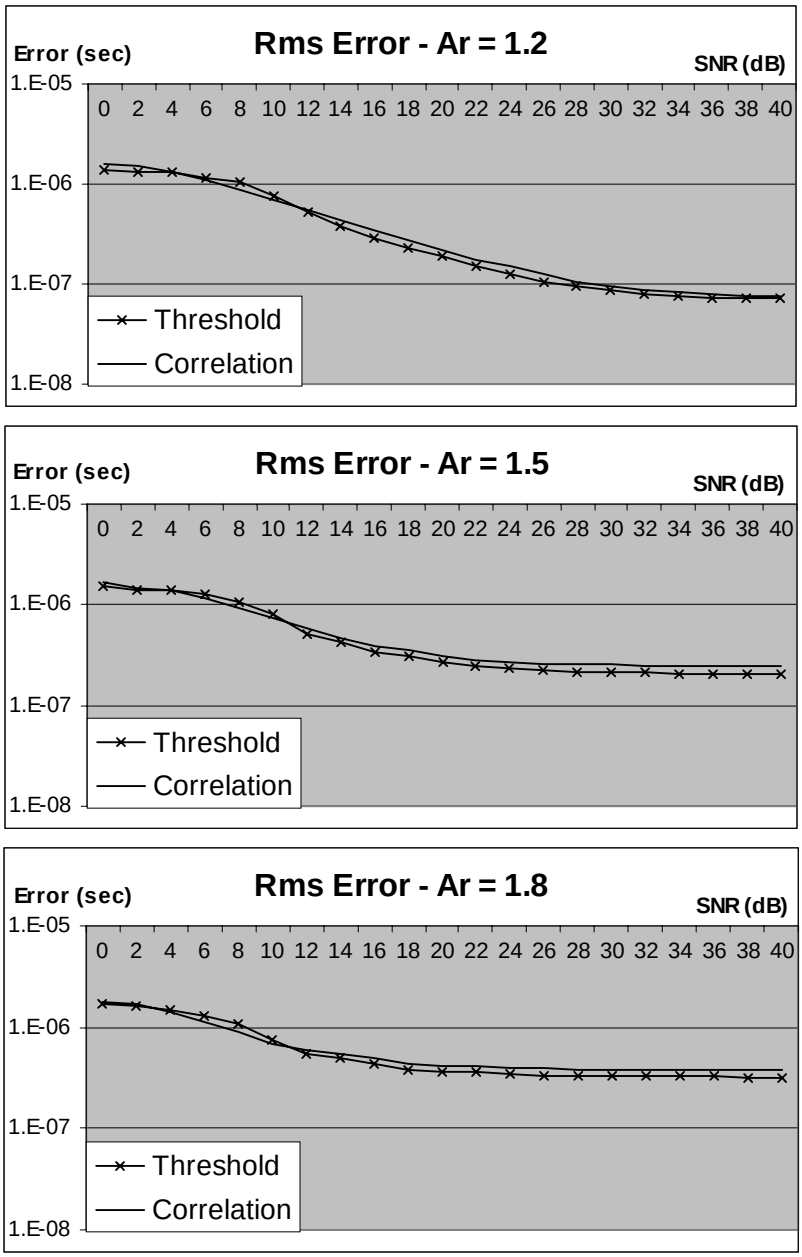

Figure 5-7 Rms error of the time measurement for symmetrical/asymmetrical pulses

5.2.2.2 Discussion

Two points can be mentioned according to Figure (5.7). The first one is that as predicted, both methods suffer from a bias in the time measurement error. This is explained graphically in Figure (5.8). This bias does not exist in the case of the time delay between two asymmetrical pulses as long as both pulses are similar.

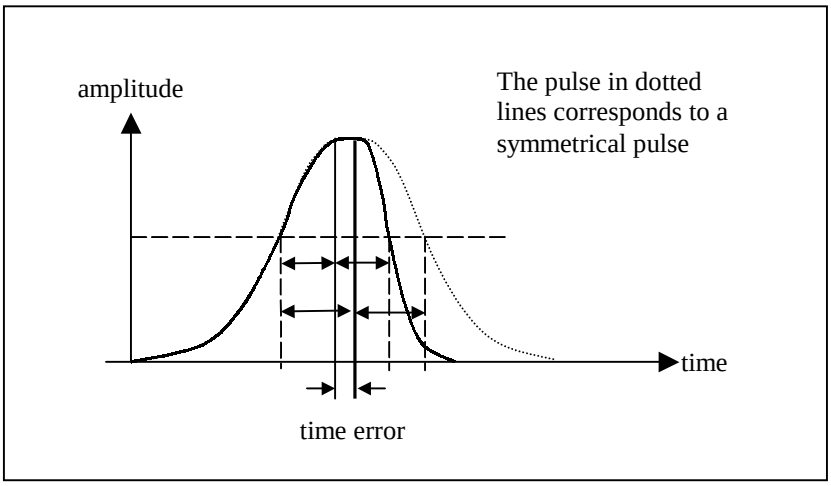

Figure 5-8 Inherent error in the location of the center of the pulse for an asymmetrical pulse as compared to a symmetrical pulse

The second important point is that whatever the ratio of asymmetry is, the correlation method provides less accurate results than the threshold method. This is simply due to the bias that is smaller in the case of a threshold process as compared to the correlation process. This result can be proved through pages of mathematical derivations. This demonstration will be avoided, but to convince oneself, one can try to correlate two discrete signals such as the vectors [0, 1, 2, 0] and [0, 0, 2, 0]. The threshold measurement at 50% of the peak of the signal (= 2) yields a time delay error of ¾, whereas the correlation method generates a 5/4 error with a threshold level at half the height of the pulse.

5.2.3 Pulses with different amplitudes

Two pulses can be received with different amplitudes, such as in systems where a detector receives pulses from two transmitters, one of which is farther away than the other. The pulse from the closer transmitter will suffer less propagation loss, and will have a higher SNR as compared to the other signal. This is equivalent to having the same noise level, but two pulses with different amplitudes.

5.2.3.1 Simulation

The simulation consisted in generating pulses with a half-power bandwidth equal to 300kHz, but with different amplitudes, and adding noise filtered at that bandwidth. The ratio ‘r’ of the higher amplitude to the lower one was made equal to 1.4, 1.7, 2, and the results are presented in Figure (5.9). The SNR scale is referred to the lower pulse.

The curve called ‘Skolnik’ is simply the rms value of the results given by equation (5.1) adapted to the SNR of both pulses. This curve is mathematically modeled by:

$$\delta T_R = \sqrt{\frac{1+\frac{1}{r^2}}{a\times\left(\frac{S}{N}\right)_{lower}}} \tag{5.15}$$

where $(S / N)_{lower}$ is the SNR of the pulse with lower amplitude.

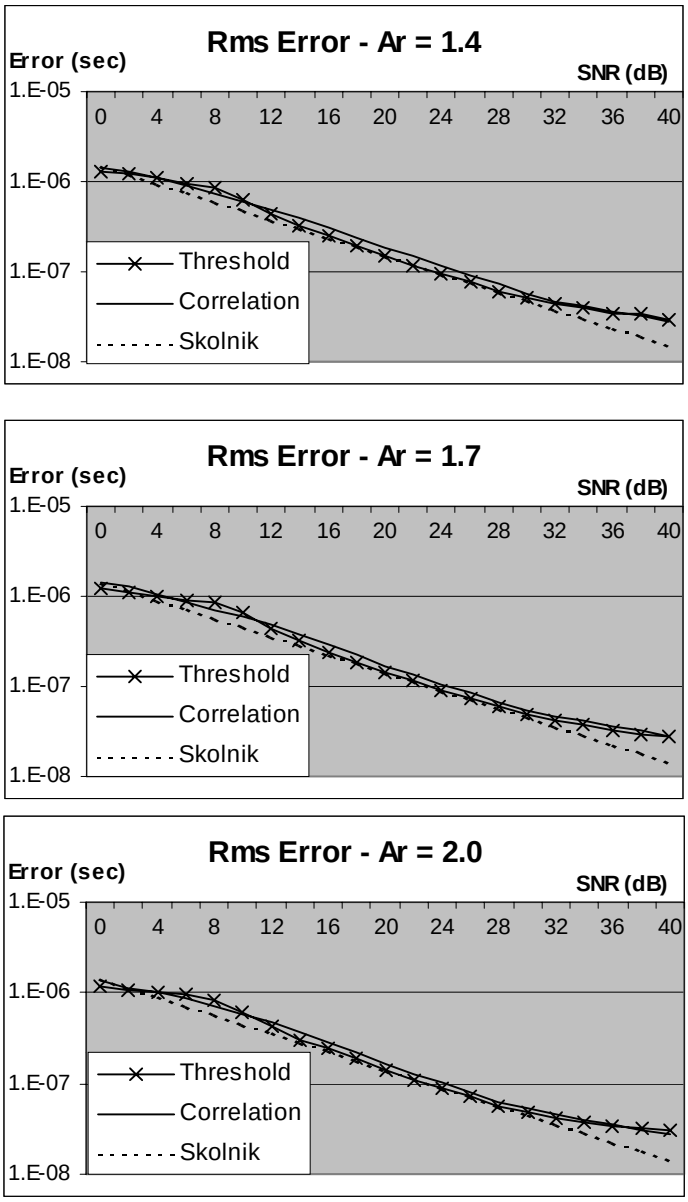

Figure 5-9 Time measurement error in the case of pulses having different amplitudes

5.2.3.2 Comments

The graphs presented in Figure (5.9) are similar with each other. This suggests that the variations in the ratio of the amplitude do not have a major impact on the results since the error is the same in each graph. Besides, the difference in accuracy between the correlation and threshold curves is constant although the ratio of amplitude is changed.

5.2.3.3 Discussion

Figure (5.9) proves again that at the bandwidth of the matched filter, the threshold method is the most accurate method to determine time delays, whatever the ratio of the pulse amplitude. This is a logical result since the rms error of the measurement is simply the root-mean-square value of the errors given by equation (5.1) for the SNR of each pulse. As compared to the case where the pulses are symmetrical and of same amplitude equal to that of the lower pulse in this simulation, the factor that has to be considered to evaluate the rms error is:

$$\text{Factor} = \sqrt{\frac{1+\frac{1}{r^2}}{2}} \tag{5.16}$$

This factor is not changed a lot as the ratio of the amplitudes changes. For instance, increasing ‘r’ by two increases the factor by 1dB. This explains why the effect on the time delay measurement of the differences in amplitude between two pulses can be neglected.

5.3 Discussion

Correlation has proved important in cases where the filtering is not perfect, in other words when the bandwidth of the noise is higher than that given by the matched filter. The bandwidth for which correlation is more accurate has been evaluated analytically, and verified practically through simulation. Yet, this result is valid as long as the pair of pulses that are measured are similar, that is either both symmetrical, or both asymmetrical. When one of the pulses is symmetrical, and the other one is not, then a bias is introduced in the measurement. This bias is bigger with a correlation measurement. Finally, when the pulses that are processed are of different amplitudes, the resulting impact on the accuracy of each method can be neglected.

Using correlation as a time measurement method is therefore suggested in cases where filtering cannot be matched with that of a matched filter.

5.4 Conclusion

The analytical developments performed in Chapter 2 and 3 of this thesis were compared to practical cases, and proved to match theoretical results in simple cases: symmetrical pulses with different noise bandwidths, and different amplitudes. In the complex cases where pulses can be asymmetric, the analytical results do not take account of the errors added.

The result of the above comparison is that correlation is an important time measurement method in cases where filtering is performed at bandwidths higher than that given by a matched filter. This is due to the filtering properties of that method. In the other cases, a simple threshold measurement will at least provide the same error, but will be more accurate in general. This comparison therefore suggests that correlation is appealing in a limited number of cases.

Yet, the discussion was based on the results given at high SNR, assuming that the pulses were always detected, and never mistaken for a noise peak. In order for this discussion to be of interest, we need to implement a method to increase the SNR of the received signals, and also detect pulses with a good probability of detection. This is the purpose of the next chapter.

Chapter 6

6. Detection Improvement

The previous chapters of this thesis have focused on the problem of determining which method between correlation and threshold is the most accurate for time delay measurements on Gaussian pulses. This discussion was based on analytical results and simulations, all performed with the ideal assumption that the expected pulses were indeed processed, in other words detected. Besides, it was shown that below a certain SNR, practical results diverge from expected ones due to numerous ambiguities. The implementation of a detection mechanism prior to the measurement system is therefore needed.

As mentioned in the literature review, it is important for a measurement system, especially a low SNR, to work with a gated-mode mechanism where time measurements errors are bounded by the window size of the observations. Since the subject of this thesis specifies that noise bandwidths be close to that given by a matched filter, noise peaks are always of width almost equal to that of pulses. Therefore, the smaller the window, the lower the potential number false alarms. As a result, a time-window algorithm where only signals within an interval of time are processed is required.

Yet, although this window of time can be thoroughly centered on expected pulses, it does not necessarily mean that the following measurement method will not fail in localizing the pulses since noise will still be present at the output of the detection process. Integration, which has the property to lower the overall noise level of a received signal, will be used for this issue.

Gathering all above ideas, this chapter deals with the implementation of a detection mechanism that ensures the processing of expected pulses within a time window of

observation corresponding to the occurrence of these signals. The combination of M/N detection and integration over a time window is proposed as the solution to this problem. M/N detection is used to detect expected pulses and generate a time window over which integration is going to clean pulses from noise.
Hence, Section 6.1 focuses on the M-out-of-N detection process, both theoretically and practically. Section 6.2 reviews the theoretical results of the integration theory, and verifies these results through simulations. Finally, Section 6.3 comments the combination of both methods.

6.1 M-out-of-N detection

M/N detection is a detection method used in many surveillance radars as introduced in the literature review of this thesis. This method is based on several threshold crossings, and provides the same detection and false alarm probabilities than a single pulse detection, but at lower SNR. While a single pulse detection may require a SNR of 12 to 16dB, M/N detection can provide the same reliability of the detection process at SNR as low as 6dB for instance. This method is described in detail in Section 6.1.1. The results of this section are used to justify the use of M/N detection in our proposed solution in Section 6.1.2. An experiment is set in Section 6.1.3 in order to check the validity of the analytical results of M/N detection on which our solution relies. Finally, Section 6.1.4 presents two methods for the determination of the parameters needed for the implementation of this method.

6.1.1 Presentation of the method

M-out-of-N detection consists in deciding that a target has been detected, upon reception of a train of N pulses, if M out of N threshold crossings occurred (M<N) at the same instant in the period of the train. A graphical explanation is provided in Figure 6.1.

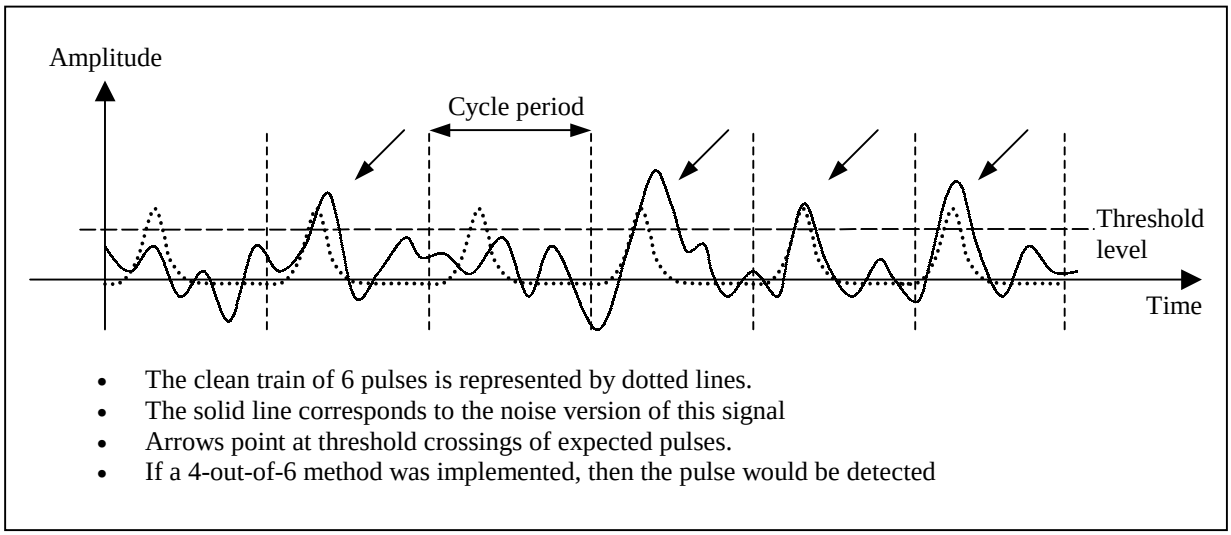

Figure 6-1 Illustration of the detection decision in a M/N detection method

Two thresholds are therefore employed: one to report all the instants of the period where a threshold occurred, and the second to count how many crossings have been experienced at these instants. Mathematically, if P_d is the probability of detection of one pulse, then the probability of detection of M pulses out of N trials is given in [Too82]:

$$P_{dM} = \sum_{i=M}^{N} \binom{N}{N-i} P_d^i \times (1-P_d)^{N-i} \tag{6.1}$$

The same formula can be applied to the probability of false alarm by replacing P_d by P_{fa}. For higher probability of detection, M, the number of crossings required for detection, has to be decreased, whereas for lower probability of false alarm, M needs to be increased.

It was proven in [Too82] that by processing N pulses the resulting probability of false alarm can be decreased while maintaining the same probability of detection. Allowing fast reductions of false-alarm rates at constant or even improved probabilities of detection thus reduces the SNR level at which a system can work.

6.1.2 Justification of the choice of the method

The presentation of M/N detection shows that this detection scheme is a form of integration. However, it is reported in [Sko80] to be less efficient than coherent integration. Integration is presented in Section 6.2 of this chapter, and considered as giving the best detection performances according to [Sko80]. M/N detection has the advantage of simplicity though. To justify this idea, one should remember that detection has to be performed over all the received signals. Integration therefore requires the storage of a complete period of the signal and summation of several cycles. Digitally, this process requires a memory equal to total number of points of a cycle times the number of bits of resolution, as given in equation (6.2).

$$\text{Memory}_{\text{integration}} = N_P \times N_B \tag{6.2}$$

N_P is the number of points of the cycle, and N_B the number of bits of resolution.

M/N detection however needs a memory to store the number of threshold crossings for each point of the signal. The memory requirement for this process is given in equation (6.3).

$$\text{Memory}_{\text{M/N detection}} = N_P \times \text{ceil}\left(\text{Log}_2(N_C)\right) \tag{6.3}$$

N_C is the number of cycles of the signal that is processed. The ceil(.) operator rounds a number up, so that ceil ($\text{Log}_2(N_C)$) is the total number of bits needed to store the number of threshold crossings of any point within N_C cycles of signal.
Typical numbers for N_B range from 8 to 12 bits of resolution. The number of cycles N_C that are studied is, in general, less than a hundred. Chapter 7 of this thesis actually presents an experiment where N_C is equal to 9, and $N_B = 8$. With such numbers, the ratio of equation (6.2) and (6.3) is equal to 2. This means than M/N detection requires half the memory of integration in the specific case presented in Chapter 7. Therefore we will prefer the implementation of M/N detection for detection of pulses rather than integration over all the received signal. Nevertheless, this solution will not prevent the use of

integration over the selected time windows, which are of insignificant length as compared to the cycle time. In Chapter 7, the practical problem that we consider has a cycle duration of 5ms, whereas the pulses are 3µs long.

Other detection methods were introduced in the literature review. These methods: inverse probability receiver, likelihood-ratio receiver, with the exception of the Neyman-Pearson observer, are all based on the knowledge of probability-density functions of the signal and/or noise, or an a-priori probability of the signal plus noise. Since the case of study that we are considering consists of different pulse shapes, within different noise environments, the application of these two methods would require a determination on the fly of the type of pulse that is analyzed in order to apply appropriate filtering. This is of course not practical unless the order of arrival of each pulse is fixed. Yet, even in that case, false alarms may cause the detection of too many pulses, making it impossible to identify the expected pulses and to implement the appropriate filter. To avoid complication that would not systematically be profitable, M-out-of-N detection was selected as the best solution based on the tradeoff of performance/complexity.

6.1.3 Choice of parameters

The choice of M and N is based on the targeted probabilities of detection and false alarm, associated with the same probabilities without M-out-of-N detection, as given by equation (6.1). Two methods can be applied to determine M and N based on the assumptions or case of study that needs considering when applying the method.

6.1.3.1 Radar approach

An economical approach for the problem of choosing M and N was originally proposed in [Sch56], and further developed in [Lin56]. J. F. Walker extended the method in [Wal71] to Swerling case 1, 2, and 5 RCS radar targets. The Radar Cross Section (RCS) of a target quantifies the amount of power reflected towards the Radar source as compared to the incident power density. A Swerling case 5 target for instance designates a target with constant cross-section, as compared to the other cases that model RCS

fluctuations. The definition of these models is provided in most textbooks on radar, yet the reader is encouraged to refer to the paper of P. Swerling: [Swe60].

The method for identifying M and N consists in considering that the signal we plan to detect follows one of the RCS target models: Swerling 1 to 5. Then, given the analytical representation of these models, and using equation (5.1), J. F. Walker reports that there is an optimum value of M that minimizes the SNR, given the targeted probability of detection, false alarm, and N. Curves summarizing the optimization are provided in [Wal71] for any kind of radar RCS.

This method is said to be economical in the sense that in complex problems where partial knowledge of the target is obtainable, it is easier to refer to ideal models and develop analytical solutions for these specific forms. In our case of study, the pulses are assumed to have constant amplitude, which corresponds to a Swerling case 5, or non-fluctuating target. In that case, we can refer directly to Figure (6.2) that gives the optimal number of minimum threshold crossings M as a function of the total number of cycles N. Yet, since this curve is an approximation – no dependence with the SNR is assumed – it is advisable to crosscheck one's result with the curves provided in [Wal71].

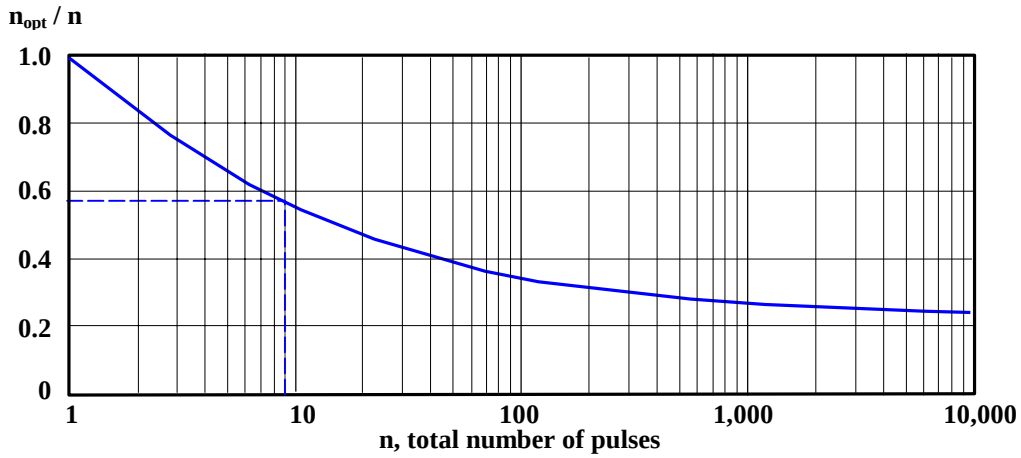

Figure 6-2 Optimum choice for M versus N in M/N detection

The blue dotted lines are used later for illustration

6.1.3.2 Practical approach

The second method that we propose is more complex but more reliable for accurate predictions. This approach allows taking into account considerations such as time

processing requirements, and consists in finding the optimum combination of the M/N detection parameters: M and N for a specific problem, based on the real distribution of the signal and noise. By collecting samples of signals at high SNR, and noise samples at low SNR, a database of the noise-free pulse and noise samples can be established. By simulating a certain SNR, in other words, taking a noise-free pulse and adding to it a noise sample at the rms value consistent with the targeted SNR, the number of threshold crossings generated by this pulse over a certain number of repetitions can be recorded. Taking the ratio of the number of times the expected pulse was detected and the number of repetitions of the experiment leads to an evaluation of the probability of detection of this pulse for a specific SNR. The same technique is applied to compute the probability of false alarm for a specific SNR by computing the number of times noise peaks resulted in threshold crossings.

These two steps allow the computation of the detection and false alarm probabilities over the SNR of interest. A binomial expansion of the two probability curves can then be added, as given by equation (6.1). Based on the specification of the problem that the design engineer faces, the maximum processing time and the SNR requirements, the probabilities he is targeting can be searched.

This method therefore involves the analysis of the signal and noise distributions prior to setting the detection system. It can be easily bypassed by the previous method when complex problems have to be considered. On the other hand, the method that we have developed allows taking account of real constraints on the system, like the processing time – linked to N – and true probabilities of detection and false alarms for the signals that are studied. Chapter 7 of this thesis provides a practical experiment where N is determined to be 9, and the appropriate value of M is 6. If Figure (6.2) is used, then the optimum value for M is 6 when N equals 9, as represented by the dotted lines. This shows that the optimum value for M is not always the value that is required for a specific problem. Our approach is needed to take into account practical constraints.

6.1.4 Simulation

The purpose of this experiment is to prove that equation (6.1), on which all the theory of the M-out-of-N detection relies, is applicable. If this equation is verified practically, then the second approach presented in Section 6.1.3.2 will be valid.

6.1.4.1 Simulation description

A noise matrix is generated using random values. Each point of this matrix is actually the result of the summation of a thousand random values contained between –0.5 and 0.5 volts. The overall distribution of the result of this process is approximately Gaussian according to the Central Limit Theorem. By convolving this matrix with the impulse response of a rectangular filter given in equation (6.4), the bandwidth of the noise is adjusted to 300kHz.

$$\text{Impulse}_{\text{rect fc}}(t) = \sin(\pi f_c t) / (\pi f_c) \tag{6.4}$$

f_c is the 300kHz cutoff frequency.

A Gaussian pulse matching that noise bandwidth was generated as given by equation (6.5) and (6.6). Equation (6.6) relates the shape of the Gaussian pulse to the near matched rectangular filter, as obtained in Chapter 5 of this thesis.

$$P_{\text{Gaussian}}(t) = A \times \exp(-a^2 t) \tag{6.5}$$

$$a \cong 2.64 \times f_c^{\,2} \tag{6.6}$$

The probability of detection P_d of the Gaussian pulse was computed for different SNR and different threshold levels by recording the number of times the pulse crossed the threshold, and dividing this result by the number of times the experiment was performed:

500 times. This leads to an approximation of the probability of detection of this signal as described in Section 6.1.3.2.

The same study was performed with the noise without any signal pulse, but with the same threshold level. The experiment was carried out over 20,000 noise points. By setting the threshold level to 50%, results for P_d and P_{fa} were then computed for several combinations of M and N: 3/5, 4/7, 5/7, and by using the binomial formula provided in equation (6.1).

These theoretical results were then compared to experimental ones by simulating each M/N method at different SNR (threshold level set at 50%), and computing the resulting detection and false alarm probabilities.

Figures 6.3 and 6.4 present the results of the simulations.

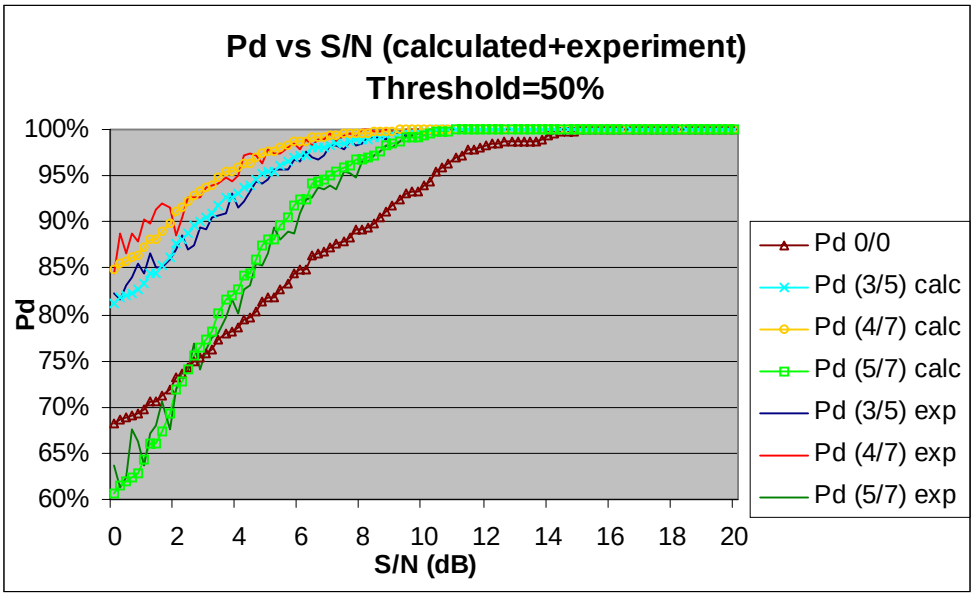

Figure 6-3 Probability of detection in practical and experimental cases

The figure in parentheses is the combination of M and N of M/N detection

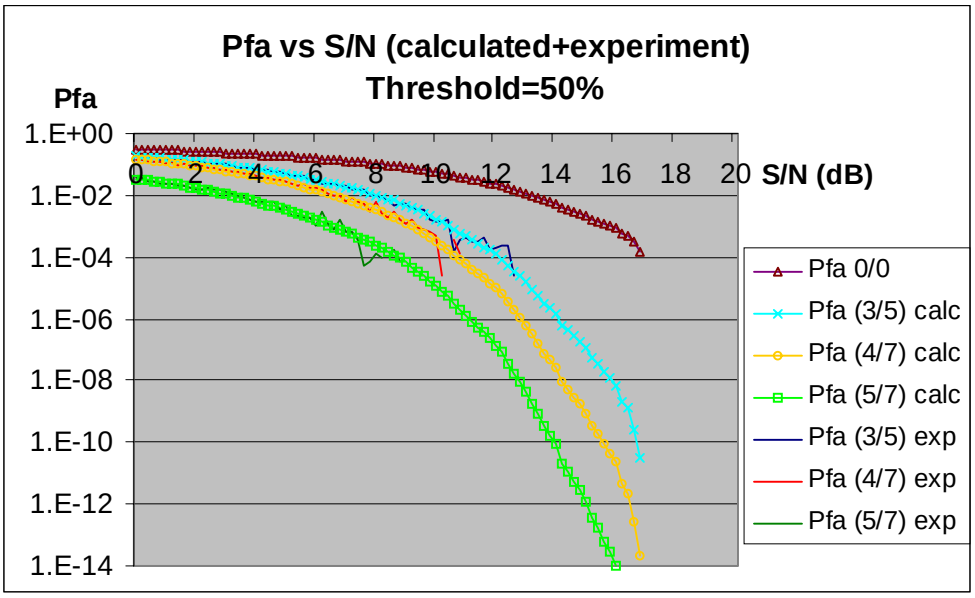

Figure 6-4 Probability of false alarm in practical and experimental cases

The figure in parentheses is the combination of M and N of M/N detection

6.1.4.2 Comments and conclusions

As seen from Figures 6.3 and 6.4, the practical curves of the evaluated detection and false alarm probabilities match closely the analytical results modeled by equation (6.1). In the case of the probability of false alarm, practical results could not be obtained below a probability P_{fa} given by one point of false alarm divided by the maximum number of points studied (20,000 points), that is 5×10^{-4}. We note however that there is a good correlation between theoretical and practical results, suggesting that the method presented in Section 6.1.3.2, which relies on equation (6.1), is valid. Consequently, this method will be used for the final experiment of this thesis.

6.2 Integration process

As discussed in Section 6.1.2, M/N detection is preferred to integration as the detection method that we plan to apply. The main reason is that integration suffers from high

memory requirements inherent to its implementation, whereas M/N detection is much simpler to employ. However, integration provides useful properties that need to be used in our detection scheme. Integration, as reported in [Too82], has the property to “dig the signal out of the noise”. This is particularly important even if the expected signals are detected, because noise will still exist at the output of the M/N detector. The presence of noise may make the time measurement fail, even in a window of time as illustrated in Figure (6.5).

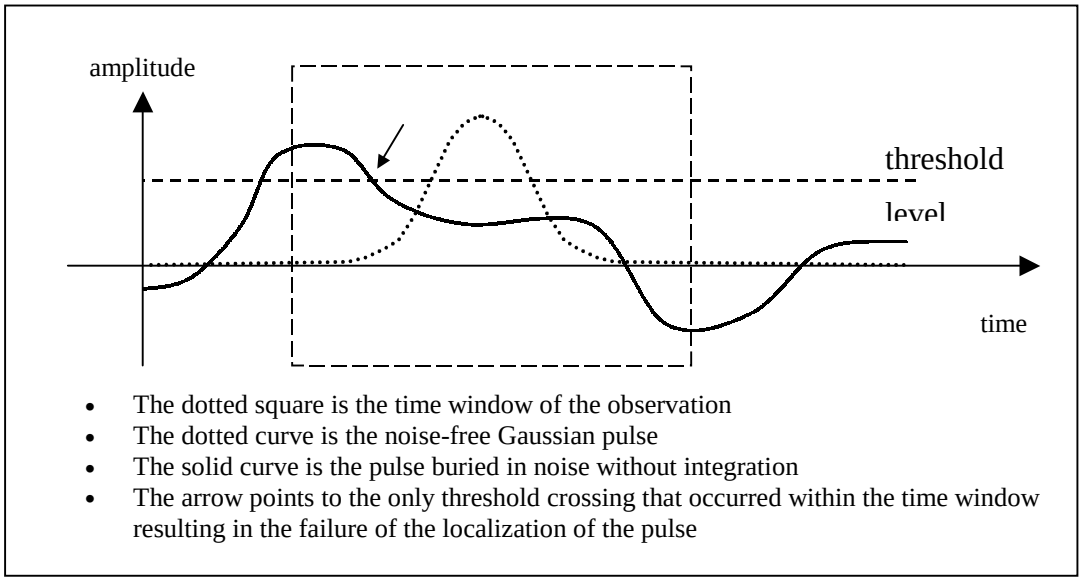

Figure 6-5 Failed threshold measurement due to noise

Section 6.2.1 therefore presents the integration method and the main associated results. Section 6.2.2 is focused on the association of M/N detection and integration. Section 6.2.3 explains how to chose the integration number. Finally, Section 6.2.4 is dedicated to the comparison of two methods: integrating Z times a signal prior to the threshold measurement, and averaging the Z threshold measurements over the same samples of signal. This discussion is needed since integrating involves a demanding processing in terms of memory and operations, whereas averaging the results of measurements is a straightforward operation.

6.2.1 Presentation of the method

Integration is the process of averaging a cyclic signal over its period. When the phase of the signal that is integrated is preserved, averaging is called a coherent integration. In a radar system, coherent integration is typically performed at IF, and the gain of this process can be mathematically calculated as equal to the number of integrated cycles, as reported in [Too82].

$$\text{Gain integration} = n \tag{6.7}$$

n is the number of pulses that are integrated.

On the other hand, post-detection integration, that means integration at the output of a video detector, is much simpler to perform. However, the loss of the phase information results in a loss as compared to the coherent gain. This loss I_{Loss} is called the integration loss, and is defined in dB by equation (6.8).

$$G_{\text{non-coherent}} = G_{\text{coherent}} - I_{\text{Loss}} \tag{6.8}$$

$$G_{\text{non-coherent}} = 10 \times \text{Log}_{10}(n) - I_{\text{Loss}} \tag{6.9}$$

This integration loss in dB can be plotted as a function of the number of pulses and the probability of detection and false alarm, and is found in Figure (6.6), but also in [Sko80].

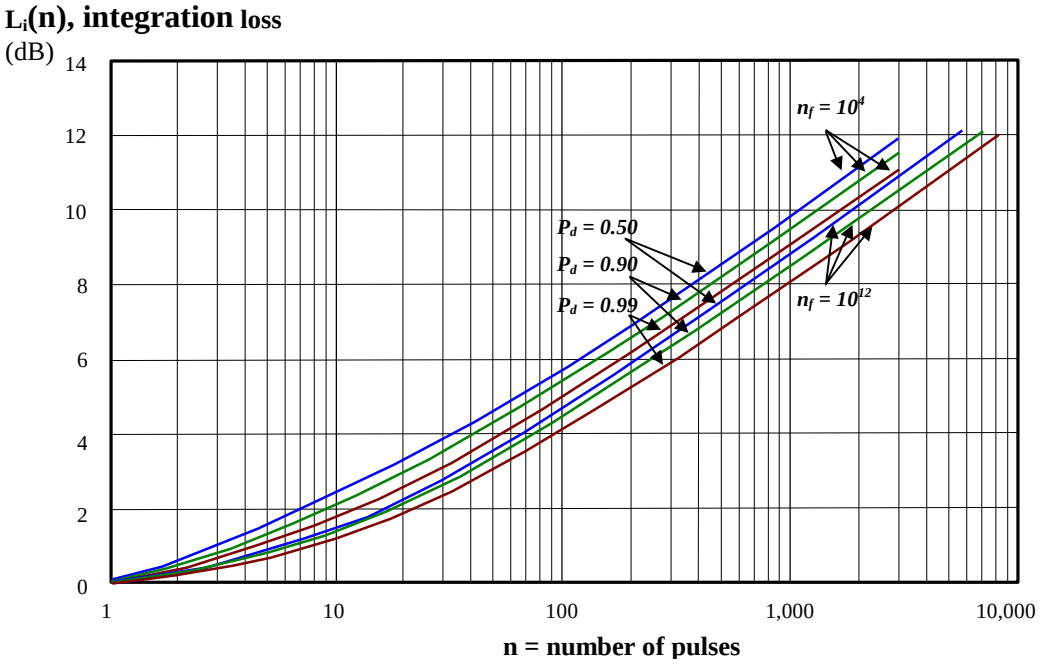

Figure 6-6 Integration loss

P_d is the probability of detection, and n_f the number of false alarms

6.2.2 Association of M/N detection and Integration

Integration is a valuable way to improve the SNR of a signal, and is fundamental in the process of detecting and performing measurements on signal samples. The association of M/N detection and integration implement both of these actions while maintaining a reasonable memory requirement for the overall process. The memory requirement of this combination of methods is derived from equation (6.2) and (6.3), and given in equation (6.10).

$$\text{Memory}_{\text{ M/N detection \& integration}} = N_P \times \{ M \times R \times N_B + \text{ceil}(\text{Log}_2(N_C)) \} \qquad (6.10)$$

N_P is the number of points of the cycle; M is the number of pulses that are processed in the integration part; R is the ratio of the number of points of the time window and N_P; N_B is the number of bits of resolution; N_C is the number of cycles of the signal that are processed. Taking the example of the final experiment of this thesis where:

$$M = 2,\ R = 10^{-3},\ N_B = 8,\ N_C = 9$$

then the ratio of equation (6.2) and (6.10) is equal to 1.99. This means that the combination of M/N detection and integration over the detected windows of time relaxes the memory requirement as compared to integration alone over all the signal cycle. The implementation of this configuration is represented in a block-diagram form in Figure (6.7).

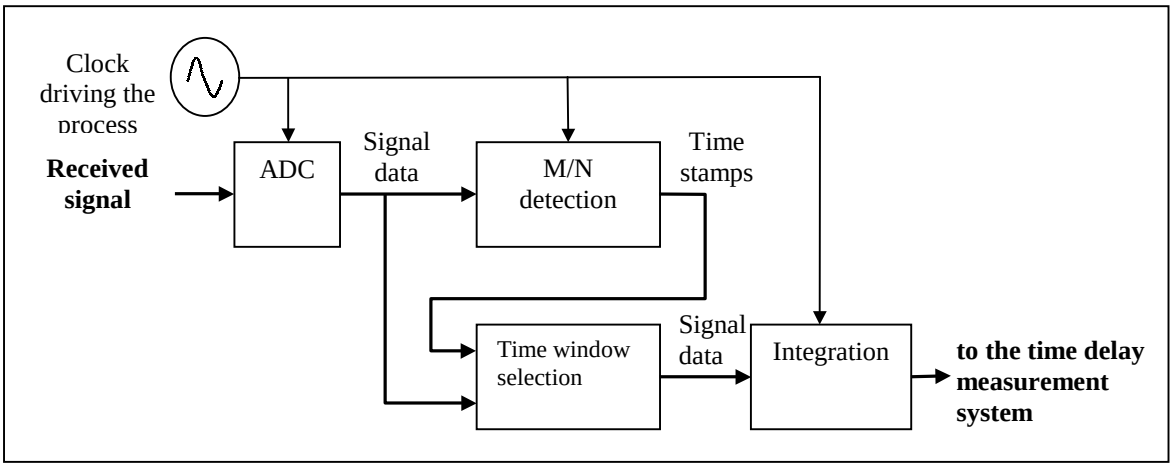

Figure 6-7 Block-diagram of the combination M/N detection and integration

The signal from the receiver is digitized in the ADC, and presented to the M/N detection block. The output consists of time stamps of the time windows associated with the detected pulses. The second flow of data samples is passed to a block that selects the samples corresponding to the determined time windows. The selected samples are then integrated. The output of integration is sent to the measurement part. It has to be noted that the design of Figure (6.7) is an illustration of the overall process that we plan to implement, and does no reflect all the problems inherent in synchronization of each subsystem. Dealing with these issues cannot be performed in an overall sense, but will be performed in the specific case of the final experiment of Chapter 7.

6.2.3 Choice of the integration number

The integration gain for coherent integration was said to be equal to the number of integrated pulses according to equation (6.7). When non-coherent integration is

considered, then a loss has to be added. Figures found in [Sko80], similar to Figure (6.6), give the loss associated with the integration number, the probability of detection, the probability of false alarm, and the type of RCS target considered. Therefore, the method for choosing the required integration number already exists and will be used as is.

6.2.4 Integrating versus averaging

The use of integration after M-out-of-N detection is needed to improve the SNR of detected pulses, as mentioned in Section 6.2.2. This improvement enables time measurements in the linear region (log/log scale) of the error curve given in Chapter 3 of this thesis. Consequently, integration is mainly used in our scheme to facilitate time localization of the pulses. However, integration is a complex and demanding process in terms of memory requirement and processing speed. It is therefore reasonable to wonder if a very simple method like averaging several results of time measurements is not a more appropriate configuration for our solution. This question is the focus of the following paragraphs.

6.2.4.1 Theoretical study

6.2.4.1.1 Gain associated with averaging

If the process of averaging Z time delay measurement errors e_j is simulated N times, then the vector of the errors ε is given by equation (6.11). Each error e_i of this vector is given in equation (6.12).

$$\varepsilon = [e_1\ e_2\ e_3\ \ldots\ e_N] \tag{6.11}$$

$$e_i = \sum_{j=1}^{Z} \frac{e_{i\ j}}{Z} \tag{6.12}$$

The mean-square value of the error vector ε is given by equation (6.13), and expanded in equation (6.14).

$$\mathrm{rms}^2(\varepsilon) = \sum_{i=1}^{N} \frac{e_i^2}{N} \tag{6.13}$$

$$\mathrm{rms}^2(\varepsilon) = \frac{1}{N}\sum_{i=1}^{N}\left(\sum_{j=1}^{Z}\frac{e_{i\,j}}{Z^2}\right)^2 + 2\times\frac{1}{N}\sum_{i=1}^{N}\left(\sum_{j\neq l}^{Z}\frac{e_{i\,j}\times e_{i\,l}}{Z^2}\right) \tag{6.14}$$

If the error e_i were due to thermal noise, we would expect the noise samples to be independent. As a result, the second term of equation (6.14) tends towards 0 as N, the number of repetition of the experiment, tends toward infinity. This conclusion leads to equation (6.15).

$$\mathrm{rms}^2(\varepsilon)_{\,N\to\infty} = \frac{1}{N}\sum_{i=1}^{N}\left(\sum_{j=1}^{Z}\frac{e_{i\,j}}{Z^2}\right)^2 \tag{6.15}$$

Hence:

$$\mathrm{rms}^2(\varepsilon)_{\,N\to\infty} = \frac{1}{Z}\times\left(\sum_{l=1}^{N\times Z}\frac{e_l^2}{N\times Z}\right) \tag{6.16}$$

$$\mathrm{rms}^2(\varepsilon)_{\,N\to\infty} = \frac{1}{Z}\times \mathrm{rms}^2(e) \tag{6.17}$$

e is the error associated with a single time delay measurement.

The result provided by equation (6.17) shows that the mean square error associated with averaging Z time delay measurements is equal to the mean square error of a single time delay measurement divided by Z.

6.2.4.1.2 Gain associated with integration

Let us now focus on the mean square error of a time delay measurement performed on Z integrated signals. The gain in SNR of the integration process, assuming coherent integration, is equal to the number of pulses integrated as given in equation (6.7).
The rms error of a threshold measurement was presented in Chapter 3 of this thesis, and is given in equation (6.18).

$$\delta T_{R\ \text{single measurement}} = \frac{1}{\sqrt{a \times \frac{S}{N}}} \tag{6.18}$$

a is constant modeling the Gaussian pulse, as given in equation (6.5).
Therefore, we can calculate the rms error of the time measurement using a threshold technique after integration of Z pulses: $\delta T_{R\ \text{Z-integration}}$ by using equation (6.7) and (6.17). The result is provided in equation (6.19).

$$\delta T_{R\ \text{Z-integration}} = \frac{1}{\sqrt{a \times \frac{S}{N} \times Z}} \tag{6.19}$$

The mean square error is written in equation (6.20) and (6.21).

$$\delta T_{R\ \text{Z-integration}}{}^2 = \frac{1}{a \times \frac{S}{N} \times Z} \tag{6.20}$$

$$\delta T_{R\ \text{Z-integration}}{}^2 = \frac{1}{Z} \times \delta T_{R\ \text{single measurement}}{}^2 \tag{6.21}$$

Equation (6.21) proves that the mean square error associated with the time delay measurement of Z integrated cycles of a signal is equal to the mean square error of a single time delay measurement divided by Z.

6.2.4.1.3 Summary

Equations (6.17) and (6.21) provide the same result. This theoretical study therefore proves that the rms error for the time delay measurements using threshold is the same for both methods:

- integration followed by a time delay measurement using threshold (equation 6.21)
- threshold delay measurement followed by averaging the results (equation 6.17)

Since both methods provides the same rms error, and since averaging Z results of time delay measurements requires insignificant memory as compared to the process of integrating Z samples of signals followed a time delay measurement, then it is sound to think that the former method should be used in our overall detection and measurement approach. Yet, this theory does not take account of the multiple threshold crossings in the vicinity of the expected pulse that was mentioned in Chapter 3 of this thesis. An experiment is therefore required to determine which method should be used.

6.2.4.2 Simulation and comparison of both methods

The experiment that we set in this section is used to determine which of the methods: integration followed by threshold measurement, and threshold measurements followed by averaging the results, is the most appropriate to our detection and measurement problem.

This experiments uses the pulse and bank of noise samples that were employed in Section 6.1.4.1. A matrix of 1000×Z lines, for Z equal to 5, 10, 15 and 20, was set. Each line of this matrix is a pulse buried in a different sample of noise. The computation of Z threshold time measurements, and the average of the results was a process performed 1000 times with this matrix. 1000 repetitions was also the number of times the process: integration of Z signals followed by the threshold time measurement was computed. Both methods were therefore tested on the same samples of signals.

The results from the 1000 trials were then averaged for each method in order to produce a statistical mean. Figure (6.8) provides the rms time measurement error versus SNR for each method. The number Z (integration or averaging) is equal to 15 in this figure. The curve called Skolnik is the analytical time measurement error obtained when a threshold crossing was performed on the integration of Z pulses, as given by equation (6.19).

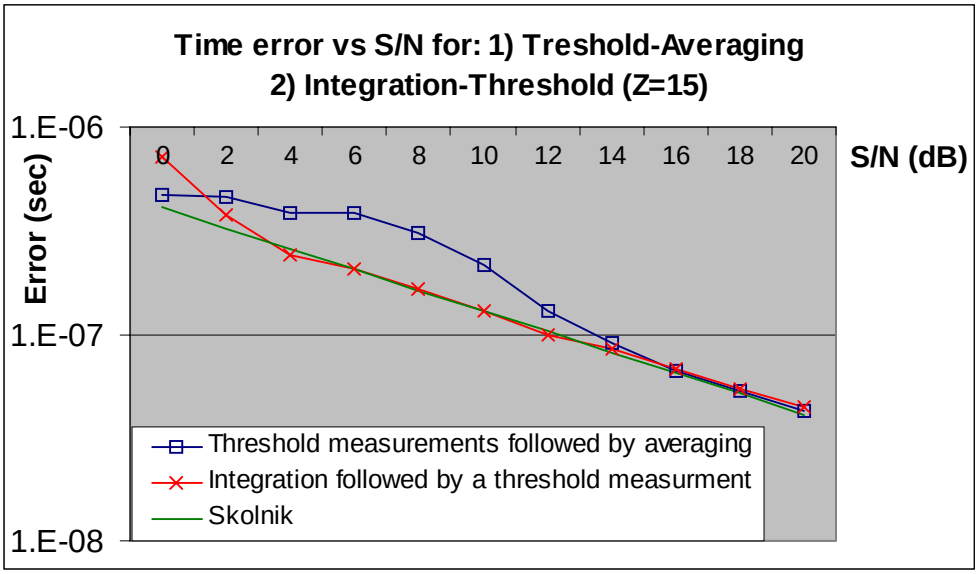

Figure 6-8 Comparison of the rms error for integration and averaging methods

6.2.4.3 Comments and conclusions

For convenience of the discussion, let us apply the following definitions:

- Method 1 refers to threshold measurements followed by averaging the results;
- Method 2 refers to integration of pulses followed by a single threshold measurement;

According to Figure (6.8), both curves reach the same theoretical curve called Skolnik, which gives the analytical accuracy of a threshold measurement performed on Z integrated pulses, for SNR above 15dB. However, Method 2 reaches this analytical limit at 2dB SNR, whereas Method 1 reaches it at 15dB SNR. Besides, in the SNR range of 4 to 12dB, method 2 is more accurate by at least 120 ns. An error of 120ns in measuring the threshold crossing time of a 3µs pulse is significant, since it represents 4%. This 120ns

error can therefore not be neglected, and this means that method 2 is far more accurate than method 1 for SNR between 4 and 12dB.

6.2.5 Discussion

The theoretical part of this section proves that method 1: threshold measurements followed by averaging of the results, and method 2: integration of the signals followed by a single threshold measurement, should yield the same result in terms of root-mean-square value of time measurement error.

Figure 6.2 proves that in the range of SNR of 4 to 12dB, performing integration prior to a threshold measurement yields significantly smaller rms error than threshold measurements followed by averaging of the results. The difference between both methods is at least 120ns within the range 4 to 12dB SNR. Yet, both methods tend to follow the theoretical accuracy given by equation (6.19) for SNRs above 15dB.

However, the comparison between methods 1 and 2 was based on the accuracy of time measurements disregarding the problems that may arise due to false alarms. Actually, it has to be mentioned that whenever a time measurement failed, due to a problem like the one illustrated in Figure (6.5), the sample was discarded. This means that the comparison between both methods was performed for a 100% success/detection case. Integrating several returns produces a signal with a higher SNR, but also produces a pulse that is closer to the ideal shape. Thus integration before thresholding is a better method to use because the probability of detection is increased and the probability of false alarm decreased. In other words, both methods 1 and 2 may give the same accuracy at high SNR (above 16 dB) with a 100% measurement success rate, but in a real case, integrating prior to any measurement will obviously yield fewer failures of the pulse localization process.

This discussion therefore justifies the use of integration in our detection process, since time measurements need to be performed on pulses with low SNR values. M/N detection

is used as the detection process for finding pulses, but integration within the selected time windows ensures that accurate measurements can be made for SNR in the range 4 to 12dB, therefore with less failure in the time measurement mechanism.

6.4 Conclusion

Section 6.1 focused on M-out-of-N detection. This process has proved to be a powerful means to lower the SNR threshold of a system while having better detection capabilities. Two methods were presented to calculate the parameters needed to implement this method. The first method is widely used in radar theory and consists in using the result of Figure 6.2 which directly provides the combination of M and N for optimum detection performances. However, this method is established with a simplistic assumption: the optimum combination of M and N is independent of the SNR of the signal, although different noise distributions and pulse shapes will result in different functions giving the detection and false alarm probabilities versus SNR. The second method that we propose is a direct approach that requires simulations using records of signal and noise samples obtained in the system that needs improvement. These records can be manipulated in order to compute the detection and false alarm probabilities of this signal at different SNR. Using the binomial expansion of equation (6.1), the probability of detection and false alarm can be predicted for any combination of M and N. The last step is therefore to pick the combination that fulfills the specification of the considered problem.

Section 6.2 reviewed the integration process, its properties, and the analytical results concerning integration gain. A discussion was established in order to know if integration followed by a threshold measurement was more appropriate than averaging several time measurement results obtained on each sample of the signal. The conclusion was that integration prior to measurement is required since it effectively increases the SNR of the signal, it allows time measurements to be performed on less distorted signals, and therefore prevents failures in the measurement section.

To sum up, the combination of M/N detection and integration is fundamental in our problem. The M-out-of-N process yields detection of the pulses with improved detection and false alarm probabilities, and integration within the selected time-windows increases the SNR of the processed signals, and decrease potential failures in the time delay estimation part.

Chapter 7

7. Practical Experiment

The previous chapters of this thesis were dedicated to the study of the main elements that we recommend as a solution to the problem of improving the detection and measurement of the time between two pulses: M/N detection, followed by an integration process. A time delay estimation method is proposed using either correlation or threshold measurements. This chapter gathers all the methods and results developed in this thesis, and applies them to a specific problem. The system that is studied is required to provide the same detection and measurement capabilities at 6dB SNR with the implementation of our architecture, whereas a SNR of 16dB is required without our improvement method. A practical experiment is set and a study of the observations will determine if the approach developed is valid.

Section 7.1 summarizes the main results and ideas reached in the previous chapters. Section 7.2 introduces the practical problem and defines the objectives that our solution has to reach. Section 7.3 focuses on the resolution of this problem analytically and presents the conditions of the experiment and the implementation of the solution.
Section 7.4 is dedicated to the observations, comments and discussion of the results of the experiment. Finally, Section 7.5 gathers recommendations for implementation of an optimal architecture.

7.1 Summary of the principal results

This section gathers the main results, ideas and methods developed in this thesis. Subsection 7.1.1 summarizes the analytical developments and main elements of comparison between the threshold and correlation methods. Subsection 7.1.2 is dedicated to the detection part of our solution.

7.1.1 Time delay measurement method

We studied and compared two methods for the time delay estimation of Gaussian like signals embedded in noise: the threshold and correlation methods. The former is simple to implement, and widely used in radar systems to detect and analyze the presence of target echoes. Correlation is, on the other hand, more complicated since it requires multiplications and summations of the values of the received sequences, although time delay estimation is obtained with only one measurement. Correlation is also widely used in radar and spread-spectrum systems, and provides high accuracy in systems like GPS where a ten-nanosecond rms timing error is practically achieved with the 1MCPS coarse acquisition code (C/A).

In a matched filter case and at high SNR, typically above 12dB, the accuracy of a threshold crossing measurement at both edges of a Gaussian pulse is given by equation (7.1):

$$\delta T_R = \frac{1}{\sqrt{\frac{a}{2} \times \frac{A^2}{N}}} \tag{7.1}$$

A is the amplitude of the Gaussian pulse, and N is the noise power; ‘a’ is the constant in units of time^{-2} modeling the Gaussian pulse represented by function p(t):

$$p(t) = A \times \exp(-at^2) \tag{7.2}$$

At high SNR, Chapter 3 reports that the rms error for correlation measurements is:

$$\delta T_R = \frac{1}{\left(\sqrt{\frac{\pi a}{8}} B_N \frac{A_2}{N}\right)^{\frac{1}{2}}} \tag{7.3}$$

where B_N is the noise bandwidth.

A SNR is considered as high when the noise peaks in which the pulse is embedded do not generate ambiguous threshold crossings in the vicinity of the threshold level, as illustrated in Figure (7.1). For a threshold method, this typically corresponds to a SNR above 12dB.

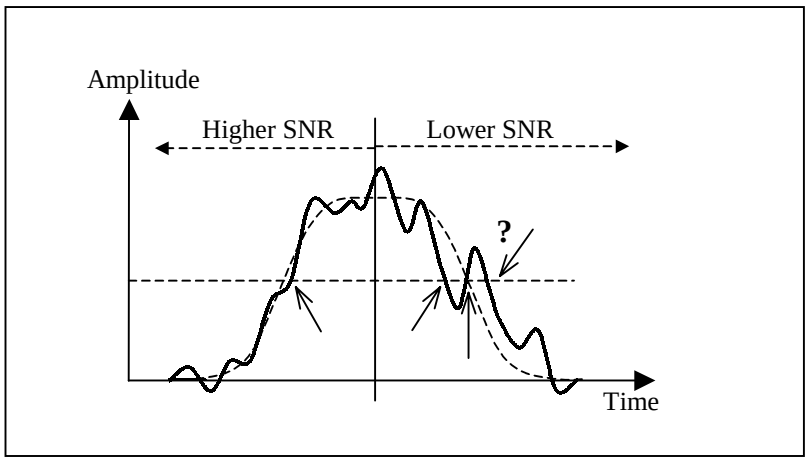

Figure 7-1 Ambiguity of a threshold time measurement

(Arrows indicate threshold crossings; "?" suggests an ambiguity in the threshold process)

Equations (7.2) and (7.3) proved that in a perfect matched filter case where the received signal is correlated with its noise-free replica, correlation suffers from a higher rms error than a threshold technique. Since a Gaussian filter cannot be practically implemented, this conclusion was reconsidered in the case of a perfect rectangular filter. The optimum bandwidth of this filter: B_{rect}, in the sense of the signal bandwidth for which the SNR is maximized in the receiver, is related to the bandwidth B_{Gauss} of the Gaussian matched filter by equation (7.4). Note that the bandwidth of the Gaussian filter matched to the

pulses represented by equation (7.2) is directly related to the constant ‘a’ by equation (7.5).

$$B_{rect} = 1.64 \times B_{Gauss} \tag{7.4}$$

$$a = \frac{(\pi B_{Gauss})^2}{4 \times \ln(\sqrt{2})} = 7.11 \times B_{Gauss}{}^2 \tag{7.5}$$

It follows that correlation has a lower rms error than the threshold technique when the noise bandwidth after filtering is given by the inequality:

$$B_N \geq 1.30 \times B_{rect} \tag{7.6}$$

Therefore, assuming perfect filtering in both the matched filter and near-matched filter cases, threshold detection will provide more accurate results than correlation. If the filter prior to the measurement fails to select these bandwidths, then correlation yields increased accuracy as compared to threshold measurements. This result is due to filtering properties that correlation provides and that threshold lacks. These conclusions have been verified in Chapter 5.

7.1.2 Detection method

The detection properties of a system are evaluated based on two probabilities. The probability that a pulse buried in noise is detected is called the probability of detection. The probability that a noise peak is detected instead of the expected signal is called the probability of false alarm. The best detection method to determine the presence of pulses buried in noise is coherent integration, which provides a gain - when the signal is processed - equal to the number of samples of signal that are integrated. However, this process has a cost: the memory required to store long samples, and the processing load needed to process the resulting data. The solution that we reached in Chapter 6 is already used in some radar systems. A M/N detection is combined with an integration process. The M/N detection is the equivalent of a double-threshold detector. The first threshold

determines which parts of the signal cycle crosses a certain level of energy, the second threshold records the number of times these threshold-crossings occurred. Mathematically, if P_d is the probability of detection of one pulse, then the probability of detection P_{dM} of M pulses out of N trials is given by equation (7.7), as reported in [Too82].

$$P_{dM} = \sum_{i=M}^{N} \binom{N}{N-i} P_d^i \times (1 - P_d)^{N-i} \tag{7.7}$$

where:

$$\binom{N}{M} = \frac{N!}{M!(N-M)}$$

The same formula can be applied to the probability of false alarm by replacing P_d by P_{fa}. This process ensures a decrease of the probability of false alarm at constant or even improved probability of detection. This procedure is not as efficient as the integration technique, but it requires less processing. The idea is therefore to combine both methods. M/N detection is used to find pulses using a certain probability of detection and false alarm, and integration is only performed within selected windows of time around the pulse.

The determination of the coefficients of the M/N detection, M and N, can be performed in two ways. We suggested a direct approach of the problem by recording samples of noise, and determining the average number of threshold crossings for a given threshold level. By taking real received pulses at high SNR at the output of the detector, a probability of detection can be established by computing the number of times the pulse embedded in noise is effectively detected. Based on the specification of the system studied, the choice of a certain combination of M and N can be established and a prediction of the detection and false alarm probabilities can be obtained through equation (7.7). Finally, the integration number is determined by the gain required in the processing part of the studied system. The gain is directly proportional to the number of integrated pulses. However, a loss analytically determined in Figure 2.8 of [Sko80] can be taken into account in the case of non-coherent integration.

7.2 Presentation of the problem

The problem that we are considering is based on a real positioning system that needs to be made more accurate over a larger operating range than its current conception allows. The problem is simplified in order to avoid accounting for all the details of this system that are irrelevant to our subject. The samples of noise and signals processed in the experiment were taken from records of received pulses in this particular system.

7.2.1 Problem and goal

The system that needs improving is processing Gaussian shaped pulses. Two pulses are sent within a cycle of time of 5ms. The pulses are 3 μs wide, and an accurate measure of the time delay between these pulses is needed. The pulse used in this system is illustrated in Figure 7.2.

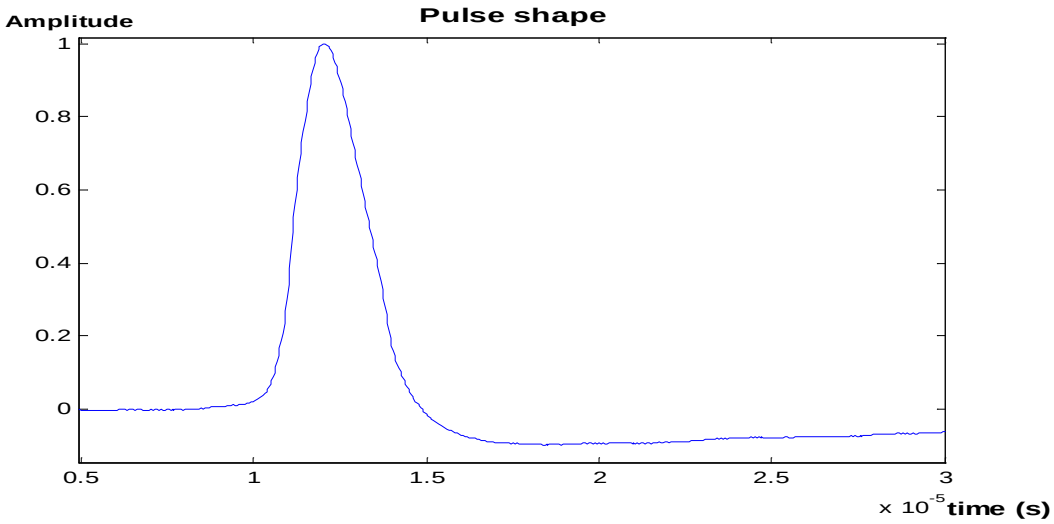

Figure 7-2 Pulse shape

The current system works with a threshold at approximately 16dB above rms noise, with a certain probability of detection and false alarm. We wish to make that system work with the same performance using a 6dB threshold.

7.2.2 Assumptions

A current version of this system is already developed to perform the detection and time delay measurement of the pulse using a threshold detector. The cycle time of the pulse is stable, but the pulses may move within this cycle. However, based on the use of this signal, the position of the pulse may be considered constant for time durations on the order of 150 ms. In order to refresh the time measurements of the pulses fast enough, a time of 300ms is granted to generate the solution. We assume that the beginning and end of a cycle time is provided to our system. The amplitude of the pulse is also given, although recommendation will be given to cope with that issue.

7.3 Resolution of the problem

The solution of this problem consists first in determining the parameters needed: the different probabilities for detection and false alarm, the accuracy of the solution, which implies the approximation of the real pulse by a Gaussian pulse, and the parameters of the detection processes M, N, and the integration number Z. We will then present the practical experiment that was used to test the validity of our solution.

7.3.1 Resolution of M, N and Z

The specification of our problem requires that we reach almost the same performances as the current system at a SNR 10dB lower. We need first to determine the current capabilities of the system. A gain of 10dB in SNR corresponds to the integration of 10 pulses in a coherent receiver, and of about 14 to 21 pulses in a non-coherent receiver depending on the probability of detection and false alarm. These numbers are found in Figure (7.3), also present in [Sko80].

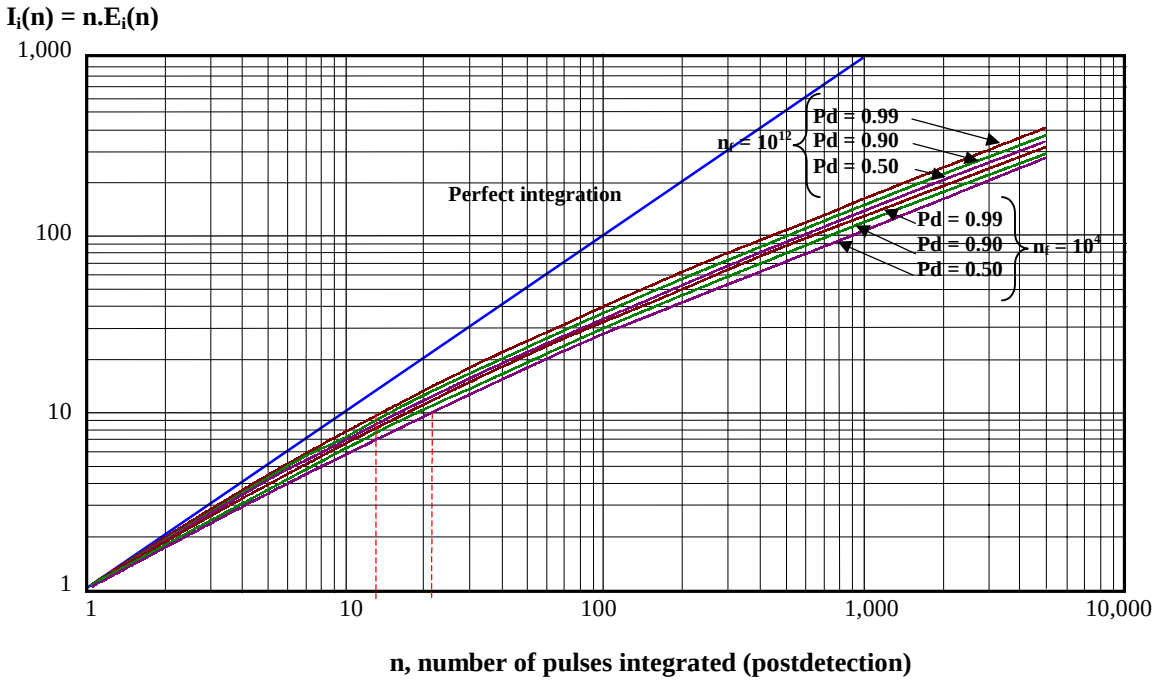

Figure 7-3 Non-coherent integration gain

P_d is the probability of detection, and n_f the number of false alarms

Since the processing time granted is less than 150ms, which represents 30 cycles of signal at 5ms, and 14 to 21 cycles are dedicated to the integration part, then N cycles of the signal should be processed in the M/N detection with N taken between: 9 (30 – 21) and 16 (30 – 14). M/N detection is the part that will fix the critical memory requirement and the computational load of the overall process; consequently, a value for N up to 9 will be targeted.

Before determining M and N, let us approximate the measured pulse that is studied with a Gaussian pulse. Figure (7.4) is the replica of Figure (7.2) with two Gaussian pulses that closely match each edge of the real non-symmetrical pulse. The constants ‘a’ given by equation (7.2) of each Gaussian pulse were determined to be:

$$a_{left} = 1{,}076\times10^{-9}\ s^{-2} \quad (7.8)$$

$$a_{right} = 374\times10^{-9}\ s^{-2} \quad (7.9)$$

where a_{left} and a_{right} correspond to the Gaussian pulses matching the measured pulse on the left and right hand side respectively.

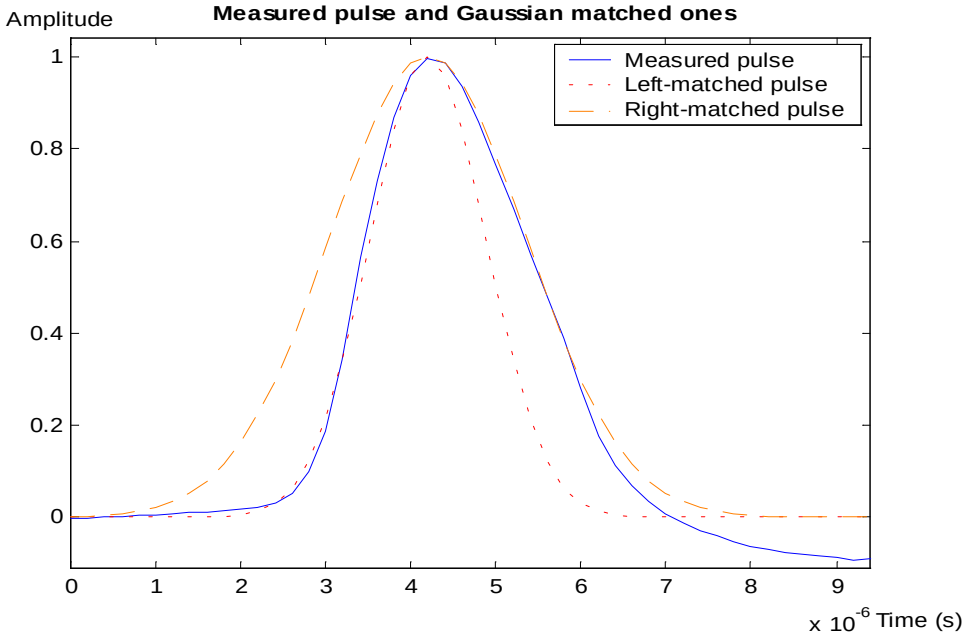

Figure 7-4 Approximation of the experimental pulse by two Gaussian functions

By taking equation (7.4), (7.5), (7.8), and (7.9), the bandwidth of the near-matched rectangular filter is 640kHz. Since the noise that was recorded had a larger bandwidth than that, the noise samples were filtered using a rectangular filter with a cutoff frequency: fc = 640kHz. This filtering was performed digitally by convolving the samples with the impulse response of the rectangular filter given by equation (7.10). Note that convolving two functions f and h in the time domain: $f(t)*h(t)$, is equivalent to multiplying the respective Fourier transforms of these functions in the frequency domain. The filtering process can therefore be carried out in the time domain just as accurately and more easily than in the frequency domain.

$$\text{Impulse}_{\text{rect 640kHz}}(t) = \sin(\pi f_c t) / (\pi f_c) \qquad (7.10)$$

The spectrum of the noise at the output of the rectangular filter is given in Figure (7.5). At 640kHz, the noise power is lowered by 6dB as compared to the average noise power

between 100 and 600kHz, and at 700kHz, the spectral component is about 11dB lower as compared to the same reference. The first sidelobe is 21dB lower than the average noise power between 100 and 600kHz.

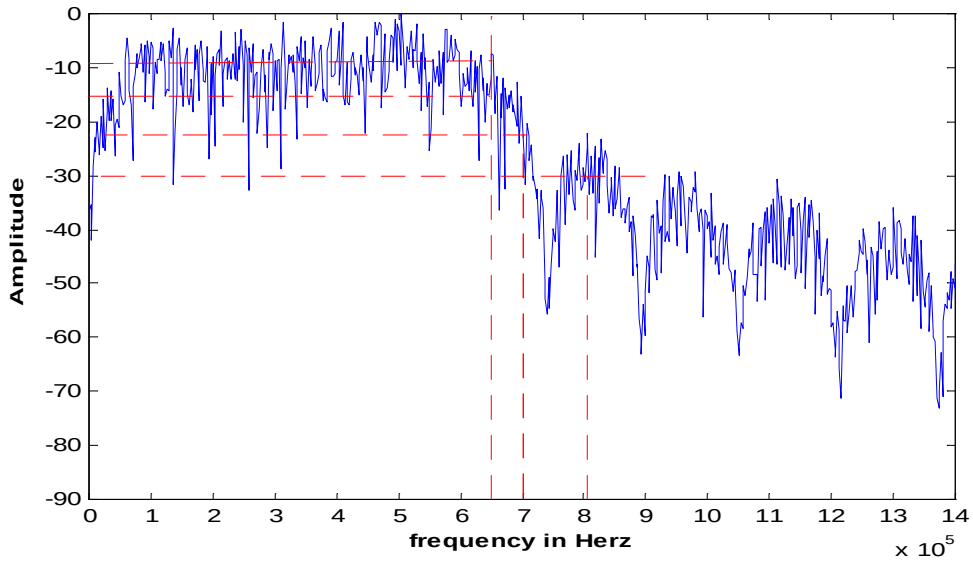

Figure 7-5 Spectrum of the recorded noise

Determining M and N requires an analysis of the noise that interferes with the pulse. This analysis consists in taking the bandlimited samples of noise, and recording the number of threshold crossings for a certain SNR. This number divided by the total number of noise points gives an approximation of the probability of false alarm. A similar method is used to evaluate the probability of detection. Noise samples are added to recorded pulses, and a test to know whether the pulse generates a threshold crossing is performed. The experiment is repeated a thousand times over different SNRs ranging from 0 to 20dB. These two analyses take less than a minute using a PC with 800MHz processor. The matrix generating noise samples is composed of 230,000 recorded points at 10MHz. Figures (7.6) and (7.7) represent the probability of detection and false alarm obtained from this study, and also the extrapolated probabilities of detection and false alarm for different combinations of M and N using equation (7.7). Values of N from 5 to 9 were studied as mentioned at the beginning of this section.

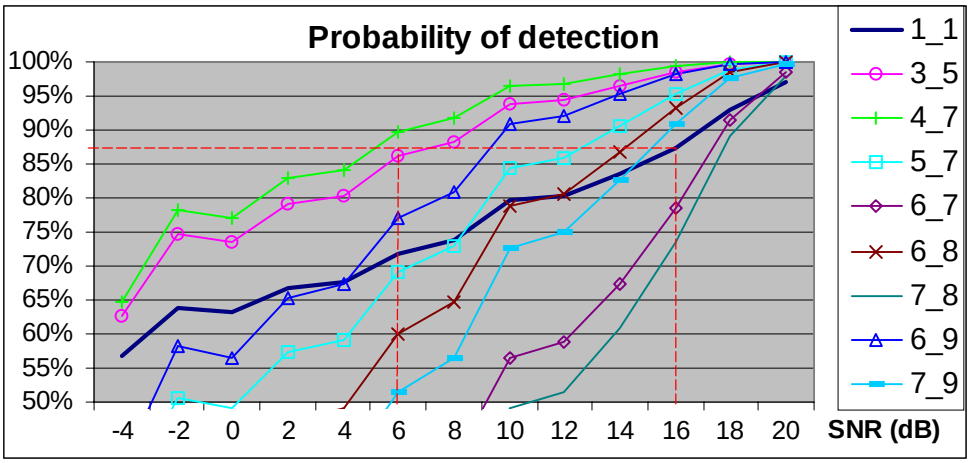

"M_N" on the right represent the type of M/N detection used

Figure 7-6 Analyzed probability of detection

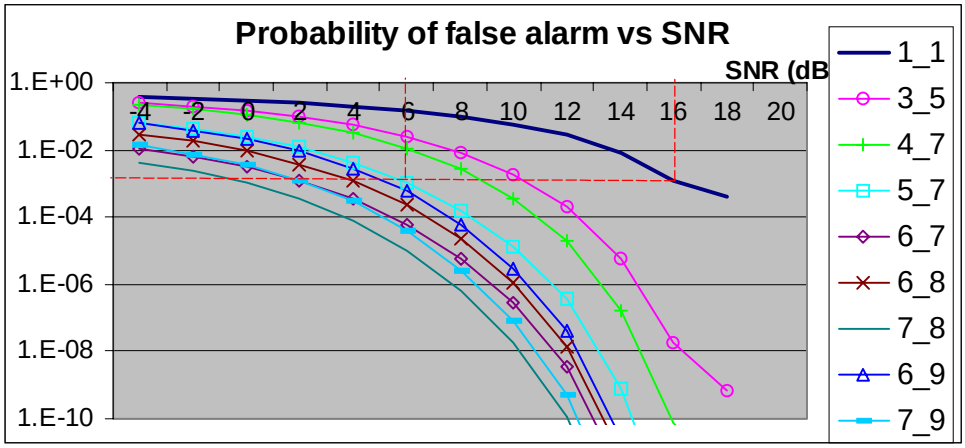

"M_N" on the right represent the type of M/N detection used

Figure 7-7 Analyzed probability of false alarm

Without M/N detection and at SNR equal to 16dB, the probability of detection reaches 87%, and the probability of false alarm is about 10^{-3}. Since the probability of detection is linked to the M/N method, which does not take into account the integration process where a confirmation of the detection can also result, the requirement on the probability of detection can be lowered to 75%. A good combination candidate is therefore (6/9) which provides a probability of detection of 77%, and a probability of false alarm of 5.74×10^{-4} at 6dB SNR.

The number of integrated pulses Z can now be increased up to Z = (30cycles – N) = 21 while still compliant with the 150ms processing time requirement. Yet, as explained later in Section 7.5, an integration number of 18 is chosen for ease of the implementation. The accuracy that is targeted is given by equation (7.1) adapted to the constants ‘a’ given in equation (7.8) and (7.9), leading to an expected rms timing error of 215 to 365ns at 6dB SNR.

7.3.2 Practical experiment

The practical experiment used to test this configuration was a simulation on a 800MHz PC with Gaussian shaped pulses and noise with a 3dB bandwidth of 640kHz, as explained in Section 7.3.1. The detection consists in performing sequentially the 6/9 detection, the integration process, and both the correlation and threshold methods for pulse detection. The algorithm is given and explained in Appendix A. The clock frequency that is recommended in Section 7.5 is 10MHz, with sampling at 2MHz for M/N detection, and 5MHz for integration. At 5MHz, the number of points in the 3µs pulse is approximately 15. However, the time window should be made larger than the pulse itself in case the pulse moves in time during the integration process. The duration of the window was chosen as 4.8µs, represented by 24 points at 5MHz. This specific number is in between the minimum size of the window corresponding to the pulse width 3µs, and a larger size that is twice this length. As mentioned in the problem resolution, our solution was designed so that the pulse timing position should not need a refreshment of the time window position within less than a complete processing cycle time. Mathematically, this corresponds to a period of the M/N detection sampling frequency, which is 0.5µs. This results in a window size of at least 4µs (= 3+2×0.5), and 4.8µs is taken as security.

In order to evaluate the error generated by the method, an accurate delay between the pulses was set prior to the experiment at 3.24ms. Although the two pulses that are used are not strictly exactly the same since they were collected respectively at different ranges from the transmitter of the real system, the time delay was thoroughly established and checked using both a correlation and a threshold method.

Due to the long samples of noise that have to be generated for M/N detection, the experiment was repeated a hundred times for SNR values ranging from 0 to 20dB with a two dB incremental step. This experiment took about 6 hours using a PC with an 800MHz processor. The experiment was performed a second time with 500 repetitions over a SNR ranging from 2 to 8dB with a 1dB incremental step in order to focus on the SNR region of interest. This second experiment took approximately 20 hours.

7.4 Observations and discussion

The results of the two experiments described in Section 7.3.2 are presented and commented on in the following paragraphs.

7.4.1 Results

Table 7.1 and 7.2 summarize the respective results of both experiments. To recall what the difference is between these two experiments, the second one is focused on SNR ranging from 2 to 8dB with 500 repetitions per dB increment, whereas the first experiment provides the results established over 100 repetitions for SNRs ranging from 0 to 20dB.

The second column of the table is the number of expected pulses that were detected divided by the number of repetitions of the experiment. The third and fourth columns provide the rms value of the measurement errors over all the repeated cycles of detection, whereas columns 5 and 6 gives the same quantity established over all the cases where the expected pulses were indeed detected.

SNR (dB)	% pulses detected	Error rms (seconds)			
		All results taken into account		Real pulses detected	
		Threshold	Correlation	Threshold	Correlation
0	15%	2.03E-03	2.03E-03	4.46E-07	3.32E-07
2	49%	1.63E-03	1.63E-03	3.55E-07	2.99E-07
4	85%	8.37E-04	8.37E-04	2.48E-07	1.95E-07
6	94%	5.07E-04	5.07E-04	1.92E-07	1.69E-07
8	100%	1.60E-07	1.41E-07	1.60E-07	1.41E-07
10	100%	1.30E-07	9.95E-08	1.30E-07	9.95E-08
12	100%	1.25E-07	9.49E-08	1.25E-07	9.49E-08
14	100%	8.49E-08	8.19E-08	8.49E-08	8.19E-08
16	100%	9.54E-08	6.93E-08	9.54E-08	6.93E-08
18	100%	8.49E-08	6.16E-08	8.49E-08	6.16E-08
20	100%	8.94E-08	4.12E-08	8.94E-08	4.12E-08

- 6/9 detection followed by 18 integrations;
- Correlation and Threshold used as timing measurement methods;
- Threshold set at half the amplitude of the pulse;
- 100 repetitions used for each Figure;

Table 7-1 Results of the first experiment

SNR	% pulses detected	Error rms (s)			
		All results taken into account		Real pulses detected	
		Threshold	Correlation	Threshold	Correlation
2	41%	1.80E-03	1.80E-03	3.22E-07	2.63E-07
3	66%	1.28E-03	1.28E-03	2.64E-07	2.16E-07
4	82%	9.08E-04	9.08E-04	2.53E-07	2.04E-07
5	91%	6.41E-04	6.41E-04	2.16E-07	1.82E-07
6	97%	3.19E-04	3.19E-04	1.92E-07	1.65E-07
7	99%	2.81E-04	2.81E-04	1.73E-07	1.46E-07
8	100%	1.59E-07	1.35E-07	1.59E-07	1.35E-07

- 6/9 detection followed by 18 integrations;
- Correlation and Threshold used as timing measurement methods;
- Threshold set at half the amplitude of the pulse;
- 500 repetitions used for each Figure;

Table 7-2 Results of the second experiment

The results given in columns 5 and 6 are represented graphically in Figure (7.8) and (7.9) respectively. A curve called “Skolnik” was added, and was computed by taking the rms of the timing error values provided by equation (7.1) for the two values of the constant ‘a’ given in equation (7.8) and (7.9): $1{,}076\times10^{-9}\ s^{-2}$ and $374\times10^{-9}\ s^{-2}$.

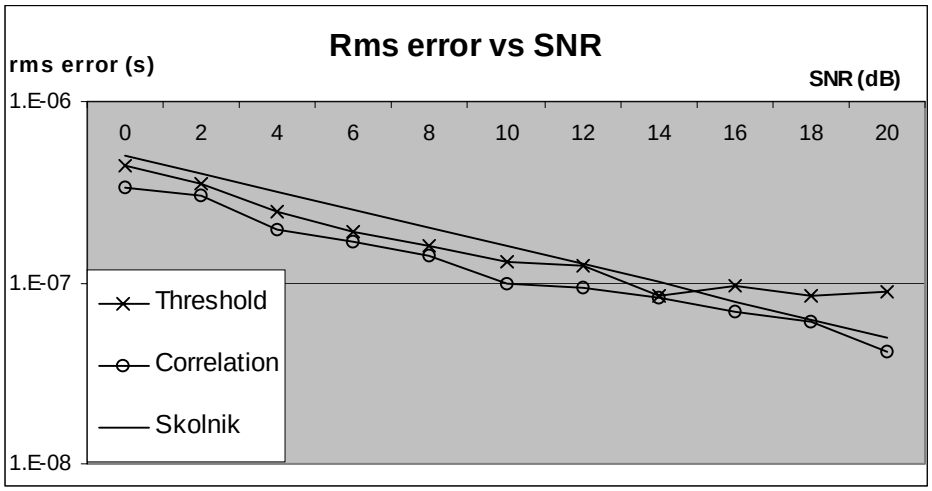

- 6/9 detection followed by 18 integrations;
- Correlation and Threshold used as timing measurement methods;
- Threshold set at half the amplitude of the pulse;
- 100 repetitions used for each Figure;

Figure 7-8 Rms time delay error for the first experiment

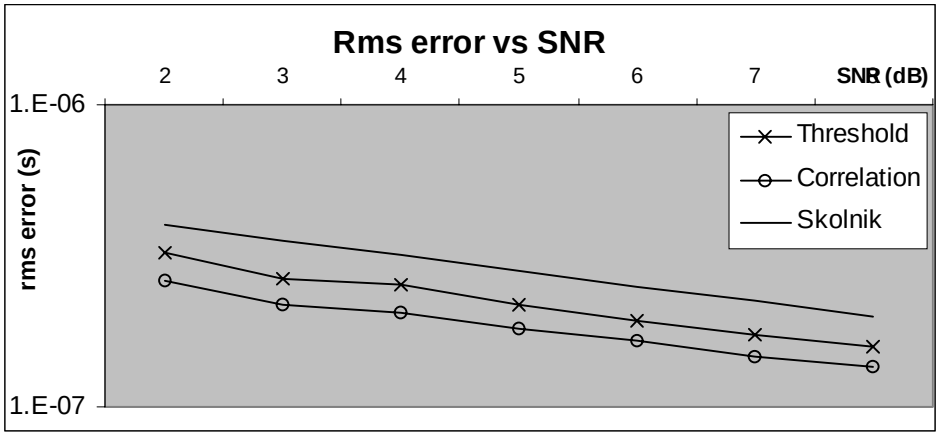

- 6/9 detection followed by 18 integrations;
- Correlation and Threshold used as timing measurement methods;
- Threshold set at half the amplitude of the pulse;
- 500 repetitions used for each Figure;

Figure 7-9 Rms time delay error for the second experiment

7.4.2 Observations and comments

Table (7.2) shows that below 8dB SNR, the probability of detection is smaller than a hundred percent, and that the probability of detection is 97% at 6dB SNR.

Considering the overall rms time measurement error, the accuracy provided by both methods is nearly the same from 0 to 6dB. Large errors due to completely missed pulses explain such a result. However, by considering only the cases where the expected pulses were detected and processed, correlation and threshold provide an rms error below 200ns. This is better than the targeted 215ns.

Correlation generates lower rms timing error than the threshold process though. This is confirmed by Figure (7.8) and (7.9) over all the SNR scale. At 6dB for instance, correlation has an rms error value 27ns smaller than that of threshold. By studying thoroughly Table 7.2, one can notice that the gain provided by correlation over threshold in terms of SNR is about 2dB.

7.4.3 Discussion

The above results prove that the designed solution meets the specification on each single point. Note however that the probability of false alarm was not evaluated since the algorithms that were implemented were simulating the real system, and the simulations would have been too long in order to put this function into operation. Yet, the probability of detection obtained at 6dB is better than that predicted in Section 7.3.1, and the rms error of each method is slightly below the targeted accuracy. As a result, one can wonder if a better design could fulfill the requirements exactly. As seen on Figure (7.6) and (7.7), the other combination that fulfill the probability of false alarm of 10^{-3} with a lower probability of detection of 69% is a 5/7 detection process. Yet, as already mentioned for the ease of the design, the integration number should be a multiple of N, which is the maximum number of cycles studied in the M/N detection. This would yield an integration number of 14 (7×12), which would not be enough to meet the desired accuracy, or 21 pulses in order to be compliant with the maximum processing time corresponding to 30 cycles. A non-coherent integration of 21 pulses yields a gain of about 11dB, whereas an integration of 18 pulses provides a 10.8dB gain referring to Figure 7.3. As a result, the 5/7 combination would decrease the probability of detection by approximately 10% as compared to the 6/9 detection, for an increase in gain of only 0.2dB. We conclude that a 6/9 detection process is preferable to the 5/7 detection.

The comparison between the correlation and threshold methods is interesting. Up to now, the comparison had been performed in ideal cases where the pulses were exactly similar, and the noise perfectly bandlimited at the optimum rectangular bandwidth. In this example, the pulses are indeed asymmetrical, not exactly similar, and the noise although filtered at the above-mentioned bandwidth, has some components at high frequencies that are not completely filtered. It follows that correlation improves the filtering capabilities of the processing chain, and therefore provides a gain in SNR. The 27ns rms error reduction when using correlation as compared to threshold at 6dB SNR may not be worth the extra computational load implied by correlation, yet, this amount of gain in accuracy is worth 2dB of SNR when compared to the correlation method at all SNRs. We conclude that correlation is indeed interesting, but the improvement in accuracy is obtained at the expense of a computational load increase.

7.5 Suggestion for implementation of the overall designed process

Several points were raised in the previous sections concerning the sampling frequency chosen, and the fact that the integration number should be a multiple of the maximum number of cycles studied in the M/N detection. Moreover, the overall architecture of the design needs clarifying, and some critical points concerning the implementation of the M/N detection are worth mentioning. The following chapters deal with these issues.

7.5.1 Choice of the sampling frequencies

We have suggested the use of several sampling frequencies for the overall system. This issue is actually linked to the memory requirement of the overall process, and more precisely of the M/N detection, which requires a critical storing space. Oversampling at 2MHz signals that have bandwidths of about 600kHz is consistent with Nyquist theorem, and obeys the need to observe several points of the 3µs pulse. This is all the more necessary since the M/N detection may determine that multiple groups of points crossed the M-threshold. The two groups of highest lengths are selected as the two expected

pulses. Therefore, the lower the sampling frequency, the lower the maximum number of sample points of the 3μs pulse that can be detected, consequently the lower the probability that the expected pulse will be chosen, although it is indeed detected. On the other hand, the higher this sampling frequency, the higher the memory required to store all these points. At 2 MHz and using a practical 8-bit quantization ADC, the memory requirement for one detection cycle reaches:

$$\text{Memory requirement} = N \times T_C \times F_S \times 8\text{bits} \tag{7.10}$$

$$\text{Memory requirement} = 9 \times 5\text{ms} \times 2\times10^{6}\text{Hz} \times 8\text{bits} = 720\text{kbits} \tag{7.11}$$

where T_c is the period of the received signal, F_s is the sampling frequency, and N is the chosen parameter of M/N detection.

The result given in (7.11) is not too high a requirement thanks to the careful choice of a 2MHz sampling frequency.

On the other hand, the sampling frequency for the integration process should be made higher since the samples of signal that are integrated are of smaller lengths, and the higher the quantization of the time scale, the more accurate the solution. Sampling at 5MHz provides 15 points for 3μs pulses. On the other hand, it requires either two ADC, one for M/N detection and one for Integration, or it requires a single ADC at the LCM of 2 and 5MHz, that is 10MHz. This is the solution that we used. However, a 6MHz sampling frequency would also be a good solution, since it is lower than 10 MHz, and already a multiple of 2MHz. This solution is the one that we recommend. It was not used in our experiment simply because the samples of noise and signals that were provided were sampled at 25MHz, which is not a multiple of 6MHz.
The memory requirement of the integration process using a 6MHz sampling frequency is:

$$\text{Memory requirement} = Z \times N_P \times T_W \times F_S \times 8\text{bits} \tag{7.12}$$

$$\text{Memory requirement} = 18 \times 2 \times 4.8\mu\text{s} \times 5\times10^{6}\text{Hz} \times 8\text{bits} = 6912\text{bits} \tag{7.13}$$

where N_P is the number of pulses detected, T_W the duration of the time window, and F_S is the sampling frequency of the integration process.

7.5.2 The integration number issue

The design of the proposed architecture yields a certain N value in the M/N detection, and certain integration number. With the requirement in terms of gain that was expected, 10dB, Z is bound to be higher than N. The simplest solution to implement the combination M/N detection followed by the integration process is to sequentially perform both processes, as given in Figure (7.10).

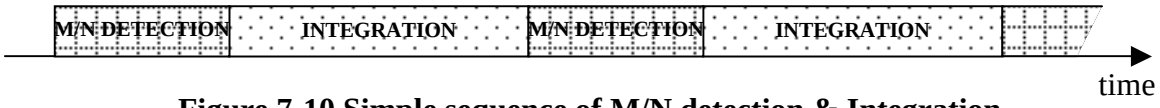

Figure 7-10 Simple sequence of M/N detection & Integration

However, M/N detection and integration are not computational demanding processes, they just require some manipulation of the memory and additions, which are two basic logic operations. The architecture presented above is therefore not optimized in terms of processing time. If the integration process is made a multiple of the parameter N of the M/N detection, then a parallel architecture is a solution that optimizes the timing of the process. The solution that we propose is illustrated in Figure (7.11). It requires of course a processor that is fast enough to determine the solution of the M/N detection in order to know when to start the integration process. A solution for this issue is proposed in Section 7.5.3.

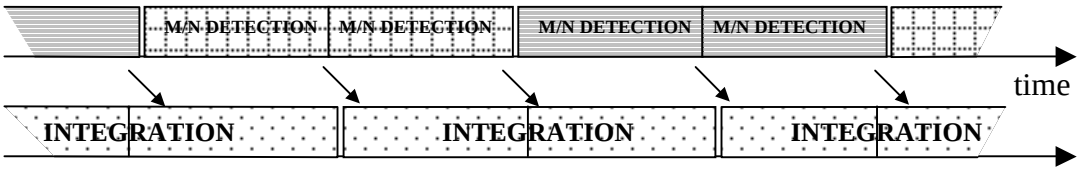

Figure 7-11 Optimized sequence of M/N detection & Integration

During a complete cycle of integration, the position of the time window determined by the M/N process is refreshed as many times as there are cycles of detection in one integration process. If the new time window that is determined is far different than the previous solution within one cycle of integration, then the new time window is discarded, and the former one is used again. Thanks to this process, the problem of having too long periods of integration as compared to the motion of the pulses is solved.

To conclude, the use of M/N detection followed by the integration of Z pulses where Z is a multiple of N is strongly recommended.

7.5.3 M/N detection processing

Two important issues concerning the operations needed during the M/N process are addressed. The first one proposes a solution to the problem that we neglected: adapting the threshold of the detection process when the amplitude of the received signal changes.
The second problem is dedicated to the synchronization issue between cycles of detection and integration as introduced in Section 7.5.2.

7.5.3.1 Adaptive thresholding

In practical communication systems, if the distance of a transmitter to a receiver is increased, then the SNR is lowered, and to be more precise, the amplitude of the received signal is decreased. In our developments, we assumed that the amplitude of the pulses was provided as an independent piece of information by the current version of the system. Yet, it is easy to implement an adaptive threshold algorithm right after the M/N detection process. It was already mentioned that after performing the double threshold operation, more than two pulses could be detected, whereas two needed identifying. Taking the two longest ones was suggested.
Let us suppose that within a certain threshold level, there are really few detected pulses. Then a decision system based on the number of detected pulses can trigger a decrease of

the threshold level. On the other hand, if too many pulses are detected, the threshold can be increased. The algorithm needed to implement this solution is therefore really simple.

7.5.3.2 Optimization of the sequence of operations

In the parallel implementation suggested in Figure (7.11), it is implied that the processor is able to compute the beginning of the first time window for the following integration process within one period of a 2MHz sampling frequency: 0.5µs. This might be difficult to perform even with a relatively fast processor. Yet, since the sequence: getting a value, comparing it to a threshold, adding it to another value and storing it, are operations that can be performed within two cycles of processing time, several other operations can be made within the detection process. Determining which pulses have already crossed the second threshold of M/N detection can be started at the M^{th} cycle; most of the pulses that will end up being detected will already have been identified prior to the processing of the final N^{th} cycle. We suggest creating chains of detected pulses containing the total number of elements within each chain before the last point of the M/N process is checked. As a result, within a period at 2MHz, that is 0.5µs, the remaining operations prior to integration consist in identifying the two longest chains, and determining the beginning of the associated time window. If there are not too many pulses detected, which limit can be fixed thanks to the adaptive threshold algorithm proposed in Section 7.5.3.1, then 0.5µs is sufficient time. The processor that is chosen for the implementation of these methods should be designed based on this requirement.

7.5.4 Design of the final architecture

The sequence of operations that we have been designing is represented in a block diagram form in Figure (7.12). Two flows of data are used in this system: the baseband signal from the receiver and the cycle time information. The signal is digitized at 6MHz using 8 bits-per-word. The stream of samples is then separated into two flows, one of which is downsampled to 2MHz for the M/N detection process, and the other one is used in the integration process. In the M/N detection branch, pulses are detected and treated

during the process itself, as discussed in Section 7.5.3.2. The first threshold used in M/N detection is adaptive and can be lowered if there are not enough pulses detected at the end of the process. The center of each pulse is then determined, and based on the cycle given in Figure (7.11), a decision can be made whether to accept the new time window, or reject it and choose the solution of the previous detection cycle as explained in Section 7.5.2. The output of this section is passed to a block that also receives the sampled data at 6MHz, and gets the period number within a signal cycle identified by the counter called: “in-cycle period counter”. This allows the identification and integration of the samples belonging to the time-window that was determined thanks to M/N detection. The output of the integration process consists of two integrated portions of the original signal, and is submitted to either the threshold process, or the correlation method for the position calculation of the pulses. Finally, the time delay is obtained by subtraction of the center time of each pulse.

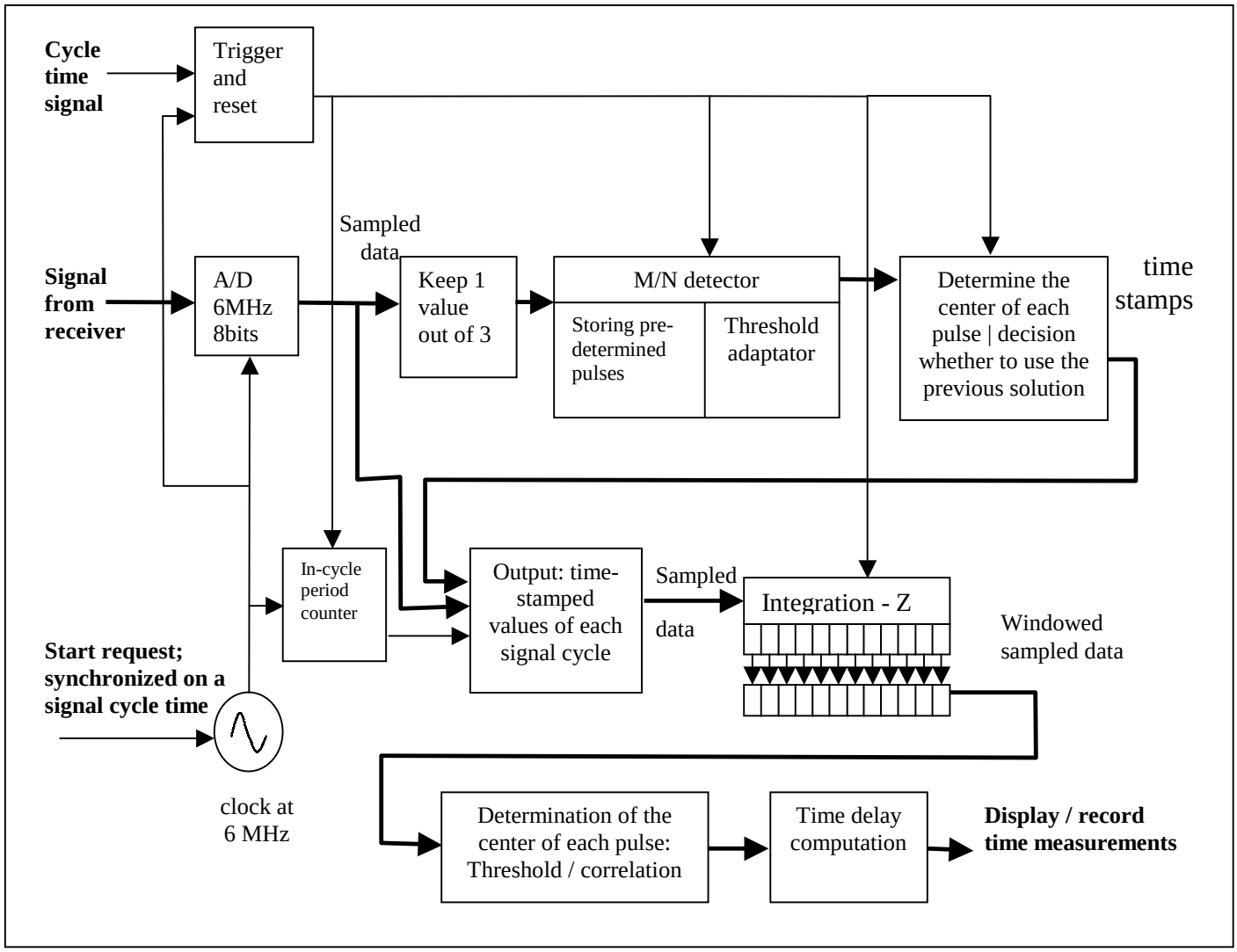

Figure 7-12 Block diagram of the designed solution

7.6 Summary

The analytical developments that we have presented throughout this thesis have been used in a practical case for evaluation of the validity of our proposed solution: the combination of M/N detection, integration and time measurement using threshold or correlation.

The practical case that we considered is a specific problem that illustrates the need for accurate time delay measurements at low SNR. We have designed a complete solution to this problem, and tested it practically. The result fulfilled the specification, and a new comparison between correlation and threshold measurements was established. In this practical case, pulses are not symmetrical, which prevents the use of a matched filter. Thanks to its filtering properties, correlation provides time delay measurements with a lower rms error as compared to the threshold process. At the targeted 6dB SNR, the gain in accuracy for correlation is about 27ns. This represents a hundredth of the pulse width, but also a gain of 2dB as compared to the threshold method. For certain applications, this improvement might prove necessary although requiring more processing.

Finally, we have designed an optimized solution to implement the operations described above, taking into account the critical problem of time synchronization of the tasks.

Chapter 8

8. Conclusion and Recommendations

This research effort focused on the better understanding of two fundamental processes needed in accurate measurement systems like GPS and radar: detection and time localization of signals. While both of these areas were treated independently, it was concluded that accurate time delay estimation could not be reached without efficient detection capabilities. Correlation was compared to threshold measurements as a time delay estimation method for Gaussian pulses. This comparison was conducted both analytically and through extensive use of simulations in various cases of study. Depending on the practical cases, one solution yields more accurate results than the other, although correlation always imposes a larger computational load on the system. As a result, a practical problem was considered, a solution was designed with both measurement techniques, and the overall configuration was tested in order to evaluate the validity of our developments. While the designed solution fulfilled the specification, it was made clear that correlation generated a smaller rms error in that specific case.

8.1 Summary of research

Chapter 2 provided an introduction to the problem under investigation. Correlation and its use in accurate measurement systems were presented through the study of several systems: CDMA based systems, radar systems, and GPS. Then matched filter theory was presented and provided a link to detection theory. Several detection methods were introduced, and especially M/N detection. Finally, a section dedicated to estimation theory raised some important issues in estimation problems, and helped familiarity with

analytical results linked to correlation. Correlation, M/N detection and integration were therefore justified as useful methods potentially applicable to the detection and time delay measurement of Gaussian shaped pulses.

Chapter 3 reviewed analytical results related to theoretical timing accuracy in radars using threshold measurements. These results were then checked through simulations. The goal of this chapter was to serve as a foundation for determining the analytical accuracy of correlation time measurements.

Chapter 4 derived the analytical law governing the accuracy of threshold measurements for the special case of correlation. Simulations were performed to test the validity of the solution.

Chapter 5 was dedicated to the comparison in accuracy of correlation and threshold processes. This study was based on both analytical results developed in the two previous chapters, and also on simulations for special cases that were not assessed by the analytical results: non-symmetrical pulses, different amplitudes, filtering at frequencies higher than matched and near-matched filters. Correlation proved more accurate than threshold in the cases where filtering is or cannot be performed at the optimum bandwidths determined by matched filter theory.

Chapter 6 focused on the detection process needed in our developments. Integration and M/N detection were studied separately. Analytical results concerning the probability of detection and false alarm, and the gain in SNR were presented and checked experimentally. It was proven that integrating several cycles of signal and then performing a time measurement was preferable to measuring time of threshold crossing first and then averaging the results. The conclusion of this part was that a combination of M/N detection and integration was an appropriate and useful solution since speed and memory requirements were relaxed as compared to the best detection technique that consists in integrating over all received signals.

Chapter 7 presents a practical problem requiring detection and time delay measurement improvements. The resolution was performed using the techniques presented in the previous chapters. The theoretical solution was implemented and tested with real samples of signals. The specification of the problem was reached, and correlation proved to

provide less rms error in the time delay estimation than threshold. Finally, recommendations were made in order to help solve specific implementation issues.
Appendix A contains the MATLAB code used in the experimental part of Chapter 6, and its explanation.

8.2 Conclusions

This research effort developed and evaluated a combination of techniques to improve the measurement capabilities of systems requiring accurate time measurement information from Gaussian shaped signals.
The combination of M/N detection and integration is a practical approach that was studied and proved powerful as a detection scheme. This solution is actually already implemented in radar systems. These two methods are essential to perform measurements on cleaned versions of the expected Gaussian pulses. However, even if this combination improves the processing of signals embedded in noise and the confidence that these signals are the expected ones, it is not sufficient to free the signal from ambiguities that may make measurements fail.
The minimization of these ambiguities can reach an optimum level if a matched filter is implemented. A matched filter shapes the received signals to a certain bandwidth for which the ratio of noise-free signal power as compared to noise power is maximum. While a matched filter is usually the targeted solution of any design, it might not always be practically feasible, especially if the shape of the expected signal is complicated. The analytical accuracy of threshold measurements will therefore be difficult to reach in practical cases. Correlation, however, is known to be a matched filter if the received signal is correlated with its noise-free replica, no matter the shape of the received signal. Consequently, if the expected Gaussian pulses are detected and processed through integration, then the conditions needed for correlation to be considered as a matched filter are almost reached, hence the SNR of the processed signal is optimized which ensures an efficient time measurement.
Correlation therefore relaxes the filtering requirements thanks to its inherent filtering properties, and increases the accuracy of time delay measurements as compared to

threshold. However, correlation is obtained through a higher computational load than threshold, which might prevent its use.

To sum up, it is not possible to give a definite answer to the question of the improvement of correlation as compared to threshold in an overall sense. Not only would this answer depend on the practical case studied, but also on the trade-off between the accuracy required and the amount of computation power available for the designed solution. However, we have however provided the analytical tools needed to evaluate this trade-off.

We therefore recommend to any designer using this solution to establish first a thorough specification of the performance that is expected, then to solve the requirements of the detection and integration problem. Considerations then need to be established in order to chose which measurement process is appropriate based on whether the implemented filter is optimum or not, and the possibility to implement practically the solution.

8.3 Recommendations for Future Research

This research effort has extended the knowledge base of the use of correlation as a time measurement method in Gaussian shaped signal cases, and the optimum use of detection methods prior to any measurement. A complete solution was designed for the association of these methods. While the developments are noteworthy, extensions of this work may provide increased benefits. The following research areas are recommended for investigation:

1. Practically implement the developed solution on an available DSP processor.
2. Investigate the possibility and benefits of triggering integration while still performing the M/N detection process.
3. Investigate a two-way interaction between the M/N detection and integration process. It could be interesting for instance to give more weight to detected pulses that lie in the previous time windowed solution instead of just taking the longest pulses. Algorithms based on feedback between M/N detection and integration can be added in order to increase the detection improvement already brought by M/N detection.

4. Study the analytical solution of correlation measurements for different shapes of pulses.
5. Determine the optimum shape of a pulse for which correlation could be the overall preferred solution for time delay measurements.
6. Investigate the possibility to estimate some parameters of the detected pulse prior to time delay measurements in order to implement weighting functions within the correlation method. This idea is based on developments presented in the literature review of this thesis that proved that the variance of correlation could be lowered by appropriate weighting functions based on the a priori knowledge of the pulses.